THE EFFECT OF POSTURE DURING CPR ON RESCUER MUSCULAR FATIGUE DEVELOPMENT AND CPR QUALITY.

ANDREW LAGREE

A THESIS SUBMITTED TO
THE FACULTY OF GRADUATE STUDIES
IN PARTIAL FULFILLMENT OF THE REQUIREMENTS
FOR THE DEGREE OF
MASTER OF SCIENCE

GRADUATE PROGRAM IN KINESIOLOGY AND HEALTH SCIENCE
YORK UNIVERSITY
TORONTO, ONTARIO

January 2019

Abstract

Introduction. The aim of CPR is to circulate oxygenated blood, while generating artificial systole and diastole. Within Canada approximately 230,000 cardiac arrest cases are treated each year, however CPR is often performed sub-optimally. Therefore, the purpose of the study was to evaluate muscular fatigue and CPR quality during four CPR positions.

Methods. In a laboratory environment, 21 CPR-certified participants performed six-minutes of CPR, on a CPR manikin at four heights (KH, LH, FH, and WH). EMG of 16 muscles, kinematics of the manikin, and kinetic data at the hands were collected.

Results. The MPF identified that four, six, four, and nine muscles fatigued during KH, LH, FH, and WH, respectively. Based on a cross-correlation analysis, three muscle groups were identified, CC initiators (RA, EO, IO), upper limb stabilizers (LD, FDS, PM, TB, ECRB), and CC terminators (LES, TES, GM). Furthermore, there was a linear decrease in CC force and CC depth over time, during all positions.

Discussion and Conclusion. Rescuers should perform CPR below WH, as the largest amount of muscles fatigued, CC force, CC depth, and perceived fatigue time decreased, additionally RPE increased. Based on the timing of the evaluated muscles three distinct muscle groups were identified. CC initiators, which initiate the CC, upper limb stabilizers, which stabilize the upper limbs during the compression phase, and CC terminators, which extend the trunk during the release phase. The TB are critical muscles in performing CPR, they produced the highest peak activation and fatigued within all CPR positions, suggesting that they play a major contributing role in stabilizing the upper limbs to allow for force transmission.

Acknowledgements

First and foremost I would like to thank my supervisor, Dr. Moore, for not only providing me with the opportunity to complete this project but also the opportunity to study in the field of biomechanics. It was volunteering in your lab where I first discovered my passion for this field. Thank you for all the support, feedback and encouragement you have given me over the years.

To my committee member, Dr. Hynes, thank you for all your support and advice over the past year. From providing the manikins and feedback equipment used during the project, to going out of your way to answer to questions I had, you were always more than willing to help. Your excitement about this project has driven me to ensure I completed it to the best of my abilities.

Kristy your love and support over the past seven years and throughout this project has meant everything to me. From spending late nights bouncing ideas off you, to volunteering to come in and help with piloting and data collection. I do not think I would have been able to finish this project without you there pushing me.

Andrew the past three years would not have been the same without you. From rush hour drives to pick up computers to late nights spent collecting data you were always more than willing to donate your time. I am glad I got to know you over the past three years and call you a friend.

Paris and Max I cannot thank you enough for the amount of hours you spent helping with the project, you both put in far more work than I had ever expected. I enjoyed all the laughs and conversations we shared and know that the future is extremely bright for both of you.

Liz, even if I have not said it before, I have always looked up to you. From the day I started in the lab you put me straight to work and because of that I gained valuable hands-on experience before entering my masters. No matter the time of day, you were always willing to talk through any questions I had. Thank you for supporting me and sparking a real desire to learn more.

To all the participants and volunteers, thank you. Without you this project would not have been completed, so thank you for all the time you gave up on your days off, travelling to York, and helping me with this project.

Table of Contents

List of Tables

List of Figures

List of Equations

List of Abbreviations

A/D	Analog to Digital
Ag-AgCl	Silver/Silver Chloride
AHA	American Heart Association
AMUP	Average Motor Unit Potential
ANOVA	Analysis of Variance
APDF	Amplitude Probability Distribution Function
BLS	Basic Life-support
BMI	Body Mass Index
BPM	Beats Per Minute
C:V	Compression to Ventilations
CC	Chest Compression
CPR	Cardiopulmonary Resuscitation
DFT	Discrete Fourier Transform
ECG	Electrocardiography
ECRB	Extensor Carpi Radials Brevis
EMD	Electromechanical Delay
EMG	Electromyography
EMS	Emergency Medical Service
EO	External Oblique
ES	Erector Spinae
FDP	Flexor Digitorum Profundus
FDS	Flexor Digitorum Superficialis
FFT	Fast Fourier Transform
FH	Finger Height
GM	Gluteus Maximus
H/L	High/Low
HR	Heart Rate

IEMG	Integrated Electromyography
IO	Internal Oblique
KH	Kneeling Height
LD	Latissimus Dorsi
LES	Lumbar Erector Spinae
LH	330 mm High
MAP	Motor Action Potential
MdPF	Median Power Frequency
MPF	Mean Power Frequency
MU	Motor Unit
MUAP	Motor Unit Action Potential
MVC	Maximum Voluntary Isometric Contraction
pH	Potential Hydrogen
PM	Pectoralis Major
PSDF	Power Spectral Density Function
RA	Rectus Abdominis
RMS	Root Mean Squared
RPE	Rating of Perceived Exertion
SEC	Series Elastic Component
sEMG	Surface Electromyography
SPSS	Statistical Package for the Social Sciences
TB	Triceps Brachii
TES	Thoracic Erector Spinae
VAS	Visual Analog Scale
WH	Waist Height

Chapter 1, Introduction

1.1 General Introduction

1.1.1 CPR Mechanics.

Cardiopulmonary Resuscitation (CPR) was introduced over 50 years ago with an aim to oxygenate blood by means of ventilations, while generating artificial systole and diastole by means of chest compression (CC) (Abella et al., 2012; Babbs et al., 1983). Within the current literature, two models offer explanations for artificial systole during CC. The compression model, takes into account the compression of the left ventricle between the sternum and spine, which produces a higher pressure within the ventricle compared to that of the peripheral arteries (Babbs, 1980). The thoracic pump model takes into account increased intrathoracic pressure during the compression phase of CC (Babbs, 1980; Niemann et al., 1980; Rudikoff et al., 1980). In turn artificial diastole, according to the thoracic pump model and compression model, is produced when the rescuer allows for chest recoil causing negative intrathoracic pressure and negative pressure within the right ventricle, respectively, which allows for return of blood to the heart (Babbs, 1980; Lurie, 1994; Niemann et al., 1980; Rudikoff et al., 1980).

1.1.2 Prevalence.

Healthcare providers, first responders, and lay rescuers, who are trained in high-performance/quality CPR, may regularly practice CPR. The importance in understanding the repetitive forces and extreme postures the human body is exposed to during CPR is first linked to its frequency of use. Current research suggests that approximately 382,800 - 424,000 citizens of the United States, 300,000 European citizens, and upwards of 3.7 million individuals across the world will suffer a cardiac arrest each year (Kudenchuk et

al., 2015; Roger et al., 2012). Of these individuals it is estimated that within the United States 294,851 - 359,400 patients and within Canada 32,160 patients will be treated for a cardiac arrest out-of-hospital by emergency medical service (EMS) (Go et al., 2013; Nichol et al., 2008). EMS respond to the largest proportion of out-of-hospital cardiac arrest cases, such that in the United States approximately 60% of cardiac arrest cases are treated by the EMS (Go et al., 2013; Roger et al., 2012). In Ontario, Canada EMS responds to 48%, of out-of-hospital cardiac arrest cases, while police/firefighters respond to 33.8% and citizens respond to 14.7% (Vaillancourt and Stiell, 2004). In-hospital cardiac arrests also plays a contributing factor to the total amount of cardiac arrest cases, with approximately 200,000 patients each year suffering a cardiac arrest (Go et al., 2013; Merchant et al., 2012).

1.1.3 Purpose

In the United States a large registry study of individuals who suffered a cardiac arrest, found the survival rate to hospital admission was 26.3% and the survival rate to hospital discharge was 9.6% (Bryan et al., 2011). Furthermore, 36.7% of out-of-hospital cardiac arrests were witnessed, while 43.8% of witnessed cardiac arrests had bystanders perform CPR (Bryan et al., 2011). Recent CPR studies have identified high-performance/quality CPR as a significant contributor to improvement in survival of a cardiac arrest (Abella et al., 2005a; Dine et al., 2008; Kudenchuk et al., 2015; Meaney et al., 2013; Sayre et al., 2008). However, hospital staff and EMS personnel often perform suboptimal CPR (Abella et al., 2005a, 2005b; Russi et al., 2016; Wik et al., 2005). Furthermore, CPR quality provided by EMS personnel was found to be significantly worse during transport compared to on-scene (Olasveengen et al., 2008; Russi et al.,

2016). Fatigue is a critical component in CPR quality, where the longer a rescuer performs CPR the lower the quality (Chi et al., 2010; McDonald et al., 2013; Russo et al., 2011). Specifically, over time CC depth and CC force decrease (Bjørshol et al., 2011, 2008a; Chi et al., 2010; Dainty and Gregory, 2017; McDonald et al., 2013; Russo et al., 2011; Sugerman et al., 2009; Trowbridge et al., 2009; Wang et al., 2015), rating of perceived exertion (RPE) and visual analog scale (VAS) scores increase (Betz et al., 2008; Chi et al., 2010; Kwak et al., 2016; Pozner et al., 2011; Trowbridge et al., 2009), blood lactate and heart rate (HR) increase (Betz et al., 2008; Cason et al., 2011; Chi et al., 2010; Shin et al., 2014; Trowbridge et al., 2009), however no muscle fatigue was found (Dainty and Gregory, 2017; Trowbridge et al., 2009; Tsou et al., 2014). The vast majority of these CPR studies have evaluated CPR while kneeling or did not report rescuer posture. To the authors' knowledge no studies have evaluated the combination of different CPR heights with local muscle fatigue, perceived fatigue, and measures of CPR quality. Therefore, the purpose of the study was to evaluate muscle fatigue and CPR quality over time at four CPR heights.

1.2 Research Questions

The main purpose of the study was to determine if muscular fatigue is evident following six-minute trials of CPR, if participants adopt muscular compensation methods during CPR positions in an attempt to maintain CPR quality, and if muscular fatigue decreases CPR quality specifically, CC force, CC depth, chest recoil, and CC rate. In addition it was to be determined if measures of CPR quality (CC depth, CC rate, and chest recoil) over time remain constant during CPR positions. Thus, the author set out to answer the following questions:

1. Do the evaluated muscles fatigue during different CPR positions and if so do they fatigue at different rates based on positions participants complete CPR in?
2. Are limiting muscles present during CPR, do these limiting muscles differ based on the CPR positions, and are compensation methods produced?
3. Are there changes in CPR quality specifically CC force, CC depth, CC rate, and chest recoil and does muscular fatigue play a role in changes to CPR quality?

1.3 Hypotheses

The following hypotheses were developed from the research questions and drove the project.

1. Limiting muscle(s) will differ based on the CPR positions.
2. The muscles evaluated for the study will fatigue at different rates based on CPR positions.
3. Over the course of the six-minute trials, muscular fatigue will develop and the participant will develop compensation methods.
4. CC force, CC depth, and change in angle of the chest will decrease over time during each CPR position.
5. Chest recoil and CC rate will increase over time during each CPR position.
6. Perceived time of fatigue will not differ from actual time of fatigue during CPR positions.

1.4 Cardiopulmonary Resuscitation Literature Review

1.4.1 Introduction.

1.4.1.1 Current standards.

CPR, like any task of concern, involves repetitive forces and extreme postures that can strain the effectiveness of the task and increase risk to the rescuer. Recent literature has cited high-performance/quality CPR as a significant contributor to improvement in survival from a cardiac arrest (Abella et al., 2005a; Dine et al., 2008; Kudenchuk et al., 2015; Meaney et al., 2013; Sayre et al., 2008). To provide rescuers with the knowledge and tools that would aid in the performance of high quality CPR, evidence based research conducted upon CPR, rescuers, and patients is a necessity. In the most recent update of international CPR guidelines (2015), focus has fallen on CC rate, CC depth, chest recoil, and CC interruptions at the basic life-support (BLS) level (Hazinski et al., 2015). Rescuers are expected to perform CC at a rate of 100 - 120 beats per minute (bpm), to a depth of 50 – 60 mm, allow full chest recoil, and minimize interruptions with a target of at least a 60% CC fraction (Hazinski et al., 2015).

1.4.1.2 Setting and posture.

Healthcare providers, first responders, and lay rescuers may regularly perform CPR. CPR quality becomes dependent on factors such as, setting, which can be further sub-classified into out-of-hospital or in-hospital cardiac arrests. First responders and lay rescuers mainly respond to out-of-hospital cardiac arrests, while healthcare providers mainly respond to in-hospital cardiac arrests. Both in-hospital and out-of-hospital cardiac arrests present unique challenges to the rescuer such as: posture, patient transport, fatigue, and total time performing CPR. According to current literature, studies have quantitatively examined various postures rescuers performed CPR in and identified

differences in CC force, CC depth, and fatigue, defined by inadequate CC depth and/or CC rate, range of motion of the elbows and lower back, in addition to the severity of back pain (Foo et al., 2010; Hong et al., 2014). Examples of such postures include, kneeling on the floor next to the patient, standing next to a bed or kneeling on the bed next to a patient. Transport of the patient is mainly a factor in out-of-hospital scenarios where the patient must be transported to advanced medical care, while still in cardiac arrest. Studies have shown that CPR quality during transport was significantly worse compared to on-scene CPR quality (Russi et al., 2016). Total time performing CPR is a factor that must also be considered for both in-hospital and out-of-hospital cardiac arrests. First responders and healthcare providers mainly work in teams, whereas lay rescuers may respond as a single responder to a cardiac arrest. Working in a team of rescuers, provides the benefit of being able to change rescuers during CPR. Whereas, lay rescuers may need to perform CPR or CC only, for a prolonged period of time, prior to the arrival medical aid.

1.4.1.3 Rescuer fatigue.

Fatigue is a critical component in all factors associated with CPR performance. Fatigue influences the rescuers ability to achieve minimum CC depth, CC rate, and chest recoil (Russo et al., 2011). Likewise, fatigue has an affect on the posture CPR is performed in, influencing endurance of rescuers in certain postures (Foo et al., 2010). Fatigue most notably influences CPR quality, where the longer a rescuer continues CC the lower the quality of CPR (Chi et al., 2010; McDonald et al., 2013). Therefore, the objective of this literature review was to evaluate rescuer fatigue pre-CPR, while performing CPR, and post-CPR, along with its effects towards the quality of CPR performed on patients.

1.4.2 Discussion.

1.4.2.1 Chest compression depth and rate.

The objective of the literature review was to evaluate rescuer fatigue while performing CPR and its effects on CPR quality. Many factors have been associated with CPR performance including: CC depth, CC rate, chest recoil, physiology, and anthropometrics of the rescuer. Within the literature a general conclusion that may be drawn is, while performing CC, over time CC depth and force decrease (Bjørshol et al., 2011, 2008b; Chi et al., 2010; Dainty and Gregory, 2017; McDonald et al., 2013; Russo et al., 2011; Sugerman et al., 2009; Trowbridge et al., 2009; Wang et al., 2015). However, CC rate remains relatively unchanged over time (Hwang et al., 2016; Trowbridge et al., 2009). There is however, disparity in the exact time a rescuers' CC becomes ineffective. Indications of rescuer fatigue may be evident as early as 40 – 90 seconds (Dainty and Gregory, 2017; Sugerman et al., 2009), providing evidence for the recommendation that rescuers should attempt to change positions approximately every two-minutes (Chi et al., 2010; McDonald et al., 2013; Russo et al., 2011; Sugerman et al., 2009). **In general, while performing CPR, over time CC depth and CC force decrease, while CC rate remains constant. However, studies are inconsistent in identifying the point in time when rescuers fatigue.**

1.4.2.2 Feedback devices.

Russi and colleagues completed a study on a paramedic population, investigating the effects of CPR during static and moving scenarios, the authors identified that CC depth was significantly lower during transport compared to on-scene resuscitations (Russi et al., 2016). A secondary analysis was completed where rescuers used a feedback device to determine its effect on CC quality. Even though correct CC depth during transport

remained relatively low, on-scene CC depth significantly improved (Russi et al., 2016). This finding aligned with similar studies that identified rescuers improved CC depth using feedback devices (Cason et al., 2011; Pavo et al., 2016; Smart et al., 2015). Feedback devices along with human feedback are associated with significant improvements in CC quality, increasing depth by approximately 7 mm, along with rescuers reporting lower levels of exertion (Cason et al., 2011; Pavo et al., 2016; Pozner et al., 2011; Smart et al., 2015). Nonetheless, significantly higher blood lactate levels have been associated with visual feedback devices (Cason et al., 2011), while metronome guidance alone is associated with decreased CC depth for the first five cycles (Chung et al., 2012). Therefore, the evidence suggests that rescuers perceived they were less fatigued during feedback conditions, even though physiologically an increased amount of work was being completed, implying that rescuers were working harder to achieve the appropriate CC depth and CC rate, however they did not perceive the increased work fatigued them. **Audio-visual feedback devices, which provide CPR metrics to the rescuer during resuscitation attempts, are found to significantly improve CPR quality. As CPR quality improved, studies found an increase in rescuer fatigue.**

1.4.2.3 Sex.

Sex of the rescuer seems to play a role in CPR quality and fatigue. A study by Zhang and colleagues, found that perceived fatigue time of females was faster than males and that males were able to reach the required depth a significantly greater proportion of the time (Zhang et al., 2013). This was in contrast to a study by Jaafar and colleagues, who found there was no difference between males and females reaching correct CC depth (Jaafar et al., 2015). In addition, a compression to ventilation (C:V) ratio of 15:2 was suggested for females, due to the fact that females generally completed shallow/rapid CC,

and perceived that fatigue had affected them during CPR (McDonald et al., 2013; Russo et al., 2011; Sayee and McCluskey, 2012). These findings were in contrast to a study by Kwak and colleagues, that identified the mean percentage of adequate CC for females was significantly higher in the 30:2 C:V group compared to the 15:1 C:V group (Kwak et al., 2016). In further evaluation of the studies by Kwak and colleagues, Sayee and McCluskey, both studies evaluated female medical students and had similar samples sizes of 22 and 16 respectively. Kwak and colleagues, were able to reach significance when comparing mean percent of adequate compression between 30:2 and 15:2 C:V groups, whereas Sayee and McCluskey did not reach significance (Kwak et al., 2016; Sayee and McCluskey, 2012). According to the authors this was due to a small sample size, however using the McNemara's test the author reached significance such that the 15:2 C:V ratio was more effective compared to 30:2 (Sayee and McCluskey, 2012). **Male rescuers tended to reach minimum CC depth a greater proportion of the time and subsequently fatigue faster than females. Studies have shown that females generally perform shallow/rapid CC, however it is inconclusive whether a C:V ratio of 15:2 or 15:1 would be beneficial.**

1.4.2.4 Body mass index.

In evaluating body mass index (BMI), rescuers whose BMI was greater than 24 kg/m^2 were more effective in performing CPR (Russo et al., 2011; Sayee and McCluskey, 2012). More specifically, fit, experienced rescuers with a high BMI correlated positively with CC quality (Körber et al., 2016; Russo et al., 2011; Sayee and McCluskey, 2012; Tsou et al., 2014). A study by Jaafar and colleagues, was in contrast with these findings, suggesting that rescuers with a BMI greater than 26 kg/m^2 were less likely to achieve correct CC depth and their CC rate was less than 100 bpm (Jaafar et al., 2015). A possible

explanation for these findings was that rescuers with a BMI greater than 26 kg/m^2 may fatigue sooner, implying that CC depth decreases early during CPR (Jaafar et al., 2015). **Physically fit and experienced rescuers with a high BMI perform more effective CPR, however a single study suggested rescuers with a BMI greater than 26 kg/m^2 were less effective when performing CPR.**

1.4.2.5 Perceived exertion.

RPE scale is a simple yet powerful measure of participant's perceived exertion and HR (Borg, 1982). Studies have shown that the rescuers' RPE increases from the start of a CPR trial as a light exercise, to the end of a trial as a moderate - hard/heavy exercise (Betz et al., 2008; Chi et al., 2010; Kwak et al., 2016; Trowbridge et al., 2009). In addition, using a VAS, rescuers' perceived fatigue significantly increases from 2 – 4 minutes (Pozner et al., 2011), further providing evidence to support the change of rescuers at two-minutes. Self reported fatigue times have also been utilized in the literature, identifying that females were faster to declare fatigue, at approximately 50 seconds, whereas males perceive fatigue at approximately 71 seconds (McDonald et al., 2013; Zhang et al., 2013). Furthermore, a study by McDonald and colleagues, found rescuers were unable to recognize fatigue until 90 seconds after their performance had decreased (McDonald et al., 2013). This again provides evidence in support of prompt rotation of rescuers. **Rescuers' perceived exertion corresponds with CPR metrics, displaying an increase in exertion over the course of the trial, however the point at which rescuers perceive fatigue dose not parallel CPR quality.**

1.4.2.6 Electromyography.

The relationship between electromyography (EMG) and force will be discussed below; for a review of EMG concepts and techniques refer to section 1.5. EMG is the

measure of electrical activity within the musculature of the body, with a frequency range of 10 – 1000 Hz (Winter, 2009). EMG signals can be analyzed using multiple techniques, which provide insight on such things as fatigue, identification of trends during muscle activation, and how EMG activity relates to force. In previous studies of CPR, EMG has been used to identify the primary muscles used during CC at kneeling height (pectoralis major (PM), tricep brachii (TB), rectus abdominis (RA), latissimus dorsi (LD) erector spinae (ES), gluteus major (GM)), however studies have not identified evidence of muscular fatigue. A study by Trowbridge and colleagues analyzed eleven muscles for the first 90 compressions and the last 90 compressions of kneeling CPR (Trowbridge et al., 2009). The authors stated that the EMG signal was integrated using the linear envelope of the EMG data, resetting the signal to zero using compressions as the mechanical time points (Trowbridge et al., 2009). Unfortunately, in using integrated electromyography (IEMG) it is difficult to understand if a reduction in signal is due to time or amplitude. However, the authors identified that the IEMG signal of the anterior deltoid, PM, bicep brachii, LD, upper trapezis, middle trapezius, and external oblique (EO) significantly decreased in amplitude during the last 90 compressions compared to the first 90 compressions. The authors suggested that decreases in CC force and CC depth were due to the decrease in IEMG amplitude of elbow and shoulder stabilizer muscles (Trowbridge et al., 2009). Many factors influence the calculations of anisometric EMG, however if the kinematics of the motion are the same (force length, force velocity, and electrode movement), then one would expect an increase of EMG for the same force with fatigue, due to increased motor unit (MU) recruitment. Results from Trowbridge and colleagues may suggest a muscular response to lower force rather than the muscles inability to

generate force (i.e. less force placed on the hands, therefore less force required to stabilize) rather than fatigue itself.

A study by Dainty & Gregory, evaluated the activity of six trunk and upper limb muscles during kneeling CPR (Dainty and Gregory, 2017). The authors found that the lumbar erector spinae (LES) and left PM increased in average activity, while the EO and left TB decreased in average activity, however the difference in muscle activation was 1-3%maximum voluntary contraction (MVC) (Dainty and Gregory, 2017). In an attempt to quantify muscular fatigue the authors had participants complete isometric back extension exercises pre and post CPR. In calculating the median power frequency (MdPF) there were no significant differences between pre and post tests, suggesting that the lumbar muscles did not fatigue (Dainty and Gregory, 2017). As the LES did not show evidence of fatigue, the increase in average activation may be attributed to longer recruitment of the back extensor muscles or increased peak recruitment of MU and/or firing rate. In regards to trunk and upper limb musculature it was suggested by the authors that there was an inverse relationship between the PM and TB, in which there may be a trade off mechanism between the two muscles when the triceps fatigue (Dainty and Gregory, 2017).

A study by Tsou and colleagues, also evaluated EMG during CPR while kneeling, and identified that the PM, RA, and LD generated the pushdown force, while the LES and GM displayed higher activation in the release phase (Tsou et al., 2014). It was also identified that the root mean square (RMS) and MdPF displayed no significant difference over time, suggesting that the PM, LD, RA, LES, and GM did not experience fatigue (Tsou et al., 2014). The author also found evidence to support balanced bilateral muscle

recruitment, defined as no significant difference in amplitude (RMS of 50% of a CC) bilaterally, during CPR, of all muscles except the GM (Tsou et al., 2014). **While there is clearly a reduction of force output over time suggesting muscle fatigue, only two studies have evaluated muscle fatigue using the power spectral density function (PSDF) and only one study has used a standardized pre-post contraction. In both cases the number of muscles tested are limited and only kneeling posture was used.**

1.5 Electromyography Literature Review

1.5.1 Physiology.

EMG is a measure of the electrical activity within muscles. In order to effectively analyze the electrical activity, cellular interactions prior to a contraction must first be understood. The smallest controllable element of the muscular contractile system is a MU, which consists of an alpha motoneuron that is divided into a synaptic junction in the ventral horn of the spinal cord, axon, and neuromuscular junction (Winter, 2009, 1980). The MU also consists of the muscle fibres the alpha motoneuron innervates, which can be as little as three or up to 2000, depending on the type of muscle innervated (Winter, 2009, 1980). The propagated signal travels along the alpha motoneuron till the neuromuscular junction, where it induces a depolarization wave traveling at a velocity of 3 – 6 m/s in both directions of the muscle fibre, called a motor action potential (MAP) (Hof, 1984; Winter, 1980). The depolarization wave is a precursor to mechanical contraction, as the wave is led into the muscle fibre by transverse tubules where calcium ions are released (Hof, 1984).

The motor unit action potential (MUAP) is the summation of MAP in the vicinity of an electrode, which are detectable waveforms of the depolarization wave, whose shape is a function of electromechanical properties of the muscle and connective tissue (Winter, 1980). The number of active MU, mechanical interaction between muscle fibres, MU firing rate, number of detectable MU, amplitude, duration and shape of the MUAP, and recruitment stability of MU all play a deterministic role in information contained within the EMG signal (Deluca, 1997). As an electrical signal, the potential also exists for causal factors such as electrode type, electrode placement, size, and orientation to influence

measurement of the depolarization wave (Deluca, 1997). **As a detectable waveform, the MUAP is the summation of waveforms travelling through the muscle at that time. Variables such as number of active MU, force-length, velocity-length, fatigue, MU firing rate, among others variables influence the shape and duration of the signal.**

1.5.2 EMG and force.

Early EMG studies used the depolarization wave as a marker for muscle timing to determine if the muscle was on or off, however a relationship between EMG and force exists (Hof, 1984). It has been identified that following the depolarization wave, maximum force is reached within 20 - 150 msec (Cavanagh and Komi, 1979; Hof, 1984). Timing however is only one component of this relationship. There are ways to control for increases in tension such as, changing the number of active MU and changing the firing rate of active MU (Deluca, 1997; Hof, 1984; Winter, 2009). Excitation of the MU is an all or nothing event; when tension increases, MU are recruited in order of magnitude, where the maximum firing rate of each MU is reached after recruitment of the next MU (Hof, 1984; Winter, 2009).

It has been shown experimentally that the mean rectified EMG is linearly proportional to force in an isometric contraction when force is quasi-static (Hof, 1984; Leedham and Dowling, 1995). In completion of an isometric contraction the contractile component can shorten in conjunction with a stretch of the series elastic component (SEC). When the contractile component length reaches a point where the force-length relation decreases, the EMG relationship will no longer be linear (Hof, 1984; Hof and Van den Berg, 1981). During an anisometric contraction multiple variables such as: the non-linearity of the force-length relation, movement of the MUAP relative to the

electrode, and increased speed of contractions influenced by the electromechanical delay (EMD) must be considered (Deluca, 1997). During an Isometric contraction muscle force is dependent on the length of the contractile component, however during anisometric contractions the muscles shortening velocity influences muscle force (Hof, 1984). **There exists a linear relationship between force and EMG during an isometric contraction when force is kept constant. Due in part to deterministic factors such as force-length, force-velocity, and EMD, during anisometric contractions, the EMG-force relationship is no longer linear.**

1.5.3 EMG frequency: non-fatigued state.

In recording EMG the most significant attribute of the signal lies within the frequency domain and depends on muscle fibre type, type and location of the electrode, and characteristics of the surrounding tissue (Winter, 1980). The frequency range for EMG is shown to range between 0.1 – 10,000 Hz for indwelling EMG and 1 – 3,000 Hz for surface electromyography (sEMG), however power is generally negligible in the higher frequencies, thus the recommend range is generally 2 - 2,000 Hz for indwelling and 10 – 1,000 Hz for sEMG (Winter, 2009, 1980). The higher frequency range for indwelling electrodes can be attributed to closer spacing between electrodes and closer proximity to muscle fibres (Winter, 2009). It is also worthy to mention that the majority of power within the EMG signal is concentrated between 20 – 200 Hz (Winter, 2009). **SEMG frequencies can range up to 10,000 Hz, however power is negligible at higher frequencies and generally found between 20 – 200 Hz.**

1.5.4 Fatigue.

Within the concept of fatigue, two components must be examined, the physiological influences of fatigue and mechanical influences of fatigue. Physiological muscular fatigue occurs when the contractile component has not been provided with sufficient metabolism due to lack of metabolic substrates or insufficient oxygen (Winter, 2009). Mechanical fatigue occurs with a decrease in tension, while assuming muscular activation remains constant (Winter, 2009). These changes in fatigue correspond to EMG power spectrum shifts, resulting in a decrease in high-frequency components (Allison and Fujiwara, 2002; Dolan et al., 1995; Krogh-Lund and Jorgensen, 1991). Changes in the EMG power spectrum have been generally attributed to a decrease in conduction velocity of the depolarization wave, a decrease in activity of larger and faster MU, and a change to MU firing synchronously (Arendt-Nielsen and Mills, 1988; Krogh-Lund and Jorgensen, 1991; Winter, 2009). In examining the interaction of force and electrical activity it is generally accepted that if a loss in force is paralleled with a loss in electrical activity it is due to failure of excitation, however if electrical activity is unchanged it is due to muscle metabolism (Bigland-Ritchie, 1981). Take for example a muscle at a constant sub-maximal force with an increase in electrical activity; this can be attributed to an increase in MU recruitment, compared to a maximal muscle contraction with a paralleled decrease in force and electrical activity which can be attributed to insufficient electrical activity (Bigland-Ritchie, 1981). Therefore, at maximal contractions, fatigue may occur from central and peripheral elements (Bigland-Ritchie, 1981; Stephens and Taylor, 1972). **Physiological fatigue, insufficient metabolism provided to the contractile components, and mechanical fatigue correspond to decreases in the PSDF.**

1.5.5 Conduction velocity.

As previously stated muscular fatigue is paralleled with a shift toward lower frequencies within the EMG power spectrum. This shift within the EMG power spectrum is due in part to a change in shape of the MUAP. It has widely been accepted that there is a progressive decrease in conductive velocity of action potentials below 4.5 m/s, accompanying fatigue (Deluca, 1997; Krogh-Lund and Jorgensen, 1991; Winter, 2009). The decrease in conduction velocity in turn influences the shape of the MUAP by increasing the time duration, which in turn compresses the EMG power spectrum (Deluca, 1997). The decrease in conduction velocity has also been associated with a decrease in pH of the fluid surrounding the muscle, due in part to sustained contractions where there is an accumulation of lactic acid (Deluca, 1997). The theory where there are linearly proportional decreases in conduction velocity and MdPF are supported by Eberstein et al. (1985) and Arendt-Nielsen et al. (1988), where endurance contractions of 60%, 70% MVC and isometric contractions of 60%, 70%, 80%, and 90% MVC saw a linear decline of MdPF and conduction velocity, respectively (Arendt-Nielsen and Mills, 1988; Eberstein and Beattie, 1985; Krogh-Lund and Jorgensen, 1991). A study by Arendt-Nielsen and colleagues, also concluded that during submaximal contractions of the vastus lateralis, conduction velocity and MdPF decreased (Arendt-Nielsen and Mills, 1988). These findings point to a relationship between conduction velocity and MdPF during contractions exceeding certain contraction levels, however for contractions below 25 - 30%MVC the reduction in conduction velocity does not seem to be a precursor for a decreases in MdPF (Krogh-Lund and Jorgensen, 1991). Krogh-Lund and colleagues identified that mean conduction velocity had almost no change after 50% of endurance time, speculating that the initial decrease in mean conduction velocity may be attributed

to the reduction of the initial MU activated during the contraction (Krogh-Lund and Jorgensen, 1991). In contrast to these results, a study by Bigland-Ritchie and colleagues suggested that minimal changes in conduction velocity during sustained maximal contractions of the adductor pollicis were insufficient to account for changes in the power spectrum (Bigland-Ritchie et al., 1981). Bigland-Ritchie speculated that the aforementioned results may have been influenced by synchronization of MU and firing frequency (Bigland-Ritchie et al., 1981). **It is widely accepted that there is a shift towards lower frequencies in the PSDF and a decrease in conduction velocity with fatigue, as seen with endurance and isometric contractions at a higher percentage of MVC.**

1.5.6 Motor unit activity.

Muscle fibres are composed of two separate types of fibres. Slow-twitch slower fatiguing fibres, are comprised of mitochondria rich, highly capillarized fibres for aerobic metabolism, which have a relatively slow rise in force twitch (Deluca, 1997; Winter, 2009). Fast-twitch, faster fatiguing muscle fibres are relatively more glycolytic and rely on anaerobic metabolism (Deluca, 1997; Winter, 2009). Therefore, fast-twitch muscle fibres have a shorter EMD, compared to slow-twitch muscle fibres (Deluca, 1997). Generally, the initial firing rate of slow-twitch fibres is 5 – 13 Hz to an approximate maximum firing rate of 15 – 60 Hz (Winter, 2009). In addition, the size principles argues that MU recruitment increases in size with increases in tension, the opposite occurs with a reduction of tension, where the larger MU drop off first (Hof, 1984; Winter, 2009). The composition of muscle fibres also varies between muscles, where generally slow-twitch muscle are used for fine controlled movements, seen in large quantities of postural

muscles, where fast-twitch muscles are required in high forces movements and are predominantly seen in muscle that are used to produce short bursts of force (Hof, 1984; Winter, 2009). A study by Nilsson and colleagues argued that a local factor within the muscles was the cause of fatigue and not the neuromuscular junction, indicating that decreases in force seen during mechanical fatigue were attributed to the drop out of fast-twitch muscle fibres (Nilsson et al., 1977). Further evidence suggests that there is a positive correlation between the percentage of fast-twitch fibres, increases in EMD, and tension during fatiguing contractions (Nilsson et al., 1977). Peak EMG and IEMG support these results, as these measures remained relatively constant throughout 100 contractions, other than the 25^{th} and 50^{th} contraction when peak EMG was significantly higher than the initial (Nilsson et al., 1977). **Muscles are composed of varying percentages of fast twitch and slow twitch fibres. The size principle states that the smallest MU is recruited first and the largest MU is recruited last, subsequently the reverse is true for reduction in tension, suggesting that the smallest MU are on for the longest period of time.**

1.5.7 Motor unit synchronization.

As previously discussed, the propagated signal travels from the spinal cord along motoneurons towards muscle fibres, and in healthy non-fatigued states fires asynchronously. In a healthy non-fatigue individual, MU fire independently within the same muscle, such that an EMG signal may be considered a summation of randomly timed MUAP (Winter, 2009). However, with fatigue there is a tendency for these MU to firing synchronously (Bigland-Ritchie et al., 1983, 1981; Mills, 1982; Winter, 2009). Additionally, synchronization of MU has been perceived to begin as early as 10 seconds

(Mills, 1982). Synchronization is also variable and is influenced by factors such as habitual physical activities performed by the individual, tasks evaluated, and muscles involved in completion of the task (Yao et al., 2000). For example, synchronization of MU is reduced in individuals who require independent control of their fingers, such as musicians (Yao et al., 2000). This is in contrast to individuals who performed gross finger movements, such as those who regularly perform resistive training, where increased synchronization occurs (Yao et al., 2000). Therefore, during prolonged activation of fatiguing contractions, individuals shift to synchronization of MU, which results in increased power in the low-frequency bands of the EMG power spectrum (Bigland-Ritchie et al., 1983, 1981). In a study by Yao and colleagues, synchronization of MU was found to have negligible affects on steady-state force, however it had substantial affects on average EMG amplitude. It was shown that moderate synchronization increased EMG amplitude by approximately 65%, while high synchronization increased EMG amplitude by approximately 130% (Yao et al., 2000). It was also shown that power within the EMG power spectrum increased with the level of excitation and amount of synchronization, as is evident with a decrease in MdPF (Yao et al., 2000). These findings are in contrast to DeLuca (1997), who argued that MU synchronization could not significantly influence the EMG power spectrum. It was suggested that a high-pass filter with a cutoff frequency of 20 Hz should be used to maintain signal stability and that synchronization affects the power spectrum at approximately 15 – 25 Hz, therefore most of the contributions of MU synchronization would be removed from the filtered signal (Deluca, 1997). **The general consensus amongst studies is that during muscle fatigue MU shift to a synchronous firing rate. Synchronisation of MU leads to increased**

power in the low frequency bands of the PSDF and increased amplitudes of the EMG signal.

1.5.8 Fatigue analysis.

As previously mentioned when examining muscles exposed to fatiguing contractions major changes to the EMG power spectrum include increases in EMG amplitude and shifts to lower frequency bands. Some of the measures used to evaluate these changes include: MdPF, mean power frequency (MPF), high/low (H/L) ratio, IEMG, average motor unit potential (AMUP), and RMS. MdPF is a frequency measure of the EMG power spectrum where half the power of the signal lies below and above a certain point. Thus, a fatigued muscle would demonstrate a decrease in MdPF as it represents a shift to lower frequency bands. A study by Allison and colleagues, demonstrated that MdPF is highly correlated to amplitudes between 15 – 45 Hz and the H/L ratio. MPF is a measure of average frequency calculated by summing the products of the EMG power spectrum and dividing it by the total sum of frequencies (Winter, 2009). Thus, similar to MdPF, a fatigued muscle would demonstrate a decrease in MPF. MdPF and MPF measures are very similar, where there is almost no difference in their correlation with independent measures of fatigue (Winter, 2009). H/L ratios represent the relationship between the high and low frequency components of the EMG signal. This method is dependent on the researchers' determination as to what specific frequencies are classified as high or low. The use of H/L ratios is not very prevalent in research, however it is used when processing a signal using the fast Fourier transform (FFT) is problematic (Allison and Fujiwara, 2002). An example of this would be when analyzing anisometric contractions or when the muscle moves with respective to the electrode, as the waveform

may become non-stationary (Allison and Fujiwara, 2002). IEMG is a measure of the integral or area under the curve. There are two strategies of resetting this measure, the first, time interval reset and the second amplitude reset. As IEMG measures the change in EMG amplitude it is assumed to subsequently be a measure of new MU recruitment and/or an increased firing rate of current MU in submaximal contractions (Viitasalo and Komi, 1977). However, it should be noted that during maximal contractions it is assumed that all motor units are active, which would likely lead to reductions in IEMG (Viitasalo and Komi, 1977). First developed by Lang and colleagues, AMUP was a way of automatically analyzing the average spatial distribution of MU potentials. Viitasalo and colleagues modified this technique to evaluate muscular fatigue (Viitasalo and Komi, 1977). AMUP requires an amplitude threshold, which determines whether an EMG spike is included in the average, the software then determines 30 digitized points prior to and after the spike to calculate a time axis (Lang et al., 1971; Viitasalo and Komi, 1977). Viitasalo and colleagues identified that the AMUP increased in duration and amplitude with fatigue along with an increased number of EMG spikes at the end of the experiment (Viitasalo and Komi, 1977). It was concluded that during fatigue, changes to the AMUP were similar to that of IEMG, rather than that of a single MU (Viitasalo and Komi, 1977). AMUP was a novel technique introduced to evaluate fatigue, however it has not been widely adopted by the research community as its use was quite limited and produced similar results as already established measures of fatigue. RMS is a time variant signal that measures the square root of the average power in the EMG power spectrum (Robertson et al., 2004). Similar to IEMG, during fatiguing sustained isometric contractions, RMS changes have been attributed to the recruitment and/or firing rate of

MU, where it has been shown that RMS increased over a wide range of submaximal fatiguing contractions (Crenshaw et al., 1997). **Current, prevalent measures of muscle fatigue include: MdPF, MPF, IEMG, and RMS. Both, MdPF and MPF measure shifts in the PSDF, however studies have shown that there is almost no difference in their measures of fatigue. IEMG and RMS measure changes in the EMG power spectrum, where during fatiguing submaximal contractions there tends to be an increase in amplitude.**

1.5.9 Conclusion.

In conclusion, EMG is a measure of MUAP, which is a summation of MAP in the vicinity of an electrode. There are also a number of factors that play a deterministic role in the information contained within the signal. In regards to fatigue, both muscular fatigue and mechanical fatigue will cause changes to the EMG signal. These changes in the signal correspond to EMG power spectrum shifts, resulting in a decrease in high-frequency components and shifts to higher amplitudes. As such, this change is generally attributed to a decrease in conduction velocity of the depolarization wave, a decrease in activity of larger and faster MU, and a change to MU firing synchronously. Notable measures used to evaluate these changes include MdPF, MPF, and RMS.

Chapter 2, Methods

2.1 Participants

York Universities' office of research ethics reviewed and approved all facets of this study (e2017-306). A total of twenty-one participants were recruited for the study, where eleven were female and ten were male. Participants' anthropometric and demographic information was presented in table 1. Two physicians, one firefighter, one paramedic, four athletic therapists, one lifeguard, and twelve civilians comprised the participant pool. Based on the participants' certification the physicians were further classified as healthcare providers, paramedic and firefighter as first responders, athletic therapists and a single civilian as first aid first responders, whereas lastly one lifeguard and eleven civilians were classified as standard first aiders (table 2).

Table 1: Participants' anthropometric and demographic information.

Sex	N	Age (years)	±1 S.D	Height (cm)	±1 S.D	Weight (kg)	±1 S.D	BMI (kg/m^2)	±1 S.D	Waist Height (cm)	±1 S.D	Finger Height (cm)	±1 S.D	Regular Smoker	Weekly Exercise	Hand on manikin
Male	10	25.8	5.07	174.46	9.31	77.5	16.23	25.38	4.62	100.55	6.38	68.63	5.68	2	3-4 Days (8) 5+ Days (2)	Right (5) Left (5)
Female	11	25.27	3.5	167.31	5.04	64.62	8.82	23.08	2.87	95.43	4.33	66.32	2.4	0	1-2 Days (5) 3-4 Days (5) 5+ Days(1)	Right (9) Left (2)
Total	21	25.52	4.21	170.71	8.07	70.75	14.17	24.17	3.89	97.87	5.88	67.42	4.33	2	1-2 Days (5) 3-4 Days (13) 5+ Days (3)	Right (14) Left (7)

Table 2: Participants' occupations and further classifications within the study.

	Occupation						Classification				Certification	
Sex	Physician	Paramedic	Firefighter	Athletic Therapist	Lifeguard	Civilian	Health Care Provider	First Responder	First Responder (first aid)	Standard First Aider	CPR-C	HCP
Male	0	1	1	1	0	7	0	2	2	6	7	3
Female	2	0	0	3	1	5	2	0	3	6	6	5
Total	2	1	1	4	1	12	2	2	5	12	13	8

2.1.1 Participant exclusion criteria.

All participants passed the exclusion criteria, which included: any musculoskeletal injuries within the past year, receiving musculoskeletal rehabilitation up to six months prior to the start of the study and presence of any diseases/injury that may influence musculoskeletal movement or discomfort. All participants noted that previous to the current study, a physician and/or qualified medical/exercise professional had not advised them against the completion of moderate to vigorous intensity exercise. All participants must also have held, at minimum, a valid CPR-C certification at the time of the study and present proof of certification to the investigator.

2.1.2 Participant recruitment and incentive.

All participants were recruited using a convenience sample. Based on a brief description of what the study entailed, individuals were offered an opportunity to participate in the study. Individuals, who exhibited interest in participating, were emailed further information about the study. Each participant was provided with a monetary incentive of a $10 Tim Horton's® 'TimCard', upon completion of the study.

2.2 Study Design

The study was a prospective randomized Latin square partial counterbalancing design, which was conducted in a lab environment using a Little Anne® CPR training manikin (Laerdal Medical., Stavanger, NO) and a CPRmeter 2 (Laerdal Medical., Stavanger, NO).

2.3 CPR Positions

Four CPR positions were evaluated during the study, which included: kneeling height (KH), 330 mm high (LH), finger height (FH), and waist height (WH) (fig. 1). KH

was chosen as first responders and lay rescuers commonly adopt this position while performing CPR. LH was chosen, as it represented on average the minimum stretcher height, which is generally seen during patient transport in an ambulance. FH was chosen, as it represented the lower end stretcher and/or bed height used to assess a patient and it was hypothesized that this position would produce the most effective CC. WH was chosen, as it represented the top end stretcher and/or bed height used to assess a patient and it was hypothesized that above this height compressions would be ineffective or quickly become ineffective, in addition to rescuers rapidly fatiguing.

Figure 1: Top left denotes KH. Top right denotes LH. Bottom left denotes FH. Bottom right denotes WH.

2.3.1 Isometric push and pull.

To determine muscular fatigue participants completed sub maximal isometric push/pull exercises using a custom rig (fig. 2). While kneeling participants used a Chatillon CSD200 (Ametek, Inc., Pennsylvania, USA) dynamometer to determine force exerted while pushing and pulling.

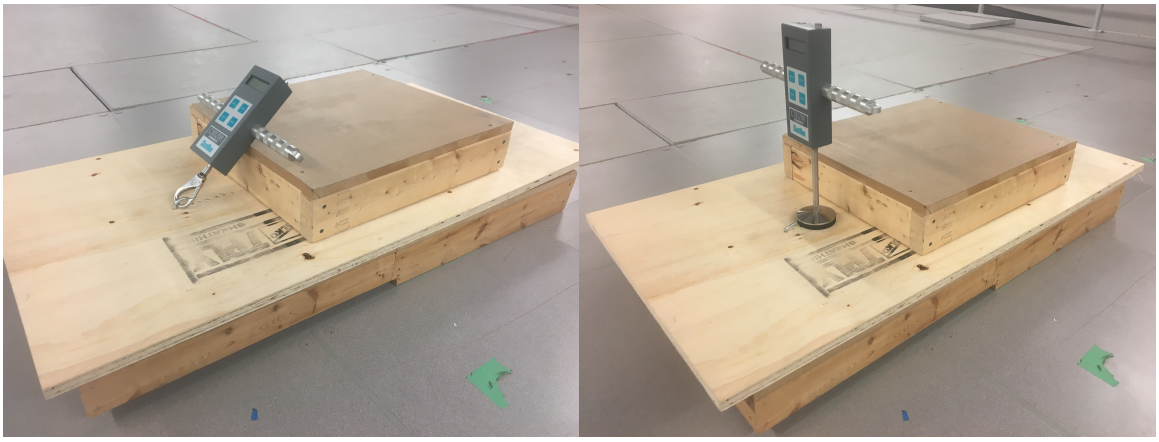

Figure 2: Kneeling rig constructed for participants to complete isometric push/pull exercises with dynamometer. Left figure is set up for pull exercises and right figure is set up for push exercises.

2.4 Collection Equipment

2.4.1 Analog to digital converter.

Kinetic and EMG analog signals were sampled and converted to digital signals using a Vicon (©Vicon Motion Systems Ltd., Denver, USA) analog to digital (A/D) board. The Vicon A/D board allowed for 64-channels of 16-bit offset binary conversions from analog sources and a 1 MΩ impedance when connected to the Vicon MX control board using a 100-way cable (see appendix F).

2.4.2 Electromyography.

2.4.2.1 AMT-8.

An AMT-8 amplifier (©Bortec Biomedical Ltd., Calgary, CA) was used to collect electrical activity of six muscles per participant (see appendix F). The signals were collected using a differential amplifier, which was set to a gain of 2000. The amplifier had a frequency response of 10 - 1000 Hz, input impedance of 10 GΩ, common mode rejection of 115 db at 60 Hz and used standard BNC connectors as the analog out. The patient unit, worn around the hip of the participant, was connected to the amplifier via a 10 m shielded patient cable. Connected to the patient unit were five APE2000 cables and one APE2000R cable. Each cable was individually taped to the participant such that cable sway was minimized.

2.4.2.2 TeleMyo 2400T G2 & 2400R G2.

A 16-channel TeleMyo 2400T G2 transmitter (Noraxon U.S.A. Inc., Arizona, USA) and 2400R analog output receiver (Noraxon U.S.A. Inc., Arizona, USA) were used to collect electrical activity of ten muscles per participant during the study (see appendix F). The signals were collected using a differential amplifier set to a sampling rate of 3000 Hz and a gain of 2000. The amplifier had an input impedance of 100 MΩ, common mode rejection of >100 db, and 16 bit resolution on all analog inputs. The EMG signal was collected using the analog output receiver, which had an input impedance of >1 MΩ and was set to a regeneration delay of 100 msec. The transmitter, which was worn around the hip of the participant, was connected to nine 2-snap/pinch active leads and one 3-snap/pinch active lead. Each cable was individually taped to the participant such that cable sway was minimized.

2.4.3 Kinematic data.

Vicon optical electronic system (©Vicon Motion Systems Ltd., Denver, USA) was used to collect kinematic data. Seven Vicon MX40 infrared cameras, mounted on tripods, encircled the capture area at varying heights (fig. 3). Each camera was no less than two meters away from the middle of the capture area and was calibrated prior to data collection to minimize movement artefacts. The following axes were defined with respect to the manikin: the z-axis represented anterior-posterior changes (global vertical), the x-axis represented superior-inferior changes, and the y-axis represented medial-lateral changes.

2.4.4 Kinetic data.

Three to four OR6-7-1000 force plates (©Advanced Mechanical Technology, Inc., Watertown US) were used depending on the CPR position, to collect kinetic data. KH had four force plates arranged in a diamond fashion (fig. 4). Three identically sized pieces of plywood (475 mm x 512 mm) were cut and placed on top of the force plates, which the participants' knee's and feet rested. A larger piece of plywood (1128 mm x 545 mm) was cut and laid on the upper most force plate, which supported the entirety of the manikin. LH, FH, and WH had three force plates arranged such that two were on the ground and one was supported by a 500lb Hydraulic lift cart (fig. 5). The force plate that rested on the hydraulic lift cart had the larger piece of plywood placed on it, which supported the manikin. As with the kinematic data the force plates axes were aligned with respect to the manikin such that the z-axis represented global vertical (anterior-posterior), the x-axis represented superior-inferior, and the y-axis represented medial-lateral changes. Three to four AMTI MSA-6 miniamps (©Advanced Mechanical Technology,

Inc., Watertown US), depending on the CPR position, were used to collect kinetic and were connected to a force plate via a 26-pin circular type connector. The miniamp allowed for an analog output range of +/-10 volts and featured a 1000 Hz low pass, 2 pole anti-aliasing filter. The miniamps were connected to the Vicon A/D board using DB25S to BNC cables.

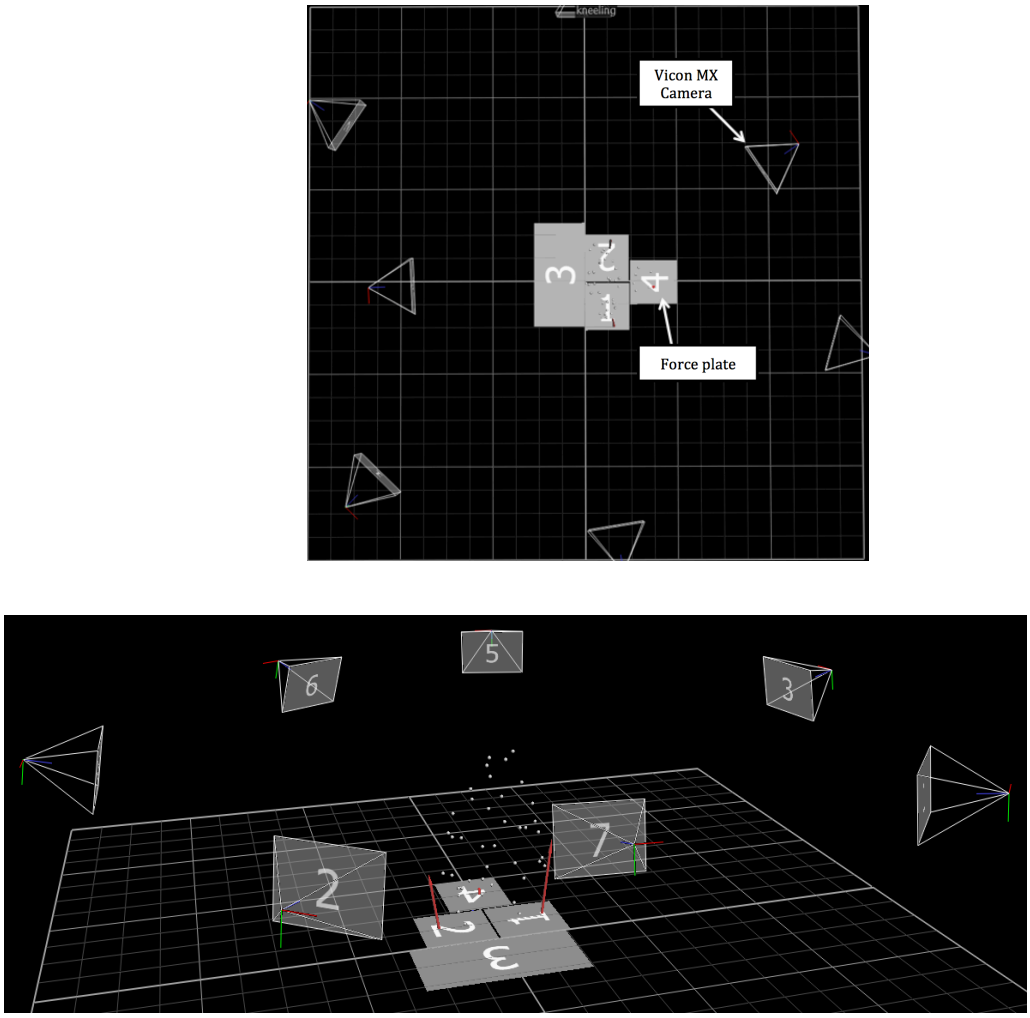

Figure 3: The top figure displays an aerial view of the locations and orientations of the Vicon cameras and force plates during KH. The bottom figure displays a side view of the locations and orientations of the Vicon cameras and force plates during KH.

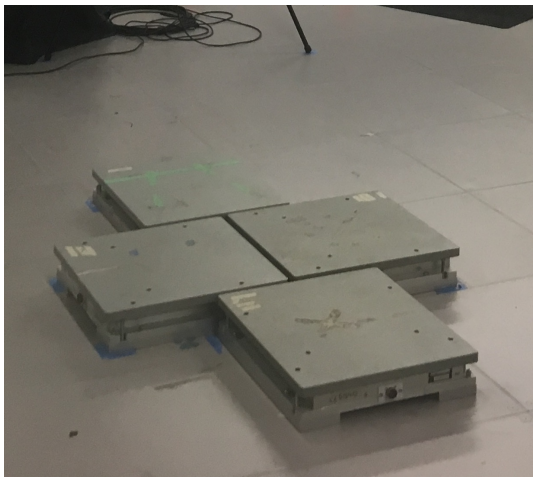

Figure 4: Force plate setup for KH.

Figure 5: Manikin, force plate, and hydraulic cart set up for LH, KH, and WH. The hydraulic cart height was adjusted to the desired height, using a foot pedal, within the CPR position.

2.4.5 Software.

Vicon Nexus software (v1.8.5) was used during data collection and data analysis. The sampling rate of the Vicon MX40 cameras was set to 100 Hz, while the sampling rate for the Vicon MX control board was set to 2400 Hz.

2.5 Electrodes and Vicon Markers

2.5.1 Surface Electrodes.

Two bipolar Ambu® BlueSensor N (©Ambu A/S, MD, USA) silver/silver chloride (Ag-AgCl) disposable rectangular electrodes (2.8 cm x 2 cm), with an interelectrode distance of no greater than 2 cm, were adhered parallel to the muscle fibres, over the muscle belly. Electrode placement sites were thoroughly cleaned using alcohol wipes and left to dry for approximately 15 seconds. Placement sites with excess hair, enough to impede the interaction of the electrode to the skin, were shaven using a disposable razor.

2.5.2 Electrode Positions.

EMG signals were collected from 6 unilateral muscles (RA, EO, internal oblique (IO), LD, thoracic erector spinae (TES), and LES). Unilateral muscles were collected on the same side of the body with which the hand was in contact with the manikin. EMG signals were also collected from 5 bi-lateral muscles (PM, TB, extensor carpi radials brevis (ECRB), flexor digitorum superficialis (FDS), and GM). Electrode locations are presented in figure 6. Specific electrode placement sites were as follows: RA, 3 cm lateral to the umbilicus (McGill et al., 1996). EO, approximately 15 cm lateral to the umbilicus (McGill et al., 1996). IO, approximately midway between the anterior superior iliac spine and symphysis pubis, above the inguinal ligament (McGill et al., 1996). LD, lateral to T9 over the muscle belly (McGill et al., 1996). TES, placed 5 cm lateral to T9 spinous process (McGill et al., 1996). LES, placed 3 cm lateral to L3 spinous process (McGill et al., 1996). PM, placed midway on a sagittal line from the point between the lateral and middle third of the clavicle to the caudal anterior axillary fold (Nieminen et al., 1993). TB, placed half way and 2 cm below the line drawn between the acromion and the

olecranon (Hermens et al., 2000). ECRB, placed 2 - 5 cm distal to the lateral epicondyle (Criswell et al., 2010; Stephan Riek et al., 2000). FDS, placed one-fourth the distance inferior to the medial humeral epicondyles on the line connecting the medial humeral epicondyles and the distal carpal sulcus (Blackwell et al., 1999; Zipp, 1982). GM, placed 50% on the line between the sacral vertebrae and the greater trochanter (Hermens et al., 2000). A reference or ground electrode was placed on the sternal end of both the right and left clavicles.

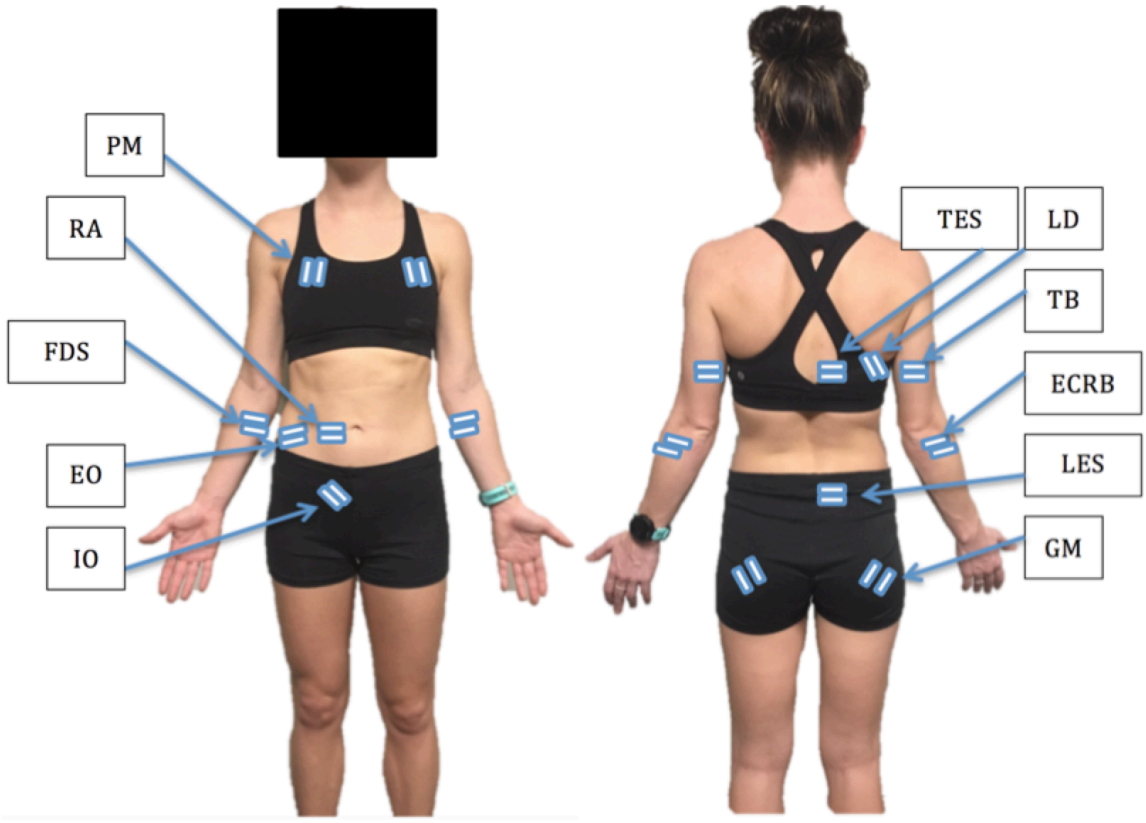

Figure 6: The white and blue bars depict the sEMG electrode placement locations and directions. Muscles collected unilaterally (RA, EO, IO, TES, LES, LD), electrodes were placed on the same side of the body with which the rescuers hand contacted the manikin. For demonstration purposes the electrodes were placed on the right side of the body.

2.5.3 Vicon markers.

Participants were fit with 43 Vicon markers according to the Vicon plug in gait model recommendations (see appendix A). In addition, the manikin was fit with six Vicon markers (fig. 7) (see appendix B)

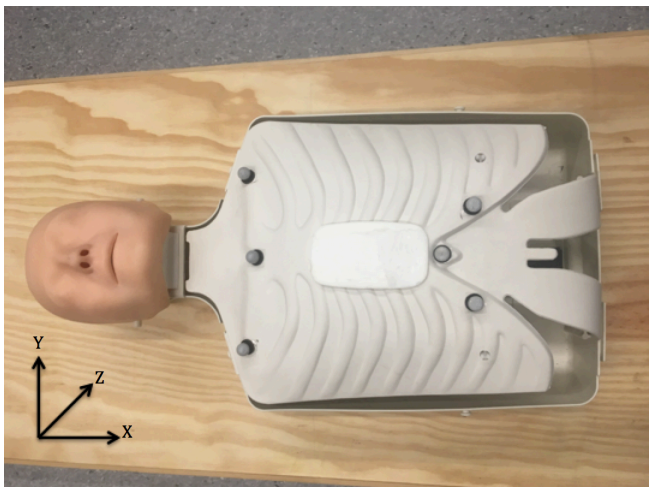

Figure 7: Reference for Cartesian coordinate system used to collect all kinematic data and Vicon marker locations on the manikin.

2.6 Maximum Voluntary Contractions

Due to the variability of EMG signals, MVC were completed to calculate a normalization coefficient. Each of the muscles evaluated had a specific isometric exercise that was resisted by the investigator. The isometric exercises were completed a minimum of two times, allowing for 15 - 30 seconds of rest between contractions. A complete description of the exercises can be found in table 3, briefly, the exercises included: back extensions, trunk flexion, lateral bends, axial twists, shoulder extensions, horizontal shoulder adductions, elbow extensions, power grasps, and hip extensions.

Table 3: Complete descriptions of the maximum voluntary isometric contraction exercises performed by all participants. Extension

Muscle	Manually Resisted Isometric Task	Reference
Rectus Abdominis, External and Internal Oblique	Resisted trunk flexion, right/left lateral bends, and right/left axial twists performed in a modified sit-up on the edge of a padded table with knees flexed to 45° and feet flat on the table.	(McGill, 1992)
Thoracic and Lumbar Erector Spinae	Resisted hanging prone trunk extension, performed on a padded table.	(McGill, 1992)
Latissimus Dorsi	Resisted shoulder extension, performed with an extended elbow, internal rotation, and 30° of abduction.	(Boettcher et al., 2008)
Pectoralis Major	Horizontal shoulder adduction performed with the shoulder in flexed to 90°, palms of the hands together, and elbows flexed to 20°.	(Boettcher et al., 2008)
Tricep Brachii	Resisted elbow extension, performed with the elbow flexed to 90° and forearm supinated to 90°.	(Dainty and Gregory, 2017)
Extensor Carpi Radialis Brevis	Maximal power grasp of a bar with wrist extension.	
Flexor Digitorum Superficialis	Maximal power grasp of a bar.	
Gluteus Maximus	Resisted hip extension, performed with the upper prone on a padded table and hips flexed to 45°.	(Rouffet and Hautier, 2008)

2.7 Spring Dynamics

The spring within the manikin was tested prior to the study using Vicon motion capture, a force plate, and custom rig. The manikin rested between a force plate and the custom rig, which had a piece of wood that spanned vertically from the sternum of the manikin to the arm of the custom rig. Three Vicon reflective markers were also attached to the piece of wood. As Vicon Nexus simultaneously collected kinetic and kinematic data the investigator fully compressed and released the spring four times using the custom rig.

2.7.1 Data Analysis.

A custom Matlab (©The MathWorks, Inc. Natick, USA) script was written to analyze the results of the spring dynamics test. First the centroid of the Vicon markers was calculated, and then the resultant force vector was calculated. The kinetic and kinematic data was then split into the compression and release phases, and subsequently

linearly interpolated between 0 – 100%. The data was then averaged across the four compressions and graphed (fig. 46).

2.8 Protocol

Upon arrival, participants were informed that they would be performing six-minutes of CPR per position using a manikin in four separate positions, in accordance to the 2015 American Heart Association (AHA) guidelines, using a feedback device. Participants then completed a consent form (see appendix E), questionnaire (see appendix C & D), and presented proof of CPR certification. Once changed into athletic clothing, participants had their height and weight measured using a mechanical scale, followed by FH and WH measurements. With participants standing upright, arms resting at the side of their body, FH was measured from the floor to the most distal part of the 3rd phalange, where as WH was measured from the floor to the iliac crest. Measurements where taken on the right and left side of the body then averaged. Participants were then fit with a Bortec patient unit, TeleMyo 2400T G2, along with EMG electrodes as outlined in section 2.4.1. Once the electrodes and cables were secured the participant they completed a quiet lying trial. The trial required the participant to lie supine and relaxed on a padded table for two-minutes. Following the quiet trial MVC exercises were completed as outlined in section 2.5. Once the MVC exercises were completed Vicon markers were attached to the participant with use of double-sided tape (see appendix A).

Prior to data collection participants were provided with instructions on how to operate the CPRMeter 2 followed by a maximum of five-minutes to practice with the unit, which provided real-time visual feedback during CPR (fig.8). Feedback included: CC depth, CC rate, chest recoil, and compression counting. Once participants finished

practicing with the CPRMeter 2 they were provided with instructions on how to execute the sub maximal isometric push/pull exercises prior to and preceding each CPR position. The push, mimicking the compression phase of a CC, and pull, mimicking the release phase of a CC, were completed using a dynamometer, as outline in section 2.3.1. Each sub maximal exercise was held for a minimum of five-seconds at approximately 200 N lower than the participants' maximum force and was completed immediately before and immediately after each CPR position, with a maximum of 20-seconds between the CPR position and sub maximal trials.

Figure 8: The CPRmeter 2 used by participants during the study. The digital display provided participants with CC counts, CC depth, CC rate, and recoil measures.

As twenty-one participants completed the study, complete counterbalancing was not possible; therefore CPR positions were partially counterbalanced using a Latin square design. The Latin square ensured participants completed each CPR position once and the position order was different between participant subgroups. Participants were randomly assigned into four subgroups and the four subgroups were then randomly assigned to four position orders.

During KH participants were instructed to kneel with their right knee on the force plate labeled “right” and their left knee on the force plate labeled “left”. The participants were then instructed to place both feet on the force plate directly behind them. Once the participants were situated the investigator would adjust the manikin to the participants’ reach. While, during LH, FH, and WH participants were instructed to stand on two force plates, placing their right foot on the force plate labeled “right” and their left foot on the force plate labeled “left”. The manikin was placed on a force plate that rested on a 500lb hydraulic cart (fig. 5). The height of the cart was adjusted depending on the position CPR was performed in. During LH the top of the cart was adjusted to 330 mm, while during FH and WH the top of the CPRmeter 2 was adjusted to the participants FH and WH measurements, respectively.

Participants were provided with the following instructions prior to each CPR trial: inform the investigator when they felt fatigued during each CPR position, perform C:V at a ratio of 30:2, CC at a rate of 100-120 bpm, compress the chest a minimum of 5 cm to a maximum of 6 cm, allow for full chest recoil, and perform ventilations with a pocket mask. Participants were also reminded to complete 3 additional CC at the start of each CPR position, as the additional compressions would be used as padding points during data analysis. Data collection and the timer began simultaneously once the participants began CPR. Immediately following the trial sub maximal push/pull exercises were completed (section 2.3.1). Following the submaximal exercises participants completed a RPE and fatigue questionnaire based on the CPR trial (see appendix C & D). Participants were then provided with 15 - 30 minute rest between CPR positions, dependent on their perceived level of fatigue.

2.8.1 Protocol timeline.

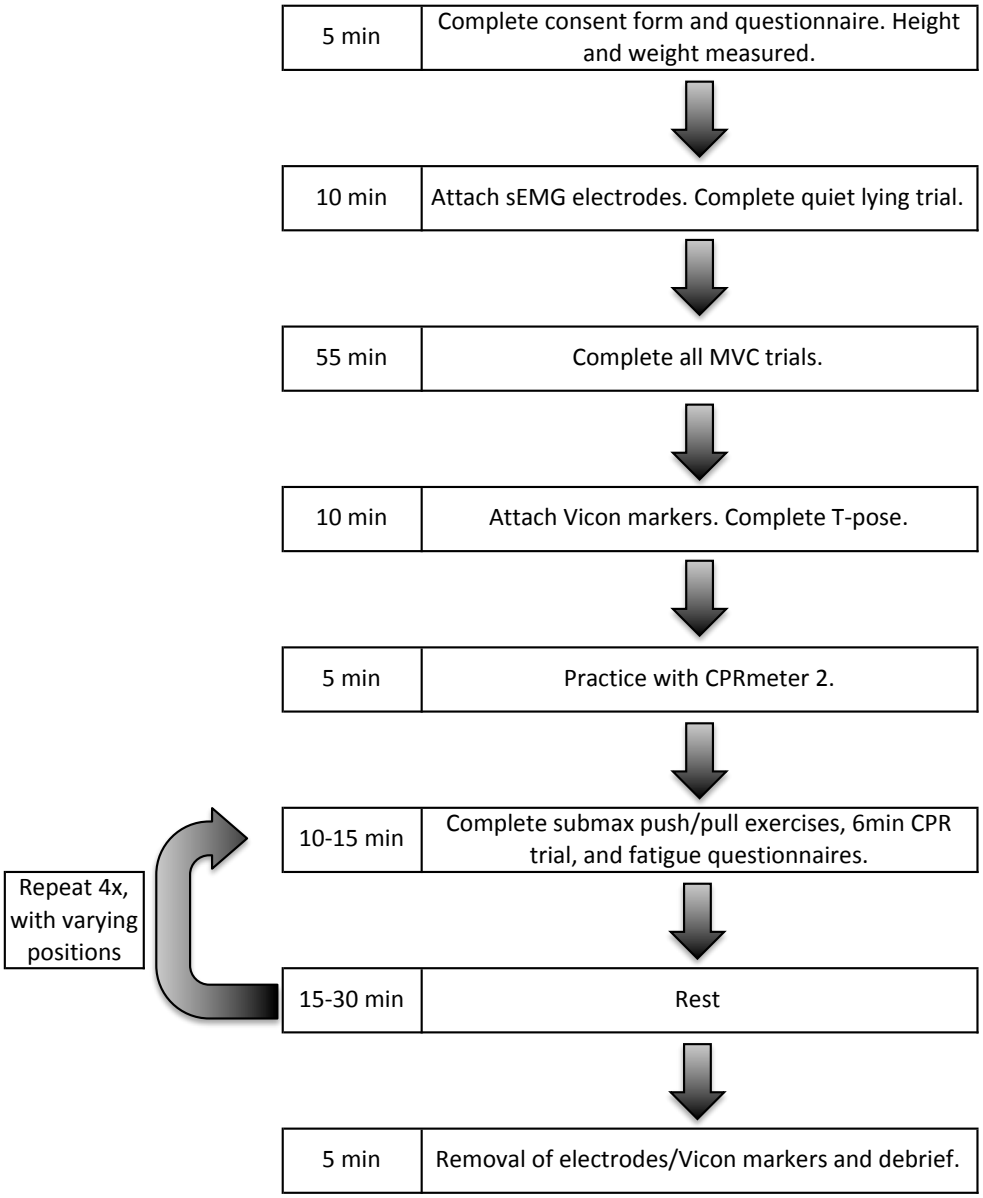

Figure 9: Study protocol and timeline.

2.9 Data Analysis

2.9.1 Kinetic data.

Data was collected at a sampling rate of 2400 Hz using Vicon Nexus (v1.8.5) for the entirety of each CPR position. Participants' CC force data was processed using a custom MatLab script. Start/end times and peak force of CC were calculated using this

data. The script first calculated resultant force using the x, y, and z-axis. The start and end time per CC were calculated by identifying the index of minimal force prior to a C and index of minimal force after the CC. Each subsequent start time became the end time for the previous CC in that cycle, ensuring a continuous signal. Peak force per CC was then calculated by identifying the maximum force between the start and end time per CC. Forces equal to 0 N lasting longer than two seconds denoted ventilations performed by the participants. Furthermore, kinetic data was ensemble averaged using a custom MatLab script, which linearly interpolated the data using the Matlab function interp1 and windowing the data from 0-100%.

In further analysis of CC force an amplitude probability distribution function (APDF) was calculated to determine the 10^{th}, 50^{th}, and 90^{th} percentile values of CC force during CC cycles. CC force during ventilations was not evaluated.

2.9.2 Chest compression rate.

A custom Matlab script was written to calculate the rate at which CC were completed. The CC start and end times (section 2.8.1) were used to identify rate. First the end time was subtracted from the start time, which calculated the total time per CC in frames. Total time was then divided by the sampling frequency, which calculated a total CC time in seconds. To convert time into BPM, 60 seconds was divided by total CC time and then averaged across each CC cycle, to calculate CC rate per cycle.

2.9.3 Kinematic data.

A custom model was created to represent the manikins' chest during CC. The three superior markers (STR, RCST, LCST) created a segment labeled 'upper sternum' and the three inferior markers (XYP, RRIB, LRIB) created a segment labeled 'lower

sternum' (see appendix B). All marker trajectories were reviewed per CPR position, if any gaps were identified the pattern fill option was used to correct the gap. Marker trajectories were then exported from Vicon Nexus via a tab delineated text file.

Trajectory data of the markers was analyzed using a custom MatLab script. First, the centroids of both segments were calculated across all three axes. The hand position was then calculated to be located one-fourth the distance away from the 'lower sternum' segment. A distance of one-fourth was chosen as the distance was measured to represent the point on the sternum where the CPRmeter 2 was attached. The resultant vector of the marker trajectories was then calculated using the CPRmeter 2 location. The general centroid equation is listed in Eq.1.

Eq.1: General 3-dimensional centroid equation. x_n = x coordinate of the vertices, y_n = y coordinate of the vertices, z_n = z coordinate of the vertices.

$$C = (\frac{x1 + x2 + x3}{3}), (\frac{y1 + y2 + y3}{3}), (\frac{z1 + z2 + z3}{3})$$

2.9.3.1 Zero position, compression depth, and chest recoil.

To correct for any hydraulic cylinder drift of the cart during the trial a moving zero position of the manikins' chest wall was calculated. First the middle time point of each pause (ventilation) was identified. A one second time period, 0.5-seconds prior to and succeeding the middle time point was captured. The segment trajectory for each one-second-time period was then averaged to identify a zero position of the manikins' chest wall. To calculate CC depth the start and end times (section 2.8.1) were used to identify each CC. The maximum CC depth was then subtracted from the minimum CC depth, which calculated total CC depth. Chest recoil was calculated using the zero position prior to each cycle of CC. Zero position was subtracted from the minimum CC depth.

2.9.3.2 Change in chest wall angle.

Changes in chest wall angle were calculated using the vector created between the 'upper sternum' and 'lower sternum' segments. The two vectors were calculated using the trajectory data at the start of a CC and maximum depth of a CC. A change in angle, in the sagittal plane, with reference to the manikin, was calculated using the dot product and vector magnitudes. Therefore, two-dimensional measurements, z-axis (anterior-posterior) and x-axis (superior-inferior) were used to calculate changes in angle of the manikins' chest.

Eq.2: General equation to calculate two-dimensional angle between two vectors. a = vector of a, b = vector of b, ||a|| = magnitude of vector a, ||b|| = magnitude of vector b.

$$\cos(\theta) = \frac{a \cdot b}{||a||\,||b||}$$

2.9.4 Electromyography.

Data was collected at a sampling rate of 2400 Hz for the entirety of each CPR position and a custom MatLab script was written to analyze the data.

2.9.4.1 Time shift, high-pass filter, and bias removal.

As the Noraxon receiver incurred a regeneration delay of 100 msec (section 2.3.3.2), 240 data points were removed from the start of each signal collected using the Noraxon receiver, to align the signals in time with the AMT-8 amplifier. As trunk musculature was contaminated by electrical activity of the heart (Drake and Callaghan, 2006), a Butterworth dual-pass, high-pass filter, with a 30 Hz cut-off frequency and 40 db/decade roll off was applied to all EMG signals, to attenuate electrocardiography (ECG) contamination (Drake and Callaghan, 2006) (see appendix G). Once the high-pass filter was applied the quiet lying trial was averaged across each muscle, this identified the

DC component or bias per muscle. The bias was then subtracted throughout all CPR positions and MVC trials, per muscle.

2.9.4.2 Linear envelope.

CPR position and MVC data was first full-wave rectified. A Butterworth single-pass, low-pass filter with a 4 Hz cut-off frequency and 40 db/decade roll off was then applied to all EMG data. The padding points at the start of each CPR position (section 2.7) were then removed from the signals. To normalize the data, the maximum value of each MVC exercise was identified per muscle. Each time point during the CPR positions was then divided by the normalization coefficient based on their respective muscle and multiplied by 100.

2.9.4.3 Ensemble average.

A custom MatLab script was written to calculate the rubber band averages using the linear envelope of the EMG data per CC. Using the start and end times of each CC (section 2.8.1) EMG data was linearly interpolated using the Matlab function interp1, windowing the data from 0 - 100%.

Eq.3: General linear interpolation equation. x = specified value of vector x, x_1 = next lowest value to x, x_2 = next highest value to x, y_1 = next lowest value to x, y_2 = next highest value to x.

$$y = f(x) = y_1 + \frac{(x - x_1)}{(x_2 - x_1)}(y_2 - y_1)$$

2.9.4.4 Amplitude probability distribution function.

A custom Matlab script was written to calculate the APDF using the linear envelope of the EMG data. The APDF was calculated for the entire trial including ventilations. The 10^{th}, 50^{th}, and 90^{th} percentiles were calculated, using the Matlab prctile function. The prctile function sorted EMG data in ascending order and then the sorted

values were calculated as percentiles (Eq.4). Percentiles that fell between 100(0.5/n) and 100([i-0.5]/n) were linearly interpolated.

Eq.4: General percentile equation. i = indices of the i^{th} location, n = number of samples.

$$P_i = 100\frac{i-0.5}{n}$$

2.9.4.5 Cross-correlation.

A custom Matlab script was written to calculate the lag times between hand force and EMG data. The cross-correlation analyses calculates how well two given signals are correlated over time (Winter, 2009), and the Matlab xcorr function was used in the script. A cross-correlation (Eq.5) was calculated across CC cycles using hand force data and the linear envelope of EMG. The time lag was identified as the maximum value of the cross-correlation sequence. To convert the lag delay to time delay, the lag delay was divided by the sampling frequency (2400 Hz).

Eq.5: General cross-correlation equation. N = number of samples, τ = phase shift, x = vector, y = vector.

$$R_{xy}(\tau) = \frac{\frac{1}{N}\sum_{N}^{n=1}[(x(n)-\bar{x})(y(n+\tau)-\bar{y})]}{\frac{1}{N}\sum_{N}^{n=1}(x(n)-\bar{x})(y(n)-\bar{y})}$$

2.9.4.6 Mean power frequency and root mean squared.

A custom Matlab script was written to calculate MPF and RMS values of the submaximal push/pull exercises (section 2.3.1). To calculate MPF, Matlabs' meanfreq function was used and set to a sampling frequency of 2400 Hz in conjunction with a frequency range of 10 - 250 Hz (Winter, 2009). The meanfreq function calculates a discrete Fourier transform (DFT) using a FFT algorithm, followed by calculating the weighted average frequency across the defined EMG power spectrum (Eq.6)

(Phinyomark et al., 2012). Matlabs' RMS function (Eq.7) was used to calculate the RMS value of the normalized EMG values.

Eq.6: General mean power frequency (MPF) equation. x_j = frequency value at bin j, p_j = EMG power spectrum at bin j, M = length of frequency bin.

$$f(x) = \frac{\sum_{j=1}^{M} x_j \cdot P_j}{\sum_{j=1}^{M} P_j}$$

Eq.7: General root mean squared (RMS) equation. x_n = value at n^{th} location, N = number of samples.

$$X_{RMS} = \sqrt{\frac{1}{N}\sum_{n=1}^{N} |x_n|^2}$$

2.10 Statistical Analysis

All statistical tests were completed using statistical package for the social sciences (SPSS) version 23 (IBM Corporation, Armonk, US) with a statistical significance level of $p \leq 0.05$.

2.10.1 CPR Measures.

A series of repeated measures analysis of variance (anova) were conducted to determine the effect of CPR position (KH, LH, FH, WH) on the dependent variables CC force, CC rate, chest angle, CC depth, and chest recoil.

A series of repeated measures anovas were conducted to determine the interaction effect of CPR position (KH, LH, FH, WH) and sex on the dependent variables CC force, CC rate, chest angle, CC depth, and chest recoil.

2.10.2 Electromyography.

A series of repeated measures anovas were conducted to determine the effect of CPR position (KH, LH, FH, WH) on the dependent variables 90th percentile, 10th percentile, and time lag of the muscles.

A series of repeated measures anovas were conducted to determine the interaction effect of CPR position (KH, LH, FH, WH) and sex on the dependent variables 90th percentile, 10th percentile, and time lag of the muscles.

2.10.2.1 Mean power frequency and RMS.

Paired-samples t-tests were conducted comparing the MPF and normalized RMS results of the submaximal isometric push/pull exercises of each muscle prior to and succeeding each CPR position.

2.10.3 Change of Rate.

A linear regression analysis was completed correlating CC force, CC depth, CC rate, chest recoil, change in chest wall angle, 90th percentile EMG values, and 10th percentile EMG values to CC cycles per participant. The calculated slopes and intercepts were then used to extrapolate values at cycle one and twenty for all dependent variables per participant.

A series of repeated measures anovas were conducted to determine the effect of CPR position (KH, LH, FH, WH) on the dependent variables slope of CC force, CC depth, CC rate, chest recoil, change in chest wall angle, 90th percentile EMG values, and 10th percentile EMG values.

Paired-samples t-tests were conducted comparing the results of the extrapolated cycle one and cycle twenty values of CC force, CC depth, CC rate, chest recoil, change in

chest wall angle, 90th percentile EMG values, and 10th percentile EMG values across all CPR position.

2.10.4 Self-Reported Statistics.

A series of repeated measures anovas were conducted to determine the effect of CPR position (KH, LH, FH, WH) on the dependent variables self-reported fatigue time and RPE.

Chapter 3, Results

3.1 Fatigue

3.1.1 MPF & RMS of pre/post EMG.

In evaluating the isometric push/pull exercises, four, six, four, and nine muscles displayed a significant decrease in MPF during KH, LH, FH, and WH, respectively, which can be found in tables 4 & 5 (fig. 10 & 11). Of particular note, during the push exercises, the right TB significantly dropped in MPF during all positions except WH, while the left TB significantly dropped in MPF during all positions. Furthermore, the LES and TES significantly dropped in MPF during FH and WH. Additionally, during the pull exercises, the TES significantly dropped in MPF within LH, while the RA significantly dropped in MPF within WH.

In further evaluation of the isometric push/pull exercises, four, three, and one muscle were evaluated to have a significant change in amplitude (RMS) during KH, LH, and WH, respectively, which can be found in tables 6 & 7 (fig. 12 & 13). Of particular note, during the pull exercises, the right ECRB displayed a significant increase in amplitude during LH.

Of the male participants two, two, one, and nine muscles displayed significant differences in MPF during KH, LH, FH, and WH, respectively. The push phase of KH displayed a significant decrease in frequency of the EO 55.4 – 50.3 Hz ($t(9)=2.3, p=.046$), while the pull phase displayed a significant decrease in frequency of the TES 71.7 – 69.1 Hz ($t(9)=2.79, p=.021$). The push phase of LH displayed a significant increase in frequency of the right ECRB 118.5 – 124.6 Hz ($t(9)=-3, p=.014$), while there was a significant decrease in frequency of the right GM 67.5 – 60.5 Hz ($t(9)=2.8, p=.024$). The

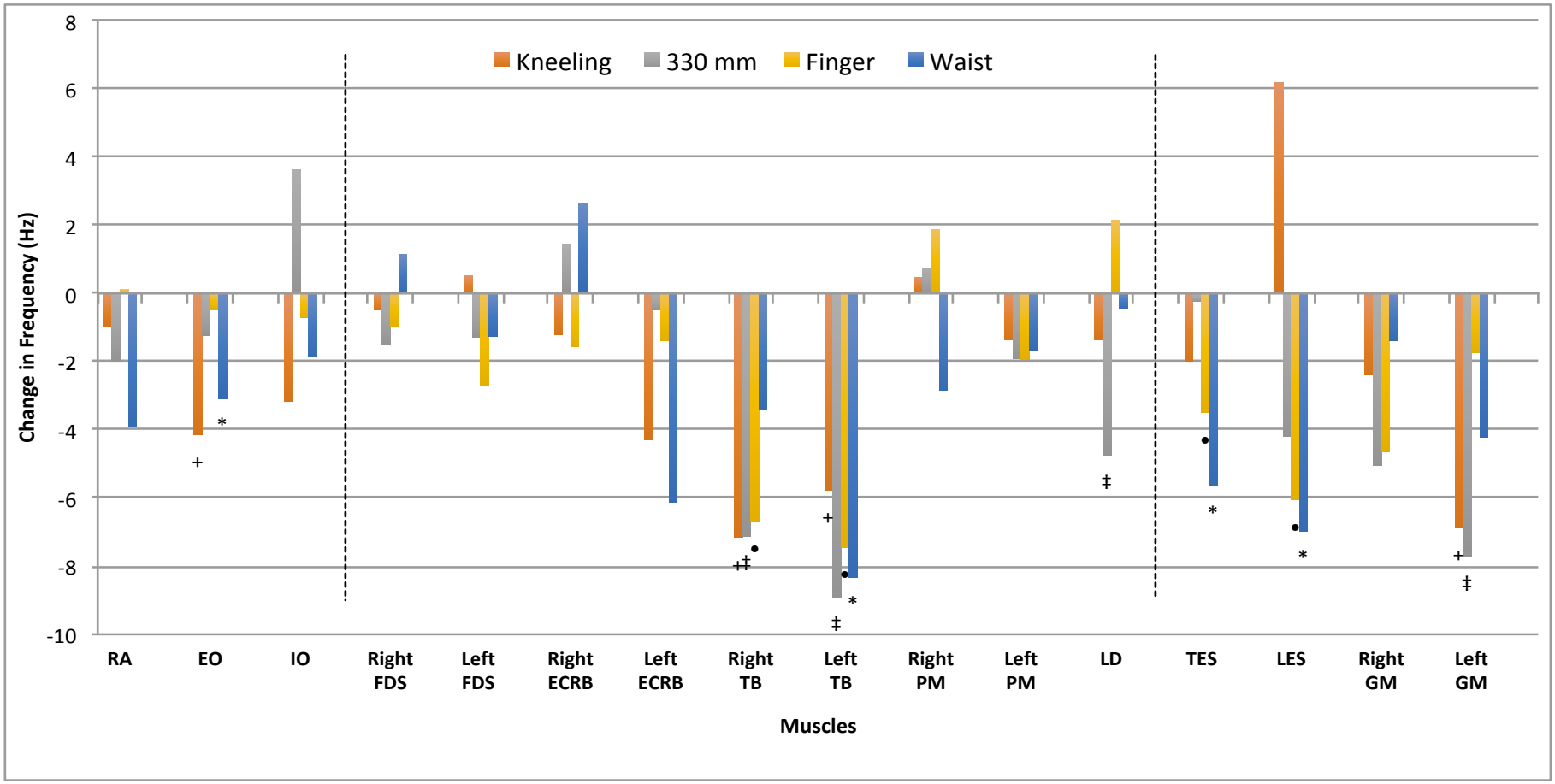

Figure 10: Magnitude and direction of the difference in MPF from pre to post isometric push exercises. Negative values denote a decrease in frequency from pre to post isometric exercises and positive values denote an increase in frequency from pre to post isometric exercises. Dashed vertical lines split the muscles into 3 groupings, CC initiators (left), upper limb stabilizers (centre), and CC terminators (right). + Indicates a significant result ($p \leq 0.05$) during KH, ‡ indicates a significant results ($p \leq 0.05$) during LH, • indicates a significant result ($p \leq 0.05$) during FH, * indicates a significant results ($p \leq 0.05$) during WH.

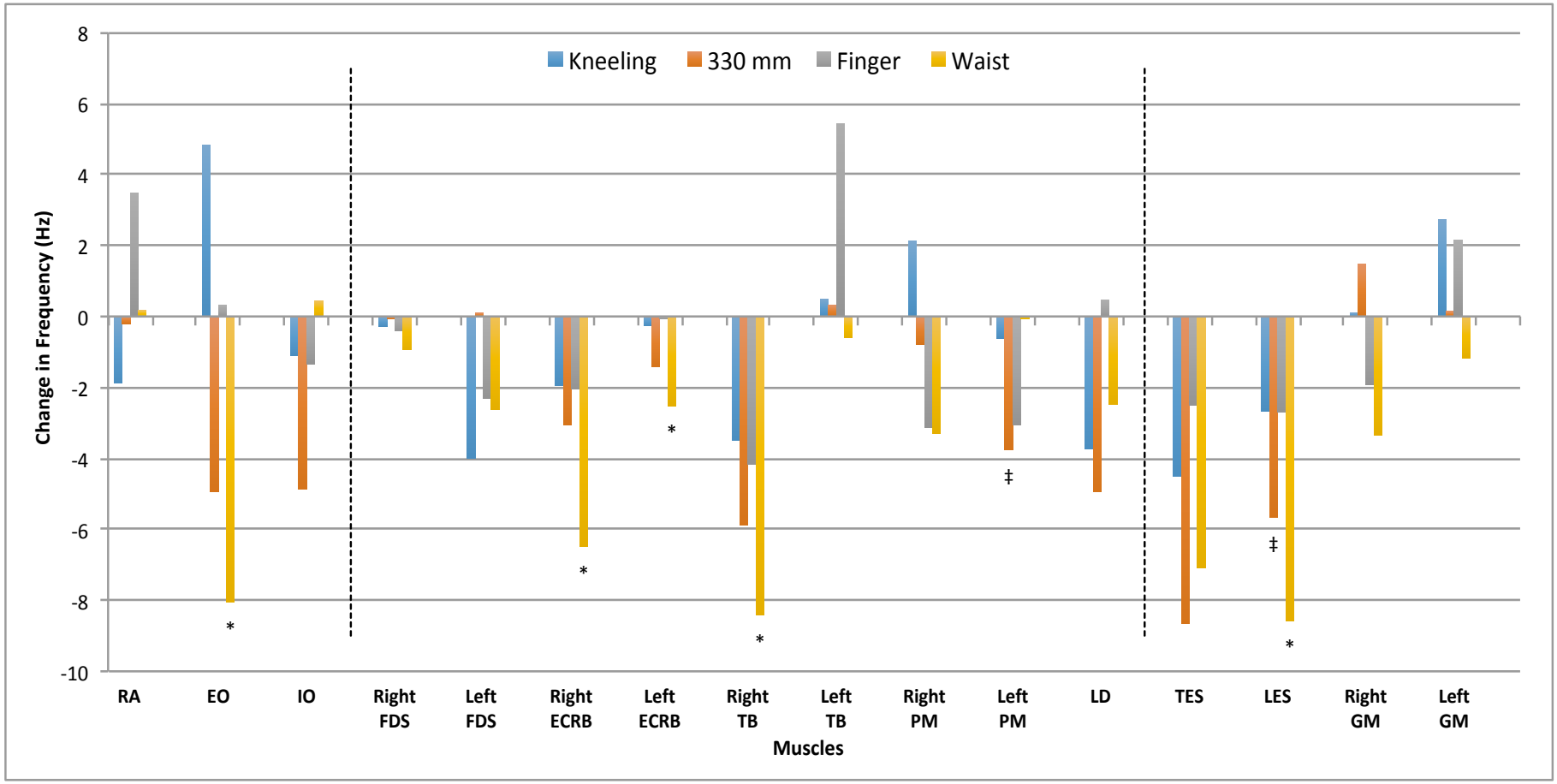

Figure 11: Magnitude and direction of the difference in MPF from pre to post isometric pull exercises. Negative values denote a decrease in frequency from pre to post isometric exercises and positive values denote an increase in frequency from pre to post isometric exercises. Dashed vertical lines split the muscles into 3 groupings, CC initiators (left), upper limb stabilizers (centre), and CC terminators (right). + Indicates a significant result ($p \leq 0.05$) during KH, ‡ indicates a significant results ($p \leq 0.05$) during LH, • indicates a significant result ($p \leq 0.05$) during FH, * indicates a significant results ($p \leq 0.05$) during WH.

Table 4: Statistical results of the paired-samples T-tests comparing MPF of the pre to post isometric push exercises per muscle and CPR position. * indicates a significant result ($p \leq 0.05$).

		Kneeling					330					Finger					Waist				
Muscle	**Timing**	**Mean**	**Std. Dev.**	**df**	**t-value**	**P-value**	**Mean**	**Std. Dev.**	**df**	**t-value**	**P-value**	**Mean**	**Std. Dev.**	**df**	**t-value**	**P-value**	**Mean**	**Std. Dev.**	**df**	**t-vaule**	**P-value**
Right FDS	Pre	103.60	13.54	20	0.23	0.819	104.71	8.67	20	0.929	0.364	103.50	11.50	20	0.64	0.529	102.51	8.49	19	-0.687	0.5
	Post	103.11	9.68				103.19	9.33				102.53	10.10				103.66	10.04			
Right PM	Pre	68.02	6.26	20	-0.26	0.799	67.22	6.76	20	-0.591	0.561	67.38	7.55	20	-2.04	0.054	70.42	7.61	19	1.291	0.212
	Post	68.49	10.01				67.96	7.89				69.24	8.52				67.57	8.22			
Right TB	Pre	123.36	16.94	20	2.49	0.022 *	120.74	11.15	20	2.337	0.03 *	122.61	15.20	20	2.92	0.008 *	118.76	12.34	19	1.104	0.283
	Post	116.19	17.19				113.62	16.87				115.91	15.41				115.37	17.20			
LES	Pre	88.71	31.34	20	-1.27	0.218	87.56	26.53	20	1.832	0.082	94.49	31.34	20	2.35	0.029 *	90.59	28.47	19	2.805	0.011 *
	Post	94.90	33.42				83.35	28.24				88.42	31.34				83.62	30.05			
Recrb	Pre	115.52	19.21	20	0.45	0.656	116.16	18.93	20	-0.578	0.569	117.08	16.38	20	0.65	0.526	113.60	15.94	19	-1.04	0.311
	Post	114.32	17.33				117.60	17.14				115.52	19.51				116.25	14.39			
TES	Pre	74.59	12.37	20	0.82	0.422	75.62	15.13	20	0.109	0.914	75.67	13.48	20	2.72	0.013 *	77.25	16.08	19	3.592	0.002 *
	Post	72.61	16.19				75.38	13.83				72.17	14.72				71.59	12.41			
Left PM	Pre	44.31	6.84	20	1.03	0.316	43.90	6.71	18	1.45	0.164	43.15	7.42	18	0.85	0.407	44.66	9.20	18	1.247	0.228
	Post	42.94	8.34				42.00	6.48				41.22	6.85				43.00	8.54			
Left FDS	Pre	80.18	12.58	20	-0.38	0.706	80.58	11.46	18	0.716	0.483	80.43	15.11	18	1.09	0.292	80.70	11.06	18	0.688	0.5
	Post	80.69	13.11				79.31	12.82				77.71	13.41				79.44	12.80			
RA	Pre	56.66	14.74	20	0.48	0.64	60.35	16.46	18	0.787	0.442	53.31	10.49	18	-0.05	0.961	59.01	12.36	18	1.033	0.315
	Post	55.70	17.71				58.37	19.40				53.43	13.88				55.09	18.59			
EO	Pre	52.24	10.71	20	2.81	0.011 *	48.60	10.75	18	0.69	0.499	46.58	10.63	18	0.23	0.823	51.89	13.47	18	2.28	0.035 *
	Post	48.10	8.00				47.38	10.04				46.10	10.01				48.80	10.62			
IO	Pre	59.15	21.28	20	1.39	0.179	54.55	15.74	18	-1.515	0.147	59.04	19.07	18	0.17	0.866	62.85	21.99	18	0.614	0.547
	Post	55.99	21.23				58.17	18.66				58.33	24.60				61.02	23.00			
LD	Pre	58.04	15.54	20	0.64	0.531	62.26	18.03	18	2.556	0.02 *	56.51	16.71	18	-0.71	0.487	59.29	16.07	18	0.407	0.689
	Post	56.67	14.62				57.51	13.90				58.65	16.42				58.83	17.14			
Left ECRB	Pre	91.48	18.56	20	1.66	0.113	90.69	16.30	18	0.151	0.882	91.39	17.50	18	0.42	0.681	92.51	17.49	18	2.064	0.054
	Post	87.18	18.88				90.20	14.35				90.01	20.46				86.39	17.87			
Left TRI	Pre	97.32	17.72	20	2.11	0.047 *	99.45	19.26	18	3.51	0.003 *	97.05	17.95	18	3.90	0.001 *	95.81	16.65	18	3.898	0.001 *
	Post	91.54	19.67				90.54	17.19				89.60	17.90				87.48	16.54			
Left GM	Pre	58.02	18.18	20	2.64	0.016 *	60.98	16.77	18	3.071	0.007 *	54.90	16.98	18	0.60	0.560	59.12	22.20	18	1.266	0.222
	Post	51.14	13.99				53.25	18.34				53.17	13.81				54.90	18.48			
R GM	Pre	59.97	19.25	19	0.77	0.451	62.30	20.13	17	1.771	0.094	61.54	21.68	17	1.24	0.233	63.79	28.13	17	0.427	0.674
	Post	57.58	23.47				57.25	23.78				56.90	16.04				62.42	27.43			

push phase of FH displayed a significant decrease in frequency of the left TB 99.9 – 94 Hz ($t(9)=2.36, p=.043$). The push phase of WH displayed a significant decrease in frequency of the LES 94.5 – 83.3 Hz ($t(9)=3, p=.013$), TES 78.7 – 72 Hz ($t(9)=2.98, p=.015$), EO 55 – 49.6 Hz ($t(9)=2.7, p=.024$), left ECRB 97 – 88.3 Hz ($t(9)=3.16, p=.012$), left TB 99.2 – 89.8 Hz ($t(9)=4.2, p=.002$), and left GM 69 – 58 Hz ($t(9)=2.5, p=.036$). Furthermore, when hand location was controlled for in evaluating the left ECRB during WH, there was a significant decrease in frequency of 12.8 Hz when the left hand made contact with the manikin ($t(4)=3.74, p=0.2$). While the pull phase of WH displayed a significant decrease in frequency of right TB 95.5 – 87.3 Hz ($t(9)=3.5, p=.006$), RA 65.7 – 54.8 Hz ($t(9)=2.3, p=.048$), and left TB 73.5 – 62.3 Hz ($t(9)=4.4, p=.002$).

In further evaluation of male participants, there were significant differences in amplitudes of five, one, and two muscles during KH, FH, and WH, respectively. The push phase of KH displayed a significant decrease in in amplitude of the right FDS 7.4 – 6.2 %MVC ($t(9)=2.3, p=.044$), right TB 5 – 3.8 %MVC ($t(9)=2.9, p=.018$), left FDS 9.2 – 7.4 %MVC ($t(9)=2.8, p=.022$), RA 7.4 – 4.5 %MVC ($t(9)=2.7, p=.023$), and IO 5.8 – 4.2 %MVC ($t(9)=2.3, p=.046$). The push phase of FH displayed a significant decrease in in amplitude of the left TB 6.6 – 5 %MVC ($t(9)=2.8, p=.021$). The push phase of WH displayed a significant decrease in in amplitude of the left FDS 10.4 - 7.2 %MVC ($t(9)=4.3, p=.002$) and a significant increase in amplitude of the left ECRB 3.3 – 4.3 %MVC ($t(9)=-2.3, p=.05$).

Of the female participants three, four, five, and two muscles had significant differences in MPF during KH, LH, FH, and WH, respectively. The push phase of KH

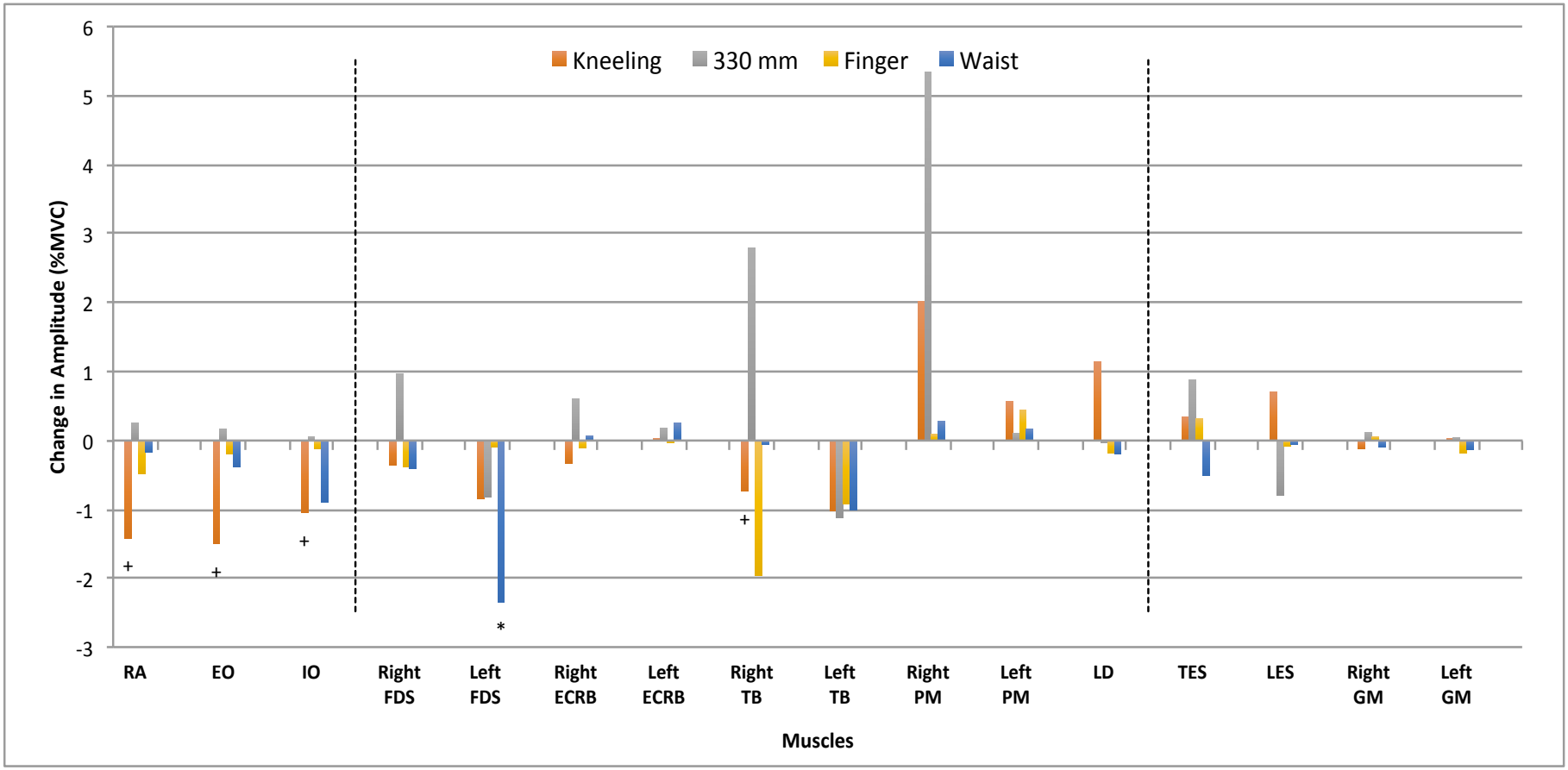

Figure 12: Magnitude and direction of the difference in normalized RMS from pre to post isometric push exercises. Negative values denote a decrease in %MVC from pre to post isometric exercises and positive values denote an increase in %MVC from pre to post isometric exercises. Dashed vertical lines split the muscles into 3 groupings, CC initiators (left), upper limb stabilizers (centre), and CC terminators (right). + Indicates a significant result ($p \leq 0.05$) during KH, ‡ indicates a significant results ($p \leq 0.05$) during LH, • indicates a significant result ($p \leq 0.05$) during FH, * indicates a significant results ($p \leq 0.05$) during WH.

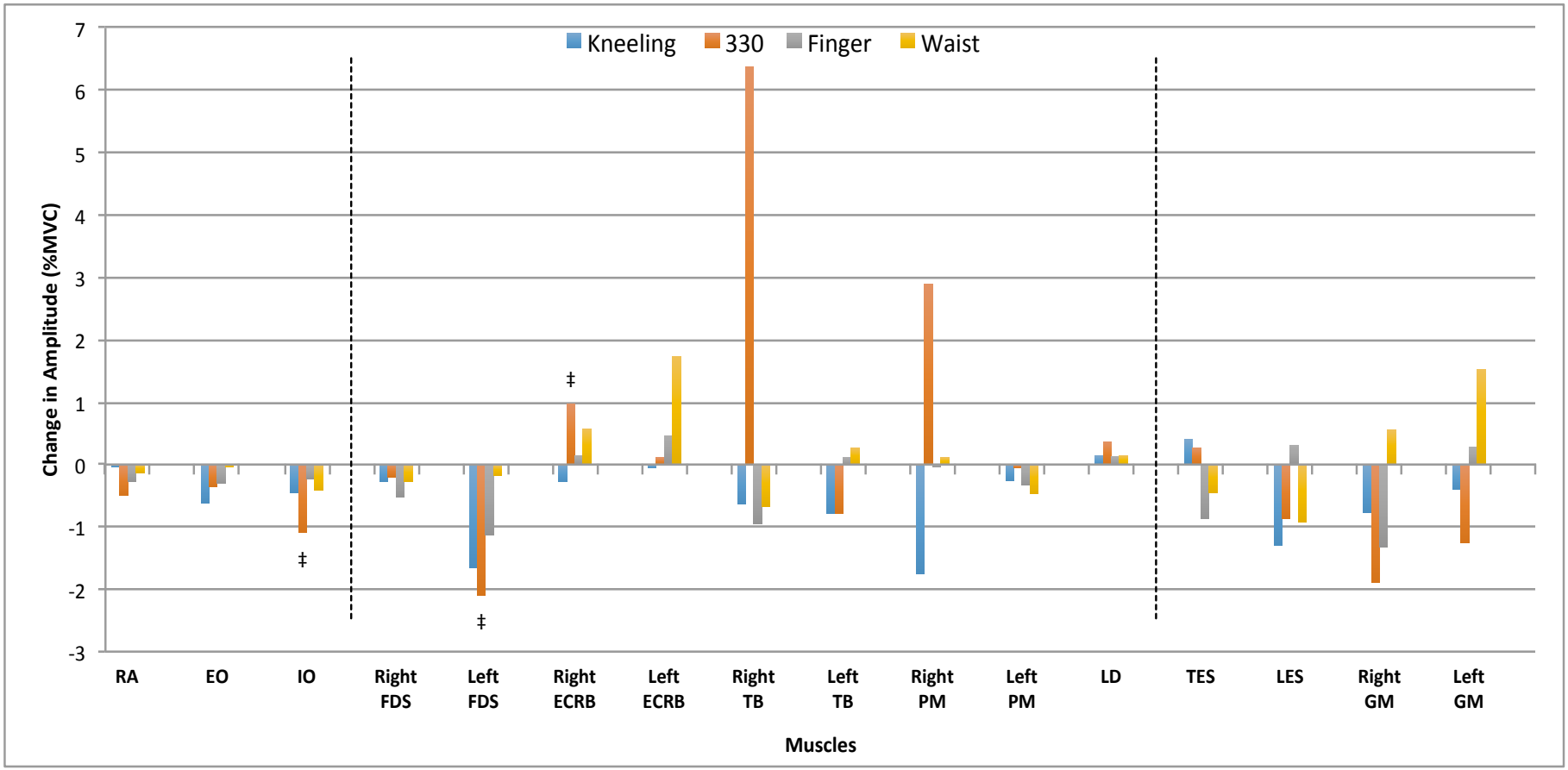

Figure 13: Magnitude and direction of the difference in normalized RMS from pre to post isometric pull exercises. Negative values denote a decrease in %MVC from pre to post isometric exercises and positive values denote an increase in %MVC from pre to post isometric exercises. Dashed vertical lines split the muscles into 3 groupings, CC initiators (left), upper limb stabilizers (centre), and CC terminators (right). + Indicates a significant result ($p \leq 0.05$) during KH, ‡ indicates a significant results ($p \leq 0.05$) during LH, • indicates a significant result ($p \leq 0.05$) during FH, * indicates a significant results ($p \leq 0.05$) during WH.

Table 6: Statistical results of the paired-samples T-tests comparing amplitude of the pre to post isometric pull exercises per muscle and CPR position. * indicates a significant result ($p \leq 0.05$).

		Kneeling					330					Finger					Waist				
Muscle	**Timing**	**Mean**	**Std. Dev.**	**df**	**t-value**	**P-value**	**Mean**	**Std. Dev.**	**df**	**t-value**	**P-value**	**Mean**	**Std. Dev.**	**df**	**t-value**	**P-value**	**Mean**	**Std. Dev.**	**df**	**t-vaule**	**P-value**
Right FDS	Pre	6.45	4.21	20	0.781	0.444	5.53	3.09	20	-1.73	0.099	6.38	3.83	20	1.071	0.297	5.73	3.00	19	1.246	0.228
	Post	6.09	3.38				6.49	3.16				6.00	3.85				5.32	2.80			
Right PM	Pre	7.45	9.41	20	-1.881	0.075	6.58	5.43	20	-1.093	0.287	7.90	11.10	20	-0.06	0.953	6.07	5.15	19	-0.433	0.67
	Post	9.47	13.64				11.93	27.07				7.99	8.58				6.36	7.06			
Right TB	Pre	4.37	2.34	20	2.513	0.021 *	6.29	8.94	20	-0.787	0.441	6.70	9.60	20	1.746	0.096	3.49	1.21	19	0.205	0.84
	Post	3.63	1.62				9.08	24.88				4.74	5.01				3.42	1.80			
LES	Pre	1.49	1.55	20	-1.87	0.076	2.68	5.03	20	0.803	0.431	2.09	2.54	20	0.337	0.74	1.68	1.72	19	0.602	0.554
	Post	2.20	2.47				1.88	2.14				2.01	2.71				1.61	1.78			
Recrb	Pre	4.23	6.91	20	0.39	0.701	3.44	4.60	20	-1.089	0.289	3.58	4.53	20	0.221	0.828	3.59	5.87	19	-0.238	0.814
	Post	3.90	3.83				4.05	5.40				3.47	5.25				3.66	6.54			
TES	Pre	5.71	6.53	20	-0.483	0.634	4.56	3.59	20	-1.065	0.3	5.32	5.64	20	-0.614	0.546	4.87	6.13	19	0.665	0.514
	Post	6.06	5.72				5.44	6.19				5.64	6.28				4.36	3.80			
Left PM	Pre	8.17	3.74	20	-0.698	0.493	7.16	2.32	18	-0.28	0.783	7.65	3.36	18	-0.418	0.681	7.27	3.61	18	-0.258	0.799
	Post	8.74	4.37				7.27	3.09				8.09	4.96				7.44	3.41			
Left FDS	Pre	8.88	4.78	20	0.968	0.344	9.30	4.76	18	1.139	0.27	9.09	5.84	18	0.113	0.911	9.23	4.26	18	3.932	0.001 *
	Post	8.04	4.08				8.49	4.08				9.00	5.14				6.88	3.67			
RA	Pre	7.37	4.73	20	2.218	0.038 *	6.24	3.94	18	-0.492	0.629	8.30	5.83	18	0.765	0.454	6.85	4.16	18	0.152	0.881
	Post	5.96	4.38				6.49	5.20				7.82	6.83				6.69	5.22			
EO	Pre	7.25	2.91	20	3.487	0.002 *	6.34	3.09	18	-0.379	0.709	7.28	4.42	18	0.36	0.723	6.74	4.03	18	0.837	0.413
	Post	5.76	2.06				6.51	3.05				7.08	4.67				6.36	2.86			
IO	Pre	6.72	3.52	20	2.651	0.015 *	7.12	4.61	18	-0.076	0.941	7.75	6.79	18	0.39	0.701	7.00	4.81	18	2.064	0.054
	Post	5.68	3.19				7.18	6.50				7.63	7.25				6.10	3.73			
LD	Pre	6.11	4.82	20	-1.194	0.246	6.41	6.50	18	0.08	0.937	6.52	5.94	18	0.294	0.772	5.76	4.51	18	0.37	0.716
	Post	7.25	6.79				6.37	5.62				6.33	4.64				5.57	4.60			
Left ECRB	Pre	3.75	4.92	20	-0.02	0.984	3.17	2.37	18	-0.401	0.693	3.38	2.27	18	0.031	0.975	3.03	2.91	18	-0.644	0.528
	Post	3.77	3.68				3.35	3.13				3.36	2.11				3.28	3.84			
Left TRI	Pre	7.23	3.94	20	1.336	0.197	6.96	2.69	18	1.898	0.074	7.33	3.44	18	2.007	0.06	6.43	2.94	18	1.431	0.17
	Post	6.22	2.88				5.84	2.91				6.40	3.62				5.42	2.58			
Left GM	Pre	2.17	2.61	20	-0.256	0.8	2.35	2.73	18	-0.485	0.633	2.53	2.80	18	1.356	0.192	2.31	2.69	18	1.479	0.157
	Post	2.18	2.50				2.39	2.56				2.34	2.53				2.17	2.44			
R GM	Pre	2.28	3.38	19	0.78	0.445	1.83	3.64	17	-1.654	0.116	2.07	3.62	17	-0.364	0.72	2.22	3.59	17	0.654	0.522
	Post	2.17	3.36				1.95	3.68				2.13	3.26				2.12	3.64			

Table 7: Statistical results of the paired-samples T-tests comparing amplitude of the pre to post isometric push exercises per muscle and CPR position. * indicates a significant result ($p \leq 0.05$).

		Kneeling					330					Finger					Waist				
Muscle	**Timing**	**Mean**	**Std. Dev.**	**df**	**t-value**	**P-value**	**Mean**	**Std. Dev.**	**df**	**t-value**	**P-value**	**Mean**	**Std. Dev.**	**df**	**t-value**	**P-value**	**Mean**	**Std. Dev.**	**df**	**t-vaule**	**P-value**
Right FDS	Pre	10.20	7.26	20	0.415	0.683	12.56	11.31	20	0.134	0.895	10.79	7.69	20	0.742	0.467	9.38	8.08	20	0.486	0.632
	Post	9.92	8.07				12.36	11.79				10.27	9.03				9.11	7.04			
Right PM	Pre	4.69	6.14	20	1.792	0.088	4.21	6.07	20	-0.929	0.364	3.13	4.88	20	0.079	0.938	3.12	5.40	20	-0.352	0.728
	Post	2.94	4.07				7.11	19.95				3.10	3.98				3.24	6.00			
Right TB	Pre	5.23	4.67	20	0.9	0.379	9.93	19.86	20	-0.95	0.353	8.36	16.92	20	0.763	0.455	4.99	4.29	20	0.962	0.348
	Post	4.60	3.97				16.31	50.35				7.40	11.87				4.32	3.35			
LES	Pre	7.03	4.38	20	1.072	0.296	7.75	4.45	18	1.734	0.1	6.78	3.71	18	-0.183	0.857	5.64	4.02	19	-0.333	0.743
	Post	6.25	3.65				6.96	4.56				6.90	4.60				5.91	3.48			
Recrb	Pre	7.10	5.41	20	1.44	0.165	8.03	6.05	20	0.711	0.486	6.06	5.13	20	-0.582	0.567	6.47	5.03	20	1.196	0.246
	Post	5.80	4.69				7.16	6.77				6.37	4.89				5.54	4.57			
TES	Pre	2.34	2.37	20	0.502	0.621	2.22	2.13	20	-2.355	0.029 *	2.32	2.12	20	-0.35	0.73	2.13	2.25	20	-1.113	0.279
	Post	2.06	2.62				3.19	3.06				2.46	2.10				2.70	2.76			
Left PM	Pre	7.01	3.91	20	-0.462	0.649	7.98	5.44	20	-0.306	0.762	8.49	5.61	20	0.796	0.435	6.43	4.05	20	1.501	0.149
	Post	7.41	4.93				8.25	5.75				7.62	5.48				5.98	4.10			
Left FDS	Pre	4.49	1.81	20	0.527	0.604	5.36	2.28	18	0.125	0.902	5.08	2.86	18	0.549	0.59	5.66	4.82	19	0.452	0.657
	Post	4.24	1.93				5.30	2.41				4.75	2.21				5.20	2.30			
RA	Pre	11.90	8.66	20	1.879	0.075	14.02	8.00	18	2.75	0.013 *	12.80	10.20	18	0.921	0.369	11.04	8.74	19	0.218	0.829
	Post	10.24	6.98				11.92	6.80				11.67	7.28				10.87	6.50			
EO	Pre	3.89	2.46	20	0.086	0.932	3.76	2.62	18	1.342	0.196	3.95	2.51	18	0.802	0.433	3.91	3.43	19	0.229	0.822
	Post	3.86	2.57				3.26	1.90				3.68	2.08				3.78	2.30			
IO	Pre	4.53	4.06	20	1.983	0.061	3.81	2.94	18	1.649	0.116	3.93	2.80	18	1.766	0.094	3.47	2.75	19	0.092	0.928
	Post	3.91	3.41				3.45	2.49				3.63	2.75				3.45	2.76			
LD	Pre	4.70	2.90	20	1.142	0.267	4.84	3.29	18	2.515	0.022 *	4.52	2.71	18	0.856	0.403	4.76	4.16	19	0.484	0.634
	Post	4.25	2.75				3.75	2.39				4.29	2.67				4.34	2.92			
Left ECRB	Pre	8.73	5.96	20	-0.232	0.819	11.34	15.75	19	-0.788	0.441	9.71	11.55	19	-0.209	0.836	7.93	6.85	19	-0.173	0.865
	Post	8.86	6.03				11.71	15.08				9.84	12.06				8.08	7.26			
Left TRI	Pre	2.57	1.66	20	0.096	0.925	2.94	2.63	18	-0.153	0.88	2.40	1.62	18	-1.451	0.164	2.45	1.97	19	-1.119	0.277
	Post	2.52	2.77				3.05	3.61				2.86	2.54				4.18	7.38			
Left GM	Pre	7.95	4.82	20	0.593	0.56	8.65	5.33	18	1.635	0.119	8.62	4.89	18	-0.355	0.726	7.93	5.21	19	-1.844	0.081
	Post	7.55	4.97				7.41	3.93				8.90	6.47				9.45	5.98			
R GM	Pre	9.30	8.15	19	0.802	0.433	10.15	10.72	18	1.726	0.102	8.50	7.18	18	1.978	0.063	7.98	7.34	18	-0.509	0.617
	Post	8.53	6.30				8.26	7.44				7.17	5.89				8.53	5.82			

displayed significant decreases in frequency of the right TB 122.7 – 111.6 Hz (t(10)=2.4,p=.037), TES 74.4 – 67.2 Hz (t(9)=2.4,p=.04), and left GM 54.8 – 46.7 Hz (t(10)=5,p=.001). The push phase of LH displayed a significant decrease in frequency of the right TB 119.8 – 110.5 Hz (t(10)=2.5,p=.034), LES 89.1 – 81.8 Hz (t(10)=2.3,p=.042), and left TB 94.5 – 84.8 Hz (t(8)=2.7,p=.025). While, the pull phase displayed a significant increase in frequency of the left PM 36.3 – 40.5 Hz (t(8)=-2.3,p=.048). The push phase of FH displayed significant decreases in frequency of the right TB 122 – 111.6 Hz (t(10)=3.1,p=.012), LES 96.9-87 Hz (t(10)=2.9,p=.017), TES 74.4 – 69.3 Hz (t(10)=2.9,p=.017), and left TB 93.8 – 84.7 Hz (t(8)=3.1,p=.015). While the pull phase displayed a significant decrease in frequency of the EO 44.9 – 40 Hz (t(9)=2.3,p=.044). The pull phase of WH displayed a significant decrease in frequency of the LD 59.7 – 55.7 Hz (t(9)=3.2,p=.01) and left TB 60.2 – 54.2 Hz (t(9)=3,p=.014).

In further evaluation of the female participants one, three, one, and one muscle displayed significant differences in amplitudes during KH, LH, FH, and WH, respectively. The push phase of KH displayed a significant decrease in amplitude of the EO 8.7 – 6.7 %MVC (t(10)=3,p=.012). The push phase of LH displayed a significant decrease in amplitude of the right TB 4.6 – 3.3 %MVC (t(10)=4.1,p=.002) and TES 3.5 – 2.7 %MVC (t(10)=2.3,p=.045). While in the pull phase there was a significant decrease in amplitude of the LES 7.1 – 4.7 %MVC (t(10)=2.8,p=.017). The push phase of FH displayed a significant increase in amplitude of the right PM 4.2 – 6 %MVC (t(10)=-2.3,p=.047). The pull phase of WH displayed a significant decrease in amplitude of the right FDS 10.9 – 9.6 %MVC (t(10)=2.5,p=.034).

3.1.2 Perceived Fatigue Time.

There were a total of twenty-seven instances over the course of the study where participants reported no fatigue. Seven participants reported no fatigue during KH (3 males and 4 females), ten reported no fatigue during LH (3 males, 7 females), eight reported no fatigue during FH (2 males, 6 females), and two reported no fatigue during WH (1 male, 1 female).

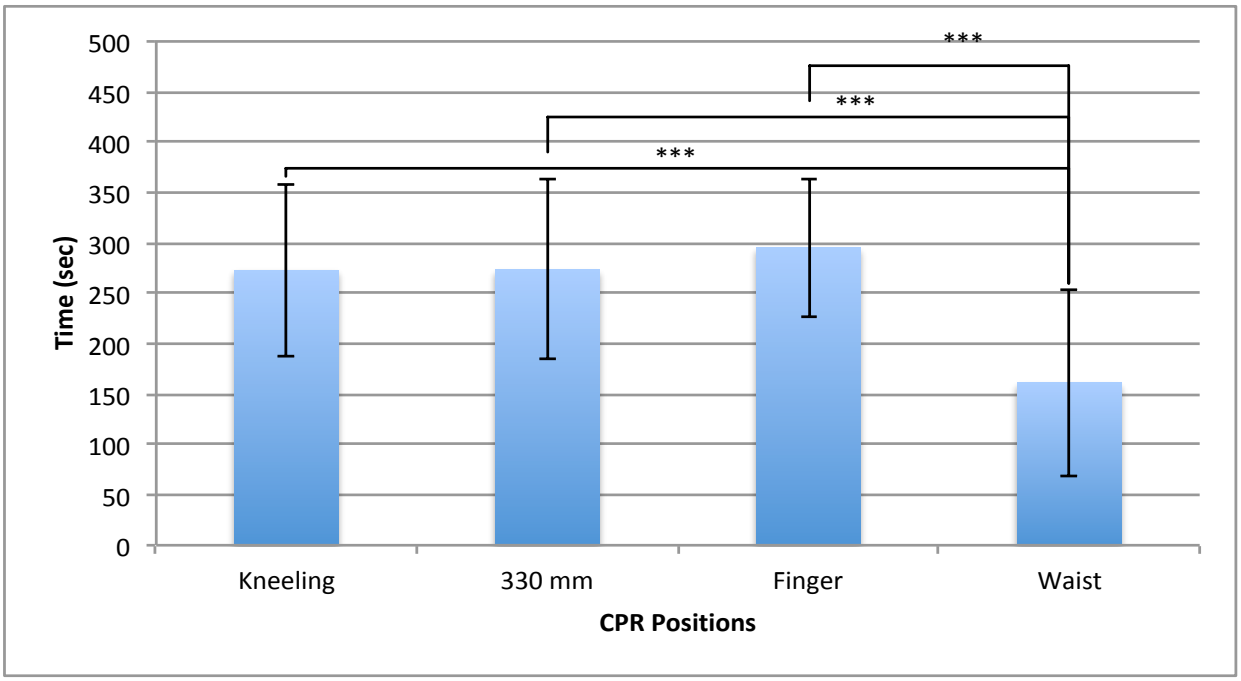

Figure 14: Average perceived fatigue time across each CPR position. Error bars indicate ±1 standard deviation. *** indicates a significance at $p<0.001$.

Participant reported perceived fatigue times during KH, LH, FH, and WH were 4 minutes 33 seconds±1 minute 25.2 seconds, 4 minutes 33.6 seconds±1 minute 28.8 seconds, 4 minutes 55.2 seconds±1minute 9 seconds, and 2 minutes 41.4 seconds±1 minute 38.4 seconds, respectively. It was further identified that during WH perceived fatigue time occurred significantly earlier compared to KH ($p<0.001$), LH ($p<0.001$), and FH ($p<0.001$) (fig. 14).

In controlling for participants' BMI the estimated marginal means of the perceived fatigue times during KH, LH, FH, and WH were 4 minutes 52.8 seconds, 4 minutes 37.2 seconds, 5 minutes 15 seconds, and 2 minutes 42.6 seconds, respectively. However, no significant differences between positions were found. Furthermore, there were no significant interactions between sex and positions.

3.1.3 Rating of Perceived Exertion.

Participant reported RPE during KH, LH, FH, and WH were 12.76±1.7, 12.86±1.59, 12.00±1.84, and 15.24±2.43, respectively. It was further identified that during WH the RPE score was significantly higher compared to KH ($p<0.001$), LH ($p<0.001$), and FH ($p<0.001$) (fig. 15).

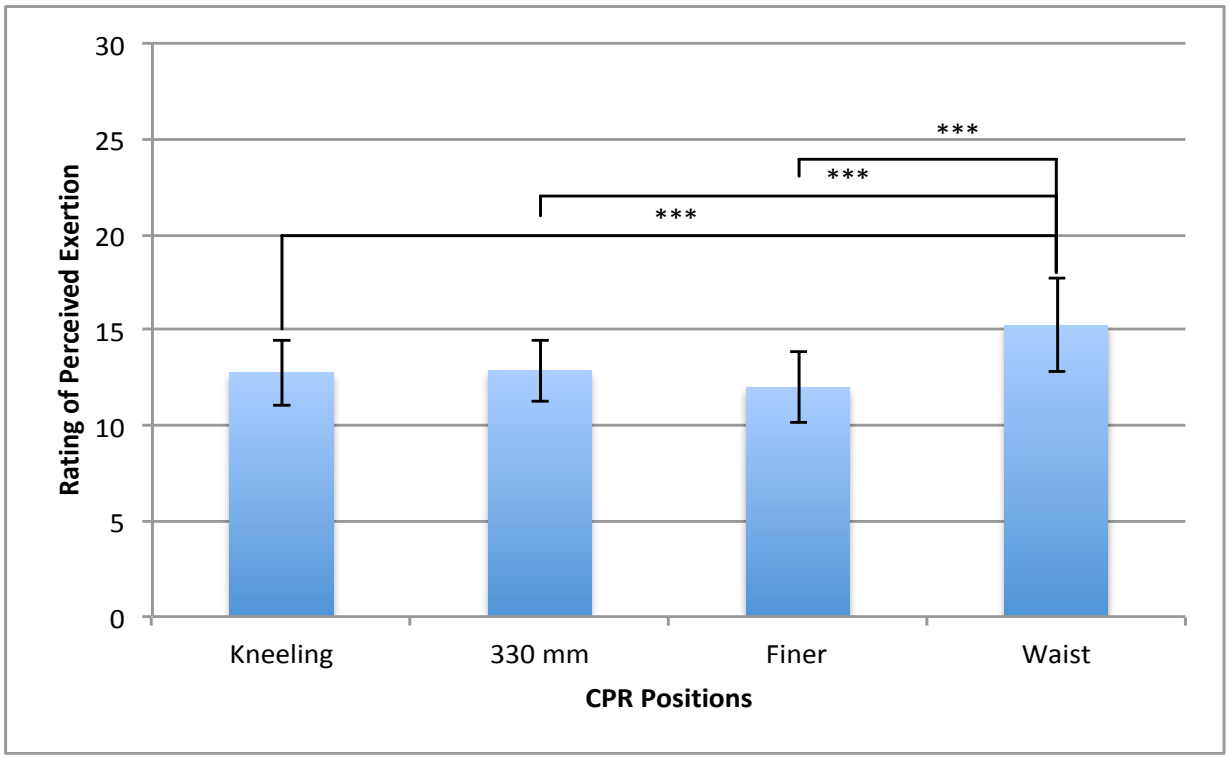

Figure 15: Average rating of perceived exertion across each CPR position. Error bars indicate ±1 standard deviation. *** indicates a significance at $p<0.001$.

In controlling for participants' BMI the estimated marginal means of the RPE during KH, LH, FH, and WH were 13.43, 13.7, 12.02, and 16.67, respectively. WH was found to have a significantly higher score compared to FH ($p=0.006$). In evaluating the interaction of sex and position, male participants displayed no significant difference in RPE, while female participants displayed a significantly higher RPE during WH (15.95) compared to FH ($p=0.014$).

3.2 EMG of CPR Positions

3.2.1 Amplitude Probability Distribution Function.

As noted in section (3.1), eight muscles displayed a significant decrease in MPF from pre to post isometric exercises. Of these eight muscles, six also displayed significant difference in RMS from pre to post isometric exercises. As peak EMG activity is closely related to peak force, the 90^{th} percentile (peak EMG activity) was examined during CPR positions (fig. 16), and identified that the right TB, LES, LD, left TB, RA, and Left GM displayed significant differences in the 90^{th} percentile when compared between positions. Of particular interest the right and left TB displayed the highest activation when compared between muscles, while the RA displayed significantly higher activation during WH. Furthermore, the TES displayed no significant differences between positions, however the LES displayed significantly higher activation during KH compared to LH.

10^{th} percentile (static EMG) EMG values were evaluated to determine low-level muscle activity during CC. Of the eight muscles that significantly decreased in MPF, from pre to post isometric exercises, four muscles (right TB, RA, LD, and left TB) displayed significant results in the 10^{th} percentile (fig. 17). Of particular interest the left TB displayed the lowest activation when compared between muscles, while the right TB

displayed the third lowest activations when compared between muscles. Furthermore, the RA displayed significantly higher activation during KH.

In evaluating the rate of change in the 90th percentile the right PM, EO, and left ECRB displayed significantly different slopes between CPR positions (fig. 18). The right PM displayed a steeper slope in KH (-0.15 %MVC/cycle) compared to FH ($p=0.047$), the EO displayed a steeper slope in KH (-0.53 %MVC/cycle) compared to WH ($p=0.042$), and the left ECRB displayed a steeper slope in LH (-0.43 %MVC/cycle) compared to WH ($p=0.002$). Furthermore, in evaluating the rate of change in the 10th percentile (fig. 19) the right TB, right ECRB, and LD displayed significantly different slopes between CPR positions. The right TB displayed a steeper slope in LH (-0.059 %MVC/cycle) compared to WH ($p=0.002$), the right ECRB displayed a steeper slope in KH (-0.14 %MVC/cycle) compared to FH($p=0.039$) and WH ($p<0.001$), while the LD displayed the flattest slope in KH ($p=0.013$), LH ($p = 0.001$), and FH ($p<0.001$) compared to WH (0.013 %MVC/cycle). Significant differences between the extrapolated cycle one and cycle twenty values per muscle across CPR positions are outlined in table 8 & 9 (fig. 20 & 21).

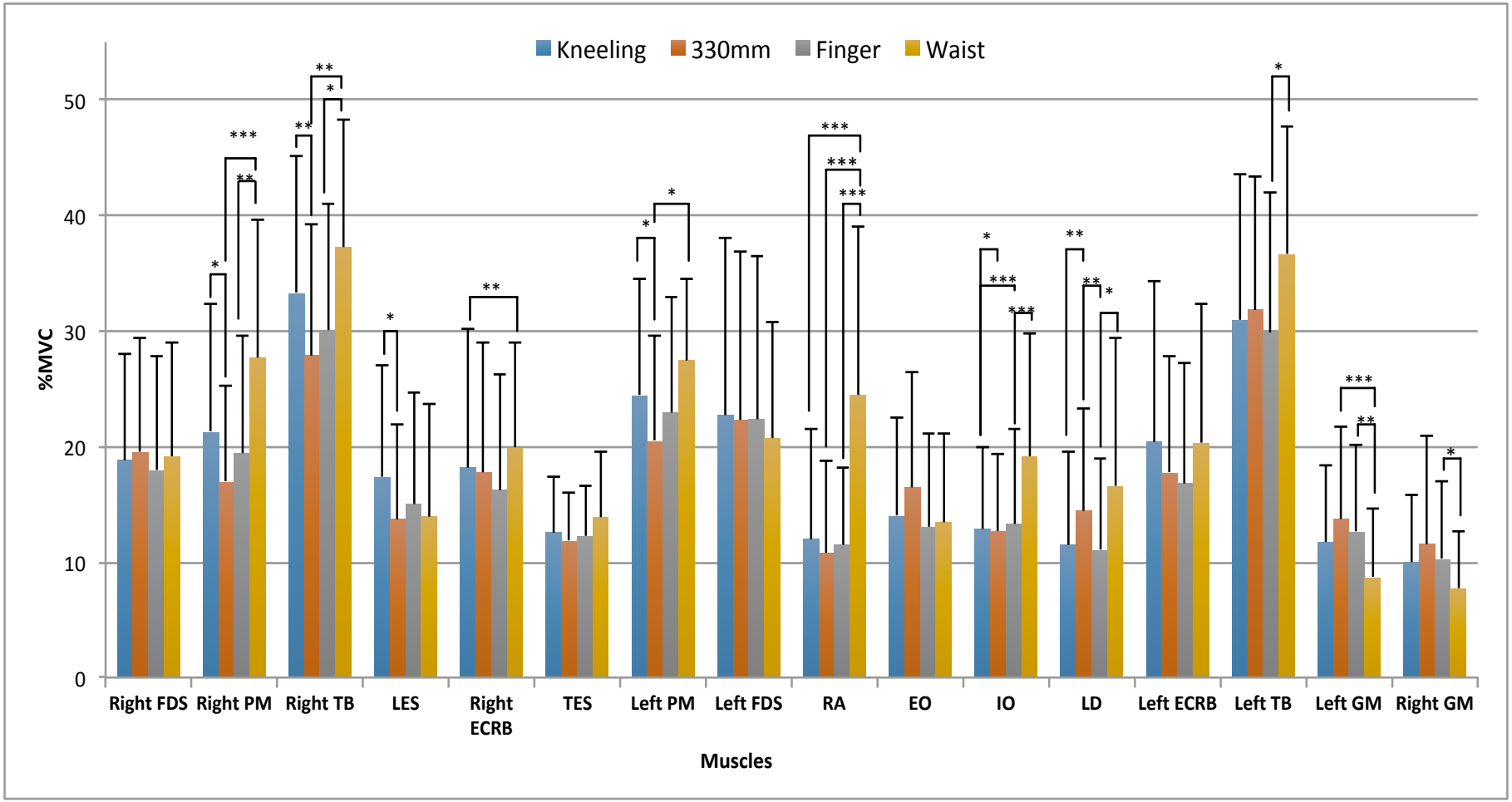

Figure 16: 90th percentile values (peak EMG) of the amplitude probably distribution function (APDF), calculated across each CPR position including breaks for ventilations. Error bars indicate +1 standard deviation. * Indicates a significant result at $p \leq 0.05$, ** indicates a significant results at $p < 0.01$, *** indicates a significant result at $p < 0.001$.

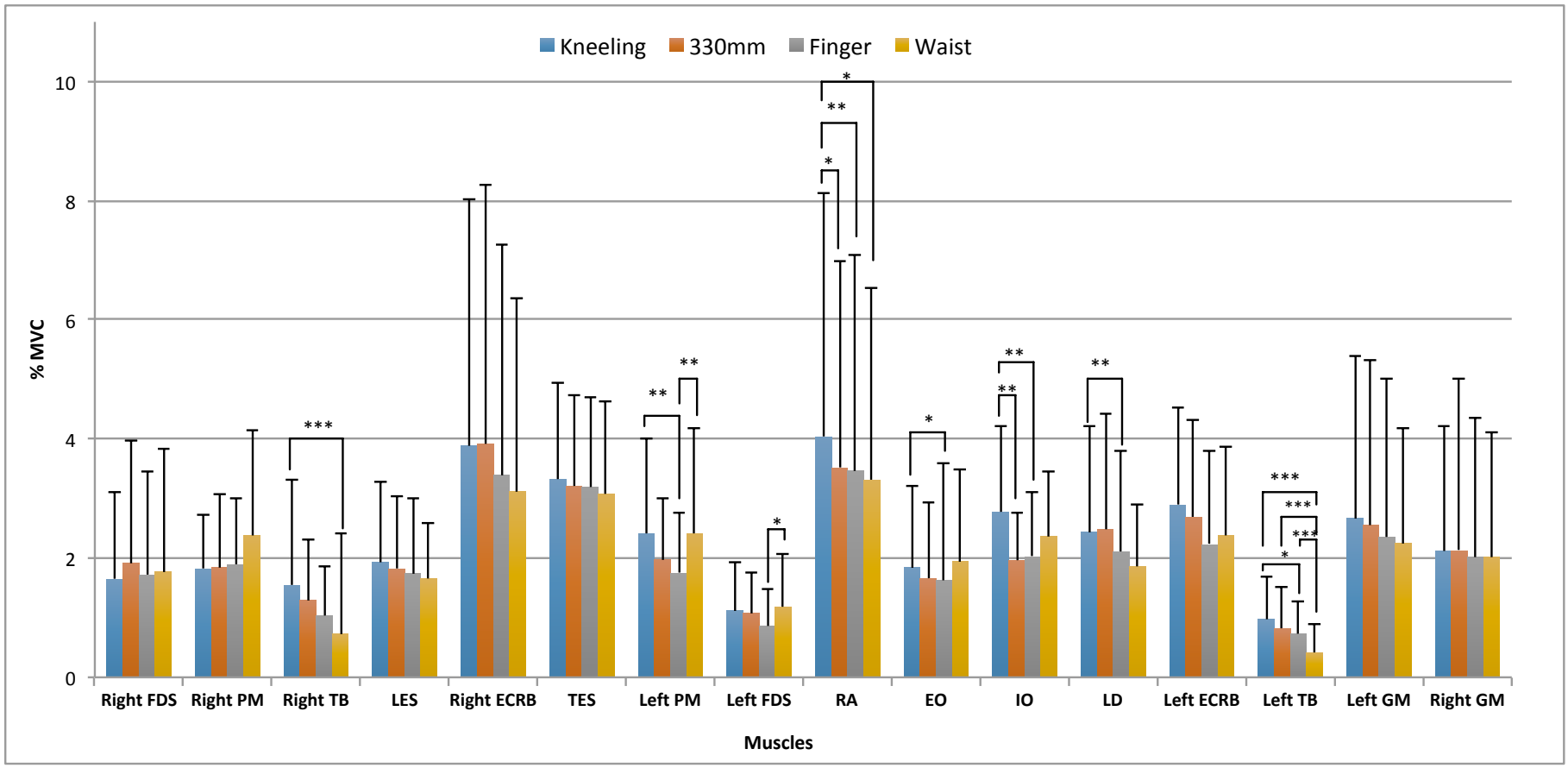

Figure 17: 10th percentile values (static EMG) of the amplitude probably distribution function (APDF), calculated across each CPR position including breaks for ventilations. Error bars indicate +1 standard deviation. * Indicates a significant result at $p \leq 0.05$, ** indicates a significant results at $p < 0.01$, *** indicates a significant result at $p < 0.001$

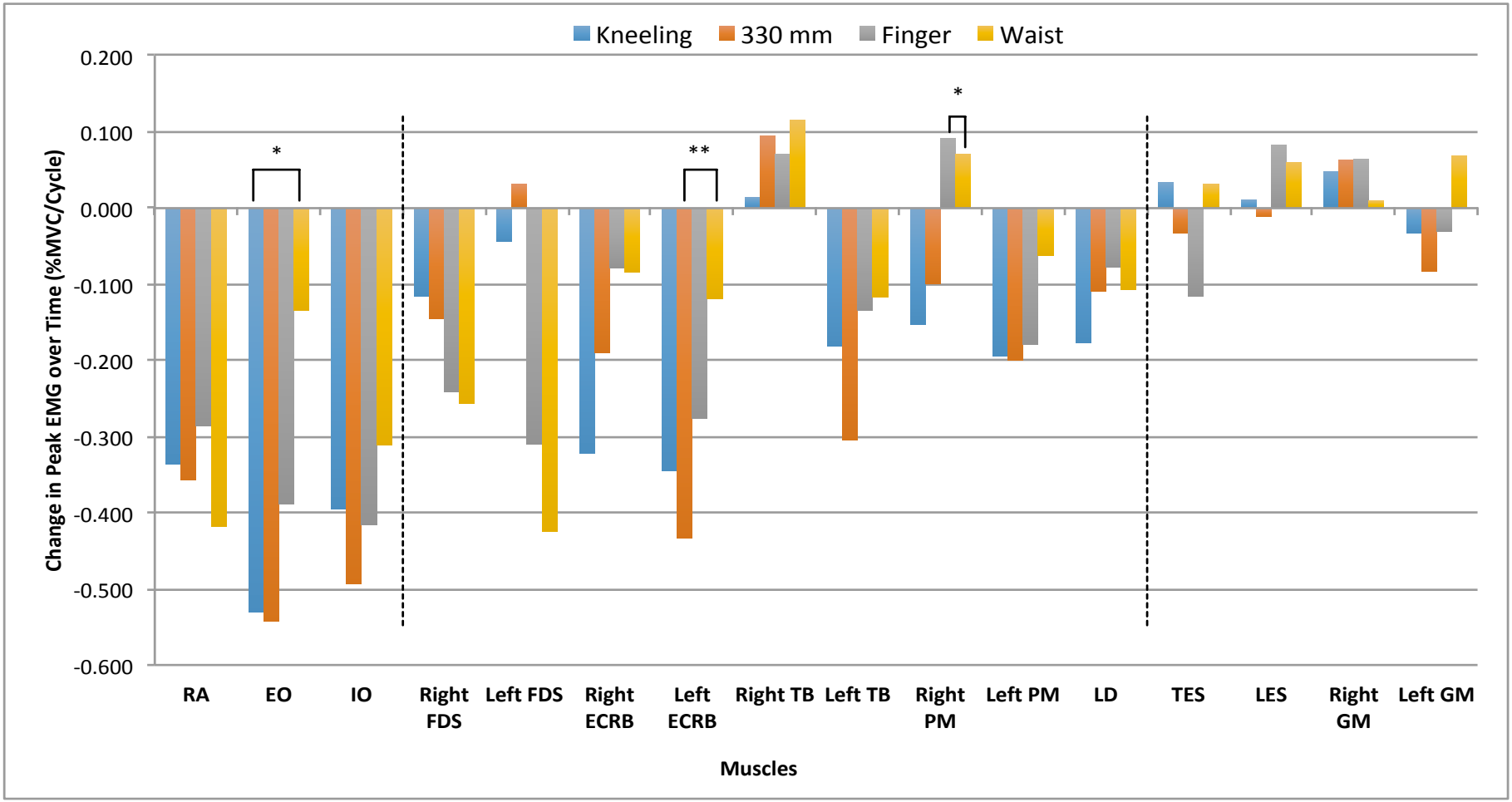

Figure 18: Change in rate of the 90th percentile (peak EMG change) from the amplitude probably distribution function (APDF), calculated across each CPR position, not including ventilations. Dashed vertical lines split the muscles into 3 groupings, CC initiators (left), upper limb stabilizers (centre), and CC terminators (right). * Indicates a significant result at $p \leq 0.05$, ** indicates a significant results at $p < 0.01$, *** indicates a significant result at $p < 0.001$.

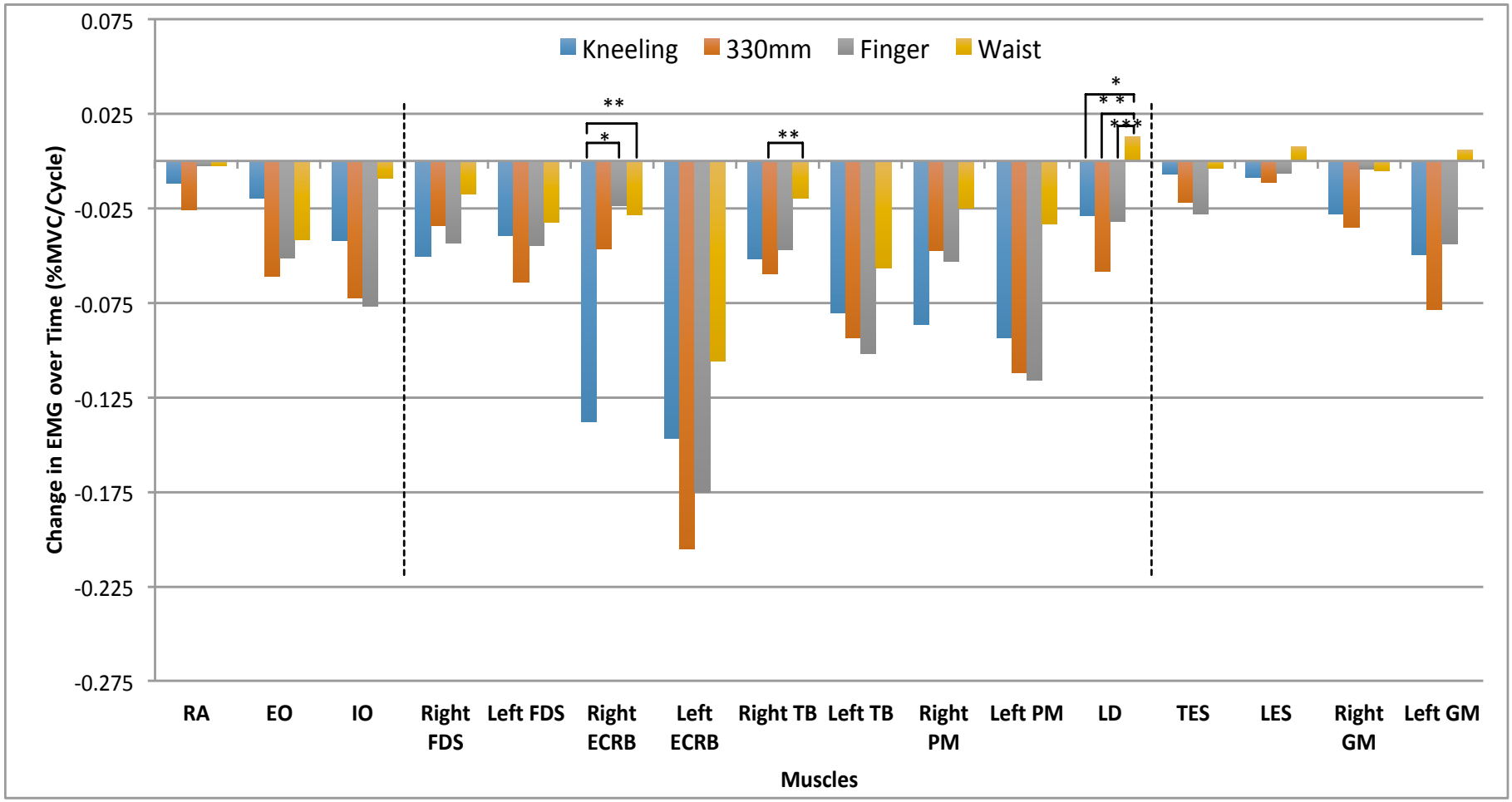

Figure 19: Change in rate of the 10th percentile (static EMG change) from the amplitude probably distribution function (APDF), calculated across each CPR position, not including ventilations. Dashed vertical lines split the muscles into 3 groupings, CC initiators (left), upper limb stabilizers (centre), and CC terminators (right). * Indicates a significant result at $p \leq 0.05$, ** indicates a significant results at $p < 0.01$, *** indicates a significant result at $p < 0.001$.

Table 8: Statistical results of the paired-samples T-tests comparing the extrapolated values using the linear polynomial equation calculating the 90th percentile (peak EMG) value of cycle one compared to cycle twenty per muscle and CPR position. * indicates a significant result ($p \leq 0.05$).

		Kneeling					330					Finger					Waist				
Muscle	**Cycle**	**Mean**	**Std. Dev.**	**df**	**t-value**	**P-value**	**Mean**	**Std. Dev.**	**df**	**t-value**	**P-value**	**Mean**	**Std. Dev.**	**df**	**t-value**	**P-value**	**Mean**	**Std. Dev.**	**df**	**t-vaule**	**P-value**
Right FDS	One	20.30	11.89	20	1.089	0.289	21.47	12.73	20	1.471	0.157	20.89	12.84	20	2.219	0.038 *	22.29	11.95	20	3.179	0.005 *
	Twenty	18.11	9.62				18.71	9.40				16.32	10.11				17.41	10.08			
Right PM	One	23.75	14.21	20	1.624	0.12	18.67	10.21	20	1.377	0.184	19.60	11.52	20	-1.069	0.298	28.67	13.19	20	-0.574	0.573
	Twenty	20.85	11.43				16.77	8.81				21.33	11.50				30.01	14.31			
Right TB	One	34.67	12.70	20	-0.194	0.848	28.71	11.87	19	-0.831	0.416	31.38	10.87	19	-0.72	0.481	38.34	13.06	20	-0.772	0.449
	Twenty	34.95	13.91				30.52	13.71				32.73	13.14				40.54	14.02			
LES	One	15.91	11.28	19	-0.154	0.879	12.81	8.16	19	0.185	0.855	12.98	10.16	20	-2.037	0.055	11.02	11.24	20	-0.63	0.536
	Twenty	16.12	10.27				12.60	9.54				14.56	10.98				12.15	12.05			
Recrb	One	21.19	13.68	20	4.329	0 *	19.72	12.73	20	1.218	0.237	17.37	9.89	20	0.83	0.416	21.23	11.43	20	0.857	0.402
	Twenty	15.09	12.27				16.11	15.10				15.88	13.06				19.64	10.13			
TES	One	10.08	5.80	20	-0.45	0.657	9.33	5.27	19	0.79	0.44	10.93	6.27	20	1.951	0.065	12.30	5.43	20	-0.562	0.581
	Twenty	10.72	7.66				8.71	4.77				8.74	5.65				12.89	8.03			
Left PM	One	27.25	11.39	20	2.235	0.037 *	23.58	9.43	20	1.902	0.072	25.54	9.81	20	1.429	0.168	29.87	10.05	20	0.444	0.662
	Twenty	23.57	12.14				19.78	12.39				22.13	14.92				28.67	9.51			
Left FDS	One	23.98	17.76	20	0.41	0.686	22.67	14.83	20	-0.217	0.83	25.80	15.94	20	2.841	0.01 *	25.62	11.18	20	4.306	0 *
	Twenty	23.14	17.01				23.28	19.16				19.92	16.99				17.57	13.18			
RA	One	15.33	12.69	20	3.232	0.004 *	14.41	10.17	20	3.773	0.001 *	14.61	8.27	20	3.688	0.001 *	29.79	16.74	20	2.485	0.022 *
	Twenty	8.94	9.54				7.63	7.02				9.18	7.51				21.85	18.42			
EO	One	18.96	12.27	20	3.512	0.002 *	22.47	13.69	20	4.362	0 *	17.10	11.09	20	3.35	0.003 *	15.28	9.02	20	1.083	0.292
	Twenty	8.89	9.69				12.18	8.74				9.71	9.23				12.73	10.95			
IO	One	16.64	10.42	20	3.512	0.002 *	17.93	12.09	20	3.48	0.002 *	17.55	12.43	20	3.35	0.003 *	23.16	13.96	20	2.028	0.056
	Twenty	9.13	7.07				8.57	4.98				9.64	6.43				17.27	13.19			
LD	One	13.34	10.21	20	4.149	0 *	16.04	9.65	19	1.591	0.128	11.97	8.19	20	1.573	0.132	18.47	12.58	20	0.942	0.357
	Twenty	9.99	7.58				13.97	10.06				10.51	9.55				16.44	15.90			
Left ECRB	One	22.76	16.19	20	2.974	0.007 *	21.23	13.52	20	4.225	0 *	18.73	12.32	20	3.018	0.007 *	21.95	13.82	20	1.447	0.163
	Twenty	16.20	13.88				13.00	8.14				13.50	10.79				19.68	13.15			
Left TRI	One	33.80	11.95	20	1.827	0.083	36.33	14.42	20	2.35	0.029 *	32.63	11.71	20	1.193	0.247	39.91	11.63	20	0.857	0.402
	Twenty	30.36	16.14				30.56	12.06				30.07	15.69				37.68	14.54			
Left GM	One	11.86	7.32	20	0.632	0.535	14.33	11.01	20	0.721	0.479	12.41	8.35	20	0.631	0.535	7.04	4.93	20	-0.901	0.378
	Twenty	11.23	6.78				12.75	8.54				11.84	7.91				8.35	7.52			
R GM	One	7.97	6.13	19	-1.4	0.178	8.05	9.71	18	-0.9	0.38	6.88	5.38	19	-1.617	0.122	4.66	3.76	19	-0.306	0.763
	Twenty	8.89	5.54				9.25	8.12				8.10	5.56				4.84	3.70			

Table 9: Statistical results of the paired-samples T-tests comparing the extrapolated values using the linear polynomial equation calculating the 10th percentile (static EMG) value of cycle one compared to cycle twenty per muscle and CPR position. * indicates a significant result ($p \leq 0.05$).

		Kneeling					330					Finger					Waist				
Muscle	**Cycle**	**Mean**	**Std. Dev.**	**df**	**t-value**	**P-value**	**Mean**	**Std. Dev.**	**df**	**t-value**	**P-value**	**Mean**	**Std. Dev.**	**df**	**t-value**	**P-value**	**Mean**	**Std. Dev.**	**df**	**t-vaule**	**P-value**
Right FDS	One	2.44	2.93	20	2.365	0.028 *	2.63	2.81	20	2.114	0.047 *	2.55	2.76	20	3.612	0.002 *	2.58	2.57	20	0.998	0.33
	Twenty	1.48	1.29				1.97	2.14				1.72	2.14				2.24	2.83			
Right PM	One	4.57	4.25	20	2.411	0.026 *	3.75	1.87	20	2.996	0.007 *	3.95	2.91	20	1.942	0.066	4.29	2.23	20	1.223	0.236
	Twenty	2.93	2.47				2.85	1.64				2.94	1.80				3.81	2.86			
Right TB	One	3.02	2.58	20	3.577	0.002 *	3.32	2.34	19	4.896	0 *	2.50	2.05	19	2.999	0.007 *	0.89	1.69	20	3.724	0.001 *
	Twenty	2.04	2.48				2.18	2.02				1.61	2.09				0.51	1.75			
LES	One	1.98	1.42	19	1.692	0.107	2.09	1.54	19	1.95	0.066	1.83	1.43	20	0.869	0.395	1.59	1.09	20	-0.729	0.474
	Twenty	1.81	1.37				1.87	1.38				1.71	1.35				1.73	0.94			
Recrb	One	7.21	5.40	20	5.166	0 *	6.29	4.42	20	1.46	0.16	5.55	4.00	20	0.764	0.454	4.79	3.74	20	1.783	0.09
	Twenty	4.59	3.68				5.40	4.82				5.10	5.14				4.25	3.16			
TES	One	3.41	1.67	20	0.863	0.398	3.48	1.63	19	2.975	0.008 *	3.54	2.02	20	1.757	0.094	3.05	1.57	20	0.601	0.555
	Twenty	3.28	1.67				3.06	1.47				3.01	1.44				2.98	1.60			
Left PM	One	5.06	4.17	20	2.869	0.009 *	4.48	2.46	20	3.785	0.001 *	4.23	3.00	20	3.191	0.005 *	4.68	2.65	20	0.986	0.336
	Twenty	3.28	2.93				2.35	1.95				2.03	3.03				4.05	3.07			
Left FDS	One	1.66	1.40	20	2.186	0.041 *	2.21	2.33	20	3.353	0.003 *	1.59	1.46	20	3.497	0.002 *	1.87	1.11	20	2.209	0.039 *
	Twenty	0.91	1.05				1.00	1.42				0.74	1.16				1.25	1.42			
RA	One	4.35	4.18	20	1.096	0.286	4.06	3.56	20	2.195	0.04 *	3.61	3.65	20	0.364	0.72	3.44	3.64	20	0.241	0.812
	Twenty	4.12	4.23				3.56	3.70				3.56	3.89				3.39	3.40			
EO	One	3.61	4.63	20	0.896	0.381	3.17	4.00	20	2.89	0.009 *	2.51	2.43	20	3.059	0.006 *	3.33	2.28	20	1.662	0.112
	Twenty	3.24	6.31				2.01	3.15				1.53	2.67				2.54	2.60			
IO	One	3.76	1.68	20	2.953	0.008 *	3.15	1.62	20	2.705	0.014 *	3.01	1.69	20	2.711	0.013 *	3.06	1.70	20	0.489	0.63
	Twenty	2.96	1.46				1.77	1.37				1.56	1.49				2.89	1.76			
LD	One	2.76	1.77	20	3.35	0.003 *	3.39	2.18	19	3.494	0.002 *	2.45	1.51	20	2.928	0.008 *	4.06	9.74	20	-1.04	0.311
	Twenty	2.22	1.68				2.28	2.18				1.84	1.76				4.30	10.52			
Left ECRB	One	6.19	4.28	20	2.579	0.018 *	6.74	4.15	20	3.6	0.002 *	5.09	3.12	20	3.661	0.002 *	4.54	3.30	20	2.339	0.03 *
	Twenty	3.40	3.36				2.84	3.00				1.76	3.44				2.53	2.53			
Left TRI	One	3.13	2.74	20	4.953	0 *	3.25	2.91	20	3.374	0.003 *	2.53	2.27	20	3.709	0.001 *	0.99	1.18	20	3.02	0.007 *
	Twenty	1.61	2.43				1.48	1.94				0.60	1.73				-0.08	0.71			
Left GM	One	3.29	3.39	20	2.581	0.018 *	4.04	3.96	20	2.492	0.022 *	3.25	3.13	20	2.113	0.047 *	2.51	2.14	20	-0.27	0.79
	Twenty	2.35	2.27				2.55	2.32				2.41	2.52				2.62	2.26			
R GM	One	2.34	2.39	19	1.999	0.06	2.38	3.55	18	1.354	0.192	2.06	2.44	19	0.498	0.624	2.13	2.37	19	0.615	0.546
	Twenty	1.80	1.75				1.71	1.84				1.97	2.16				2.03	1.94			

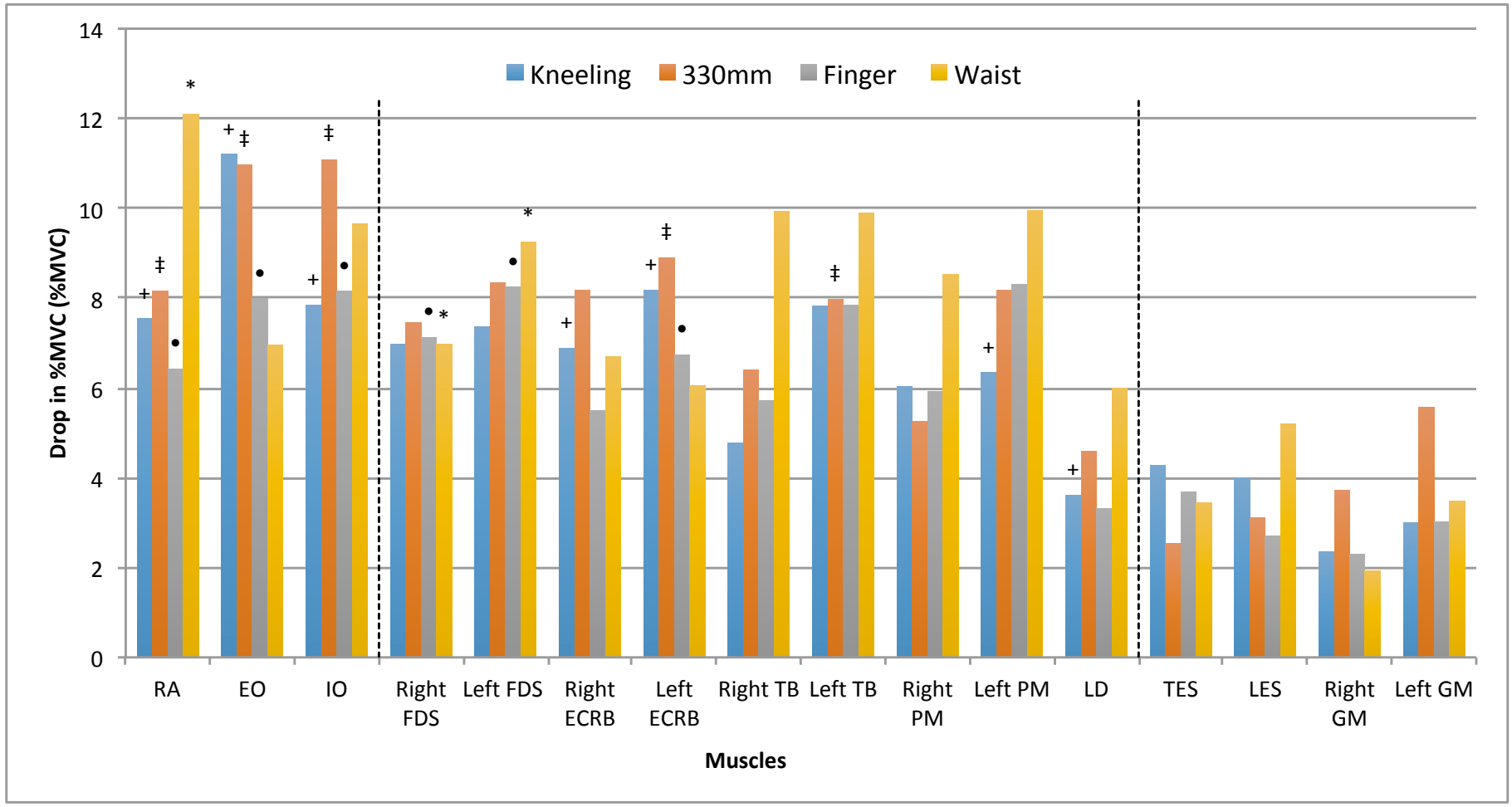

Figure 20: Magnitude of the difference between cycle one and cycle twenty of the extrapolated 90th percentile (peak EMG) values. Dashed vertical lines split the muscles into 3 groupings, CC initiators (left), upper limb stabilizers (centre), and CC terminators (right). + Indicates a significant result ($p \leq 0.05$) during KH, ‡ indicates a significant results ($p \leq 0.05$) during LH, • indicates a significant result ($p \leq 0.05$) during FH, * indicates a significant results ($p \leq 0.05$) during WH.

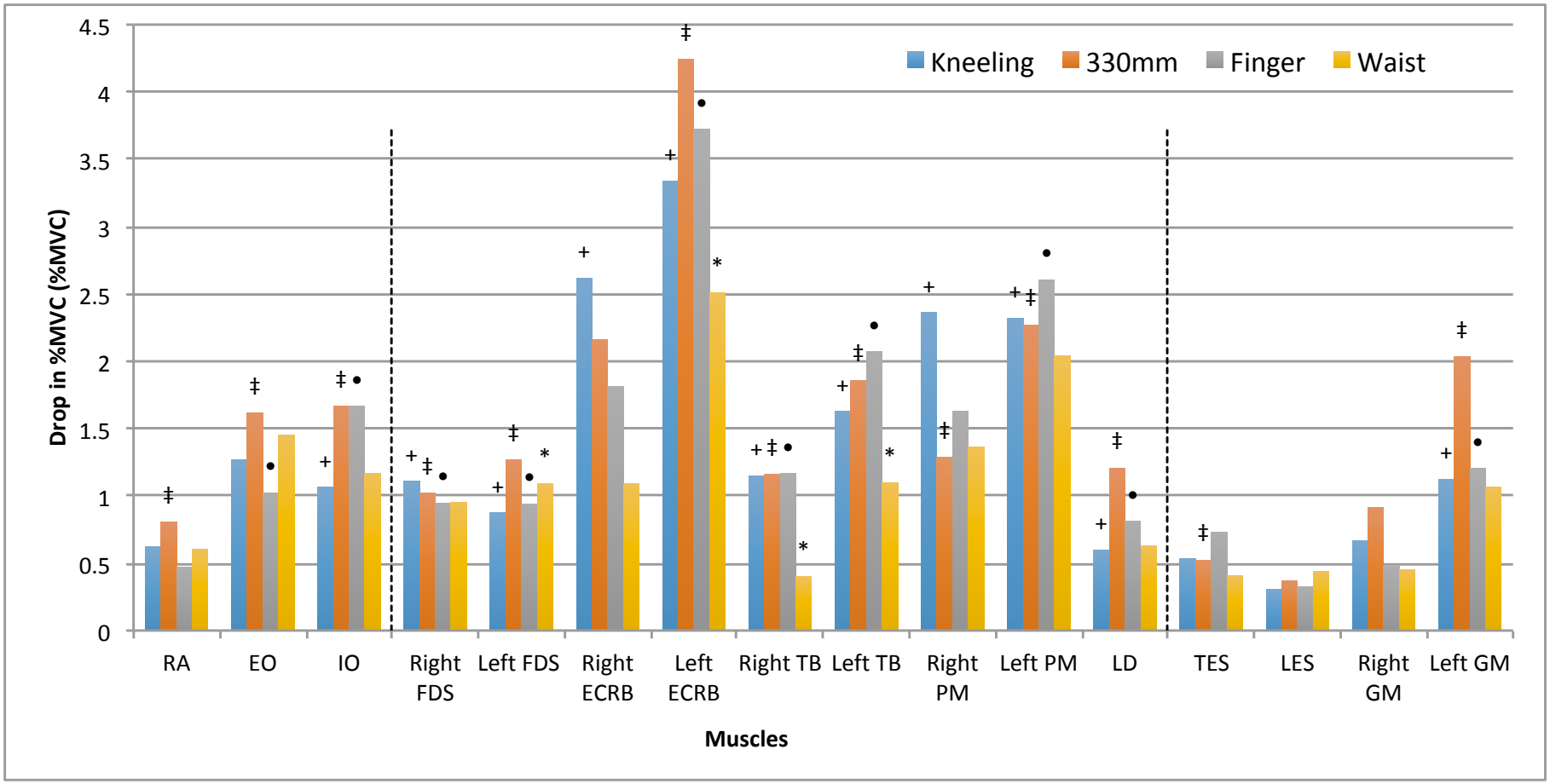

Figure 21: Magnitude of the difference between cycle one and cycle twenty of the extrapolated 10th percentile (static EMG) values. Dashed vertical lines split the muscles into 3 groupings, CC initiators (left), upper limb stabilizers (centre), and CC terminators (right). + Indicates a significant result ($p \leq 0.05$) during KH, ‡ indicates a significant results ($p \leq 0.05$) during LH, • indicates a significant result ($p \leq 0.05$) during FH, * indicates a significant results ($p \leq 0.05$) during WH.

3.2.2 muscle timing.

To determine the order of over all muscle activation per trial, CC were evaluated per cycle and then averaged across twenty CC cycles (fig. 22-25). The subsequent data represents the firing order of muscles, it is presented in order of onset to completion of a CC. Muscle order during KH was: EO, IO, RA, right FDS, left FDS, right ECRB, left PM, LD, right TB, left TB, left ECRB, right PM, TES, LES, right GM, and left GM. Muscle order during LH was: EO, RA, IO, LD, right FDS, left FDS, left PM, right ECRB, left TB, right TB, left ECRB, right PM, TES, left GM, LES, and right GM. Muscle order during FH was: RA, EO, IO, right FDS, left FDS, left PM, LD, right ECRB, right TB, left TB, left ECRB, right PM, TES, LES, left GM, and right GM. While, muscle order during WH was: RA, EO, IO, left TB, left FDS, right FDS, right TB, left PM, LD, left ECRB, right PM, right ECRB, left GM, right GM, LES, and TES.

Of the sixteen muscles evaluated eight displayed significant differences in timing between trials and were as follows: right TB, right ECRB, RA, IO, LD, left TB, left GM, and right GM. The right TB displayed significantly earlier activation during WH when compared to KH ($p=0.002$) and LH ($p=0.024$) positions, while the LH displayed significantly earlier activation compared to KH ($p=0.015$). The right ECRB displayed significantly earlier activation during KH compared to WH ($p=0.04$). The RA displayed significantly earlier activation during WH when compared to KH ($p=0.005$) and LH ($p=0.002$). The IO displayed significantly delayed activation during KH when compared to FH ($p=0.01$) and WH ($p=0.002$). The LD displayed significantly earlier activation during LH when compared to WH ($p=0.022$). The left TB displayed significantly earlier activation during WH compared to KH ($p<0.001$), LH ($p<0.001$), and FH ($p<0.001$). The

left GM displayed significantly earlier activation during WH when compared to KH ($p<0.001$), LH ($p=0.035$), and FH ($p<0.001$). Lastly, the right GM displayed significantly earlier activation during WH when compared to KH ($p<0.001$), LH ($p<0.001$), and FH ($p<0.001$).

The extrapolated values of cycle one and twenty of the right and left TB were evaluated to determine if there was a significant change in timing of the TB during each CPR position. The right TB displayed a significant increasing in timing of 10.7 – 18.6 msec ($t(20)=-5.7, p<.001$) while the left TB also displayed a significant increase in timing of 10.7 – 15.6 msec ($t(20)=-2.4, p=.002$) during KH. The right TB displayed a significant increasing in timing of 7.96 – 13.8 msec ($t(20)=-3.8, p=.001$) during LH. The right TB displayed a significant increasing in timing of 13.4 – 19.8 msec ($t(20)=-5.5, p<.001$) while the left TB also displayed a significant increase in timing of 12.7 – 19.7 msec ($t(20)=-3.3, p=.004$) during FH. The left TB displayed a significant increase in timing of 22.4 – 27.9 msec ($t(20)=-3.3, p=.004$) during WH.

In controlling for participants' BMI, nine muscles displayed a significant interaction between sex and position. Male participants displayed significantly delayed activation of the right PM during LH compared to FH ($p=0.005$) and WH ($p=0.013$). Female participants displayed significantly earlier activation of the right TB during WH compared to male participants ($p=0.001$). Male participants displayed significantly earlier activation of the TES during KH compared to female participants ($p<0.001$). Male participants displayed significantly earlier activation of the TES during KH compared to FH ($p<0.001$). Male participants displayed significantly earlier activation of the TES during WH compared to FH ($p=0.008$). Female participants displayed significantly earlier

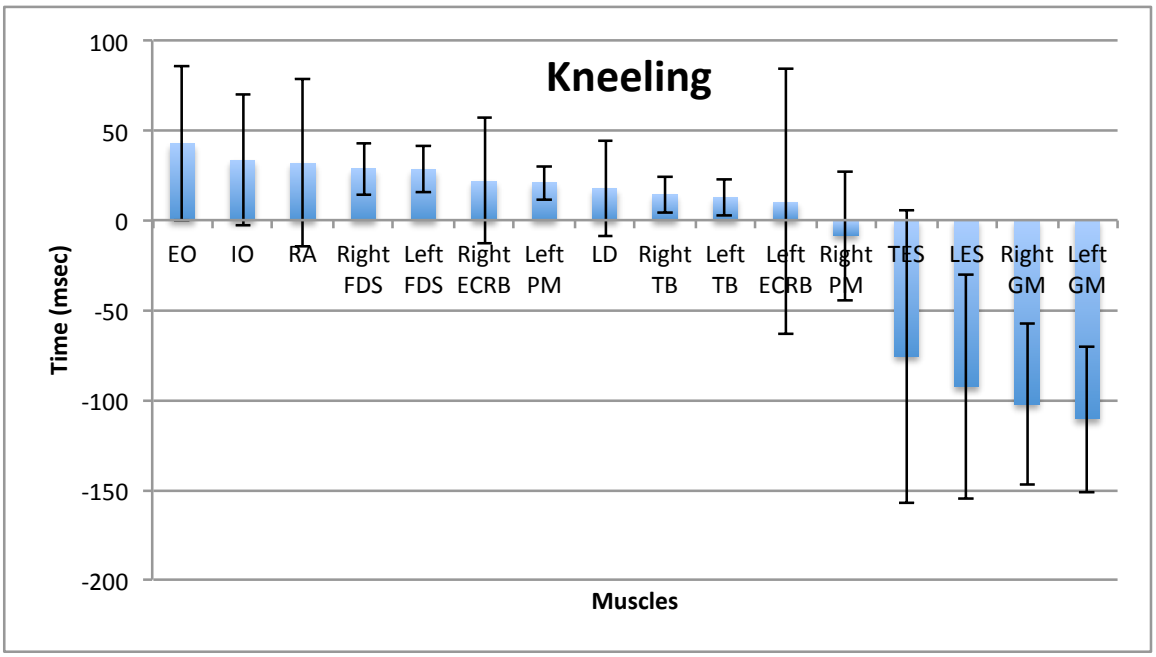

Figure 22: Average muscle time lag during KH when compared to CC force. Time lag was averaged across all CC cycles and sorted in descending order. Positive values indicate onset prior to CC force and negative values indicate onset after CC force. Error bars indicate ±1 standard deviation.

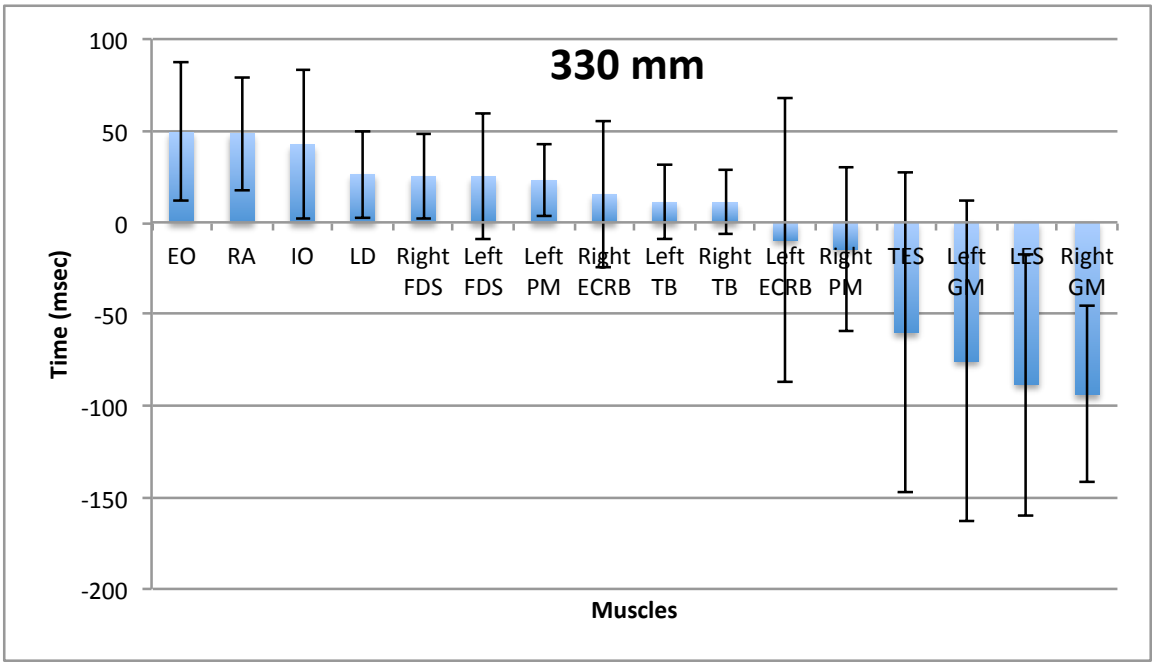

Figure 23: Average muscle time lag during LH when compared to CC force. Time lag was averaged across all CC cycles and sorted in descending order. Positive values indicate onset prior to CC force and negative values indicate onset after CC force. Error bars indicate ±1 standard deviation.

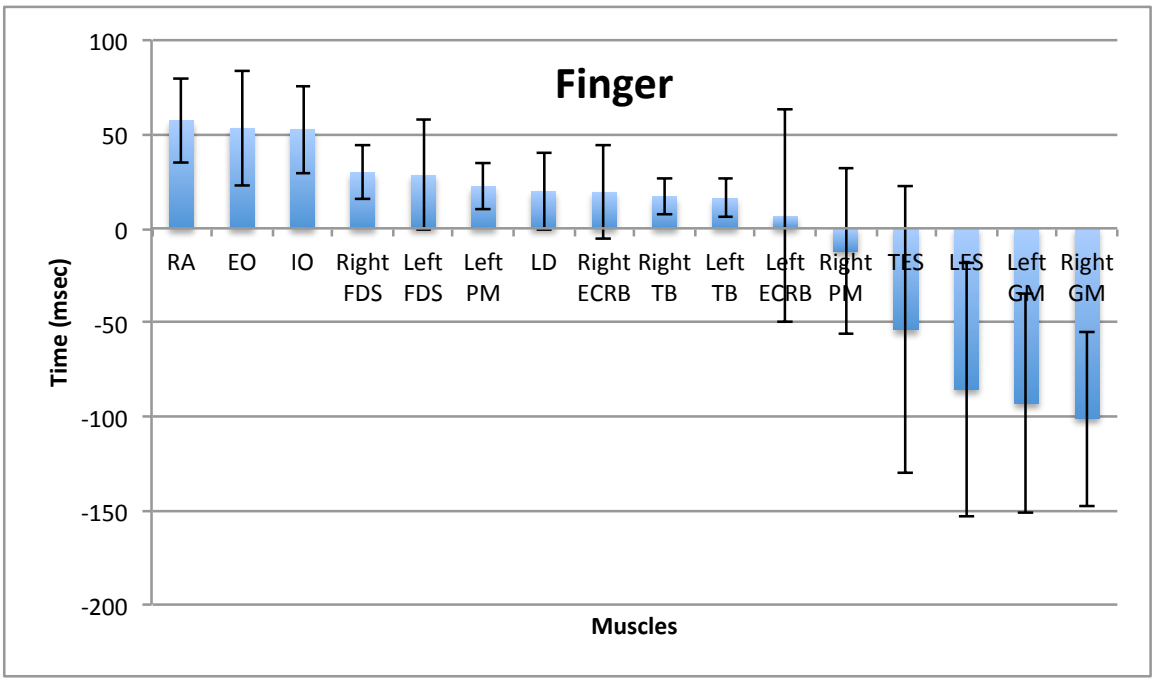

Figure 24: Average muscle time lag during FH when compared to CC force. Time lag was averaged across all CC cycles and sorted in descending order. Positive values indicate onset prior to CC force and negative values indicate onset after CC force. Error bars indicate ±1 standard deviation.

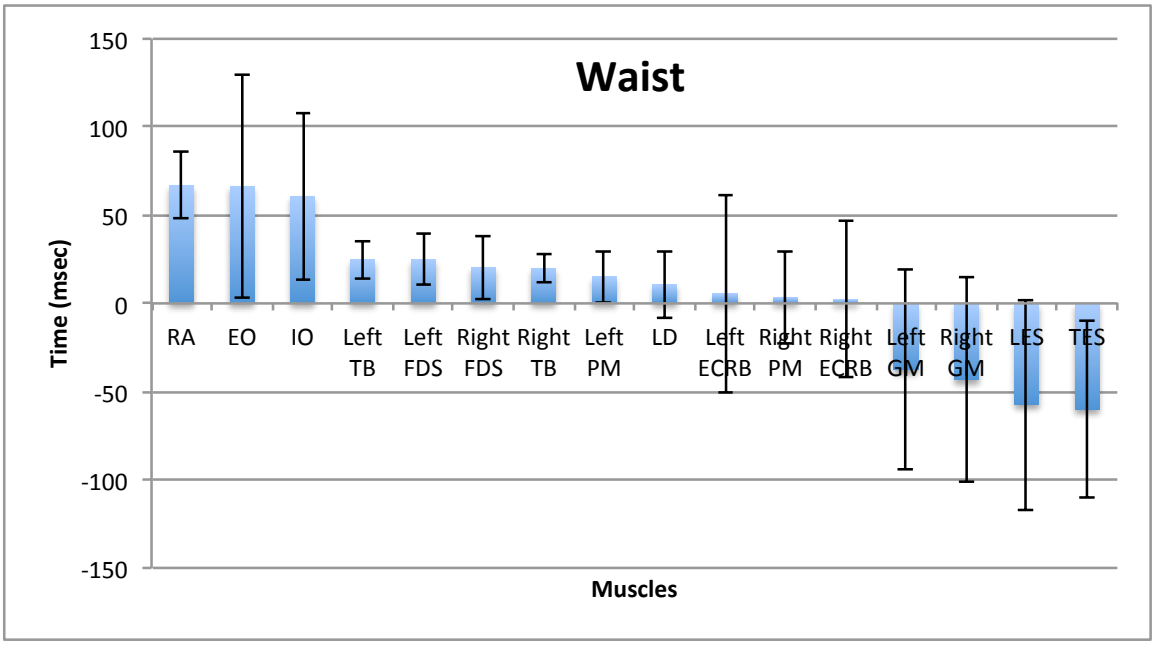

Figure *25*: Average muscle time lag during WH when compared to CC force. Time lag was averaged across all CC cycles and sorted in descending order. Positive values indicate onset prior to CC force and negative values indicate onset after CC force. Error bars indicate ±1 standard deviation.

activation of the TES during KH compared to FH (p=0.001). Female participants displayed significantly earlier activation of the TES during WH compared to FH (p=0.001). Female participants displayed significantly earlier activation of the EO during WH compared to FH (p=0.004) and LH (p=0.002). Male participants displayed significantly earlier activation of the IO during WH compared to KH (p<0.001) and LH (p=0.034). Female participants displayed significantly earlier activation of the IO during WH compared to KH (p<0.001), LH (p=0.002), and FH (p=0.004). Female participants displayed significantly earlier activation of the LD during FH compared to the male participants (p=0.004). Male participants displayed significantly earlier activation of the LD during the WH compared to FH (p=0.001). Female participants displayed significantly earlier activation of the LD during LH compared to FH (p=0.003). Female participants displayed significantly earlier activation of the left TB during KH compared to male participants (p<0.001). Male participants displayed significantly earlier activation of the left GM during the WH compared to FH (p=0.049). Female participants displayed significantly earlier activation of the left GM during WH compared to FH (p=0.03). Male participants displayed significantly earlier activation of the Right GM during WH compared to LH (p=0.018). Male participants displayed significantly earlier activation of the right GM during WH compared to LH (p=0.039).

3.2.3 ensemble averages.

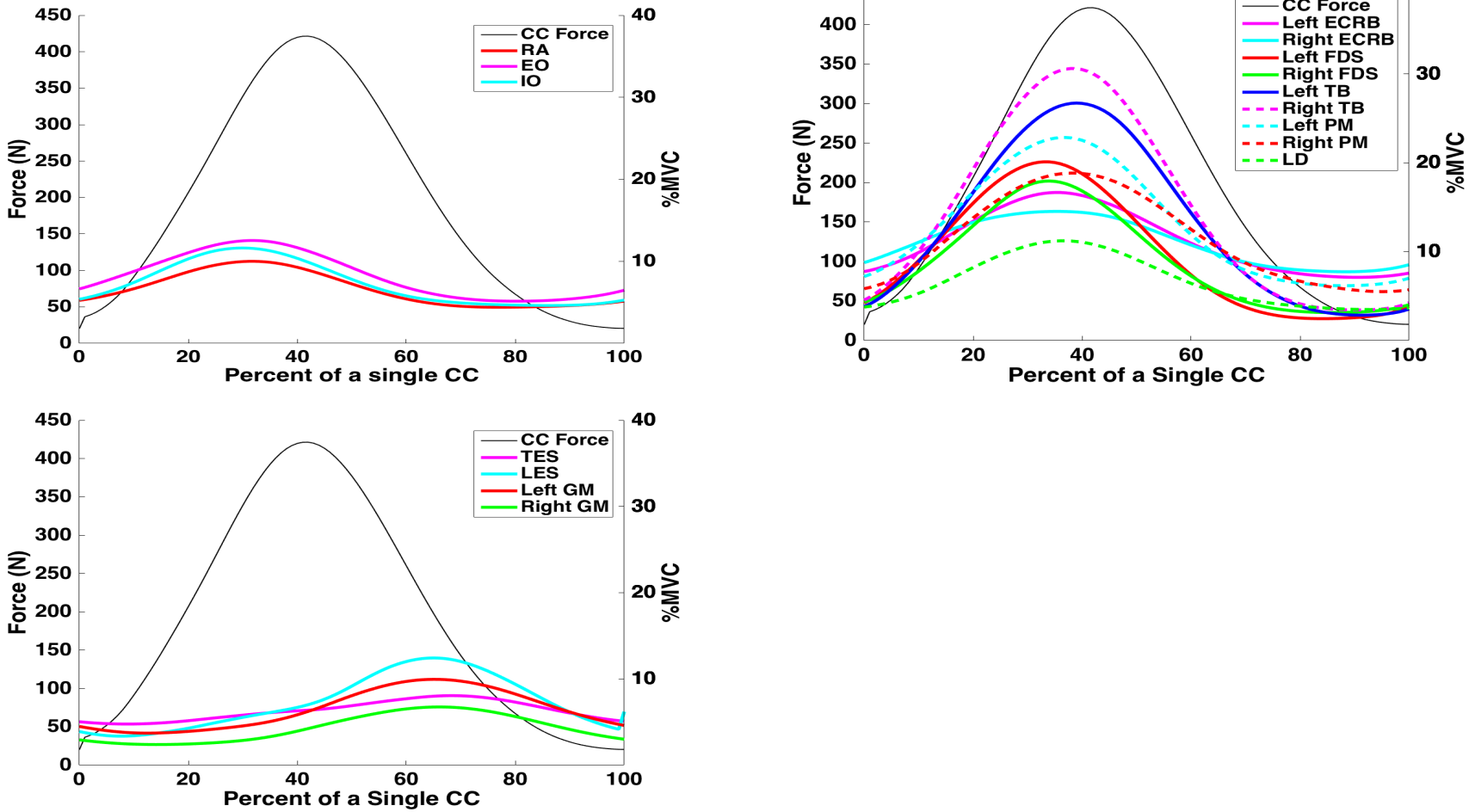

Figure 26: Ensemble averages of EMG values of each muscle and CC force during KH. 0% represents the initiation of a CC and 100% represents termination of a CC. Averages were calculated across all CC during KH. Top left represents CC initiators. Top right represents CC stabilizers. Bottom left represents CC terminators.

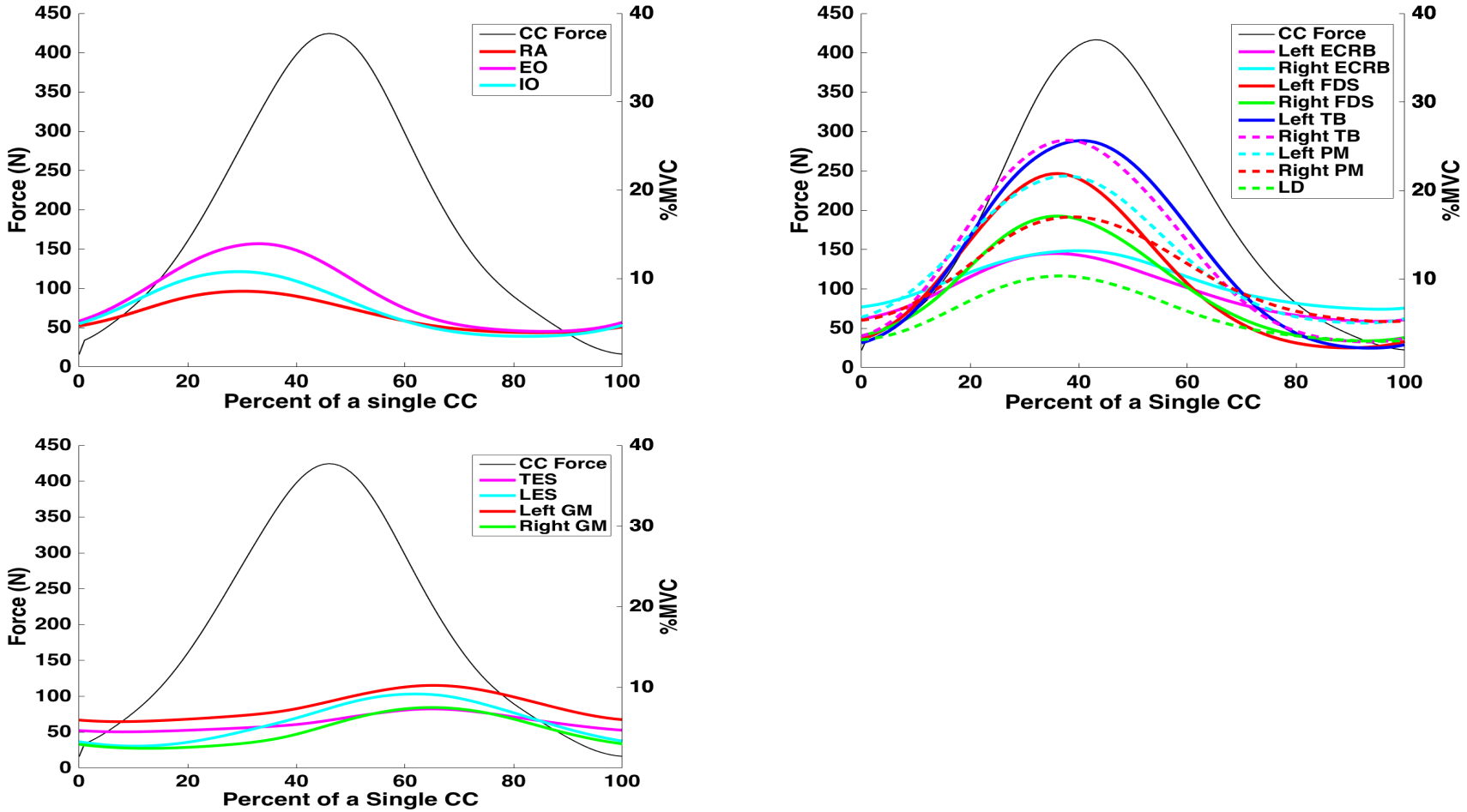

Figure 27: Ensemble averages of EMG values of each muscle and CC force during LH. 0% represents the initiation of a CC and 100% represents termination of a CC. Averages were calculated across all CC during LH. Top left represents CC initiators. Top right represents CC stabilizers. Bottom left represents CC terminators.

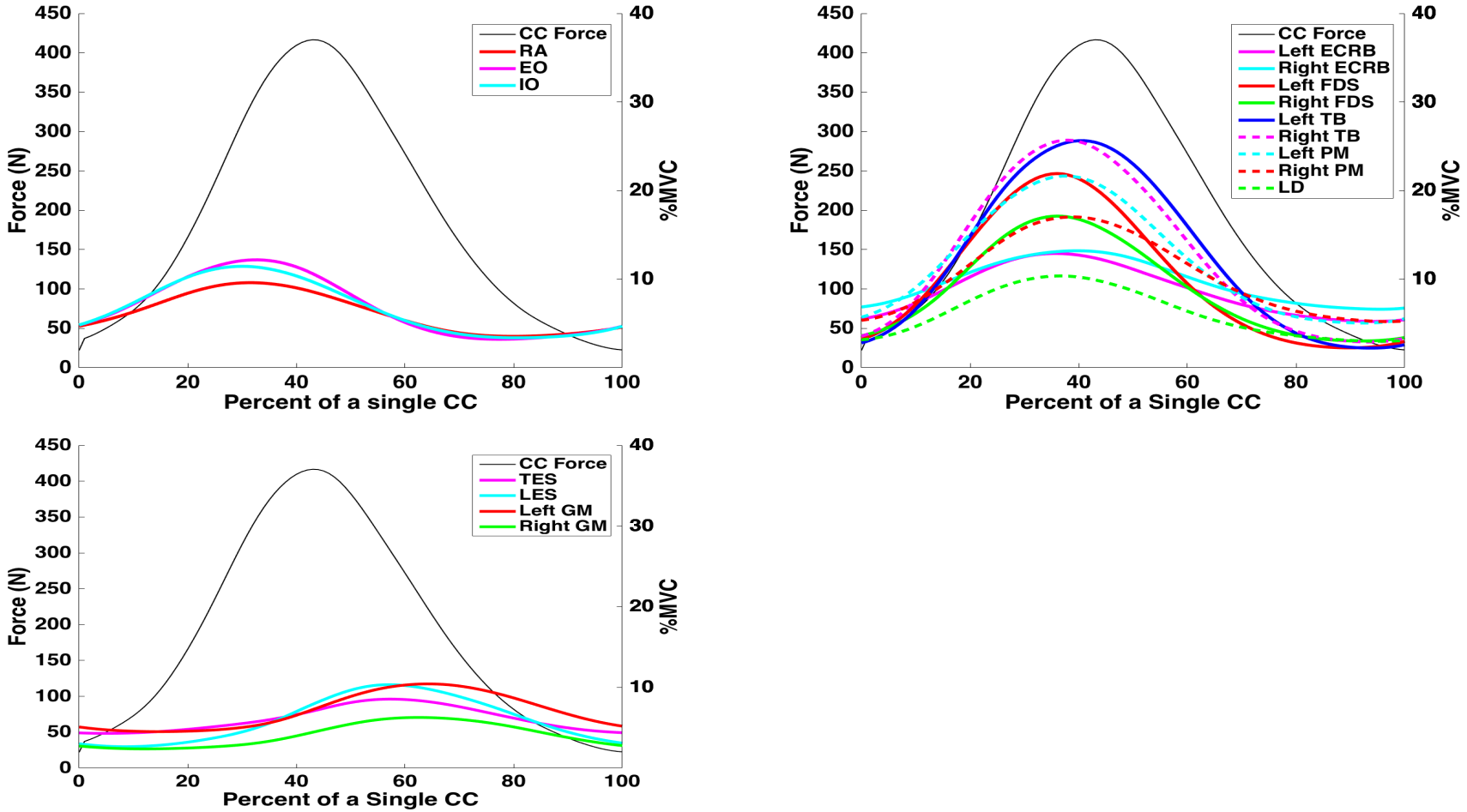

Figure 28: Ensemble averages of EMG values of each muscle and CC force during FH. 0% represents the initiation of a CC and 100% represents termination of a CC. Averages were calculated across all CC during FH. Top left represents CC initiators. Top right represents CC stabilizers. Bottom left represents CC terminators.

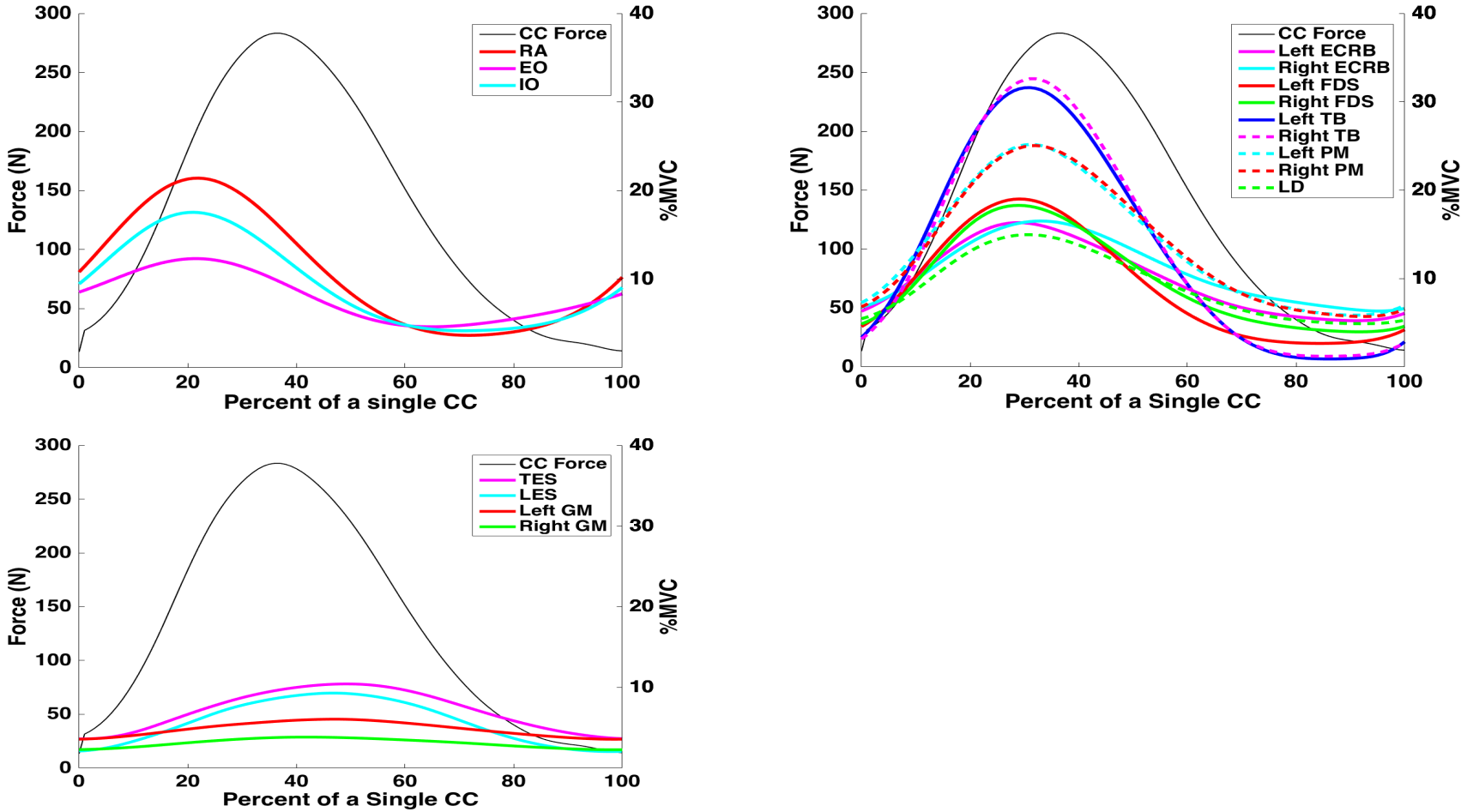

Figure 29: Ensemble averages of EMG values of each muscle and CC force during WH. 0% represents the initiation of a CC and 100% represents termination of a CC. Averages were calculated across all CC during WH. Top left represents CC initiators. Top right represents CC stabilizers. Bottom left represents CC terminators.

3.3 CPR Functionality

3.3.1 chest compression force.

Averaged across twenty CC cycles, CC force during KH, LH, FH, and WH were 517.22 N±152.62, 528.75 N±173.93, 529.44 N±183.48, and 488.49 N±181.73, respectively. WH was found to have a significantly lower CC force compared to KH ($p<0.001$), LH ($p<0.001$), and FH ($p<0.001$) (fig. 30).

In examining each CC cycle the maximum force did not exceed 600 N and all four positions displayed a linear decrease in force over the course of the trial. The slopes of KH, LH, FH, and WH were -5.5 N/cycle, -3.96 N/cycle, -3.29 N/cycle, and -4.22 N/cycle, respectively.

In evaluating the 10^{th} percentile of the APDF, CC force during KH, LH, FH, and WH were 354.25 N, 369.52 N, 351.41 N, and 214.07 N, respectively. 50^{th} percentile values of CC force during KH, LH, FH, and WH were 496.26 N, 475.61 N, 455.32 N, and 354.38 N, respectively. 90^{th} percentile values CC force during KH, LH, FH, and WH were 748.02 N, 849.77 N, 859.07 N, and 499.24 N, respectively.

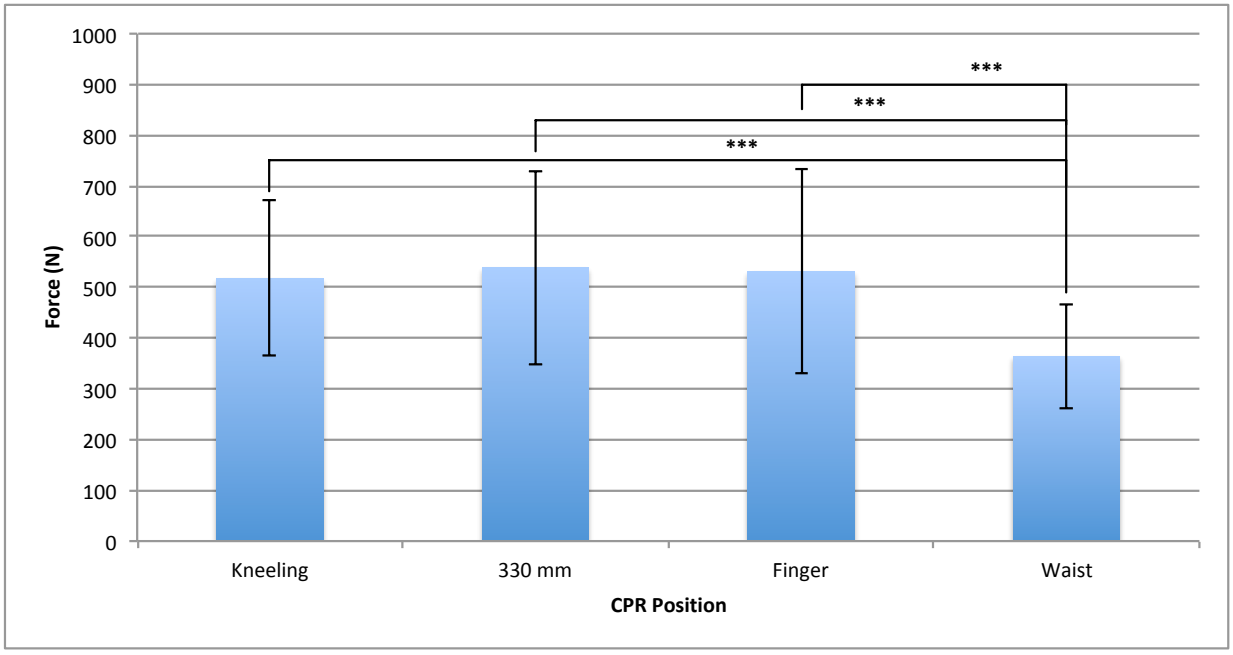

Figure 30: Average CC force across each CPR position. CC force was averaged across all CC and CC cycles per CPR position. Error bars indicate ±1 standard deviation. *** indicates a significance at $p<0.001$.

During KH, cycles ten ($p=0.012$), eleven ($p<0.001$), twelve ($p=0.002$), thirteen ($p=0.001$), fourteen ($p=0.001$), fifteen ($p=0.007$), sixteen ($p=0.017$), seventeen ($p=0.005$), and eighteen ($p=0.047$) were found to be significantly different from cycle one (581N). Displaying a significant decrease in force at approximately 2 minutes and 9.34 seconds. During LH cycles eight – eighteen ($p<0.01$) were found to be significantly lower that cycle two (595.8 N), displaying a significant decrease in force at approximately 1 minute and 37 seconds. During WH cycles five – nine ($p<0.029$) and eleven to sixteen ($p<0.032$) were found to be significantly lower that cycle two (419.5 N), displaying a significant decrease in force at approximately 59.91 seconds. While, there were no significant differences found between cycles during FH (fig. 31).

In controlling for participants' BMI the estimated marginal means of the overall CC force during KH, LH, FH, and WH were 409.61 N, 359.04 N, 388.62 N, and 315.63

N. KH was found to have significantly higher CC force compared to WH (p=0.005). Furthermore, in examining the interaction effect of sex and position, male participants had significantly lower CC force during WH compared to KH (p<0.001), LH (p=0.043), and FH (p=0.005). However, there was no significant interaction between sex and position for female participants.

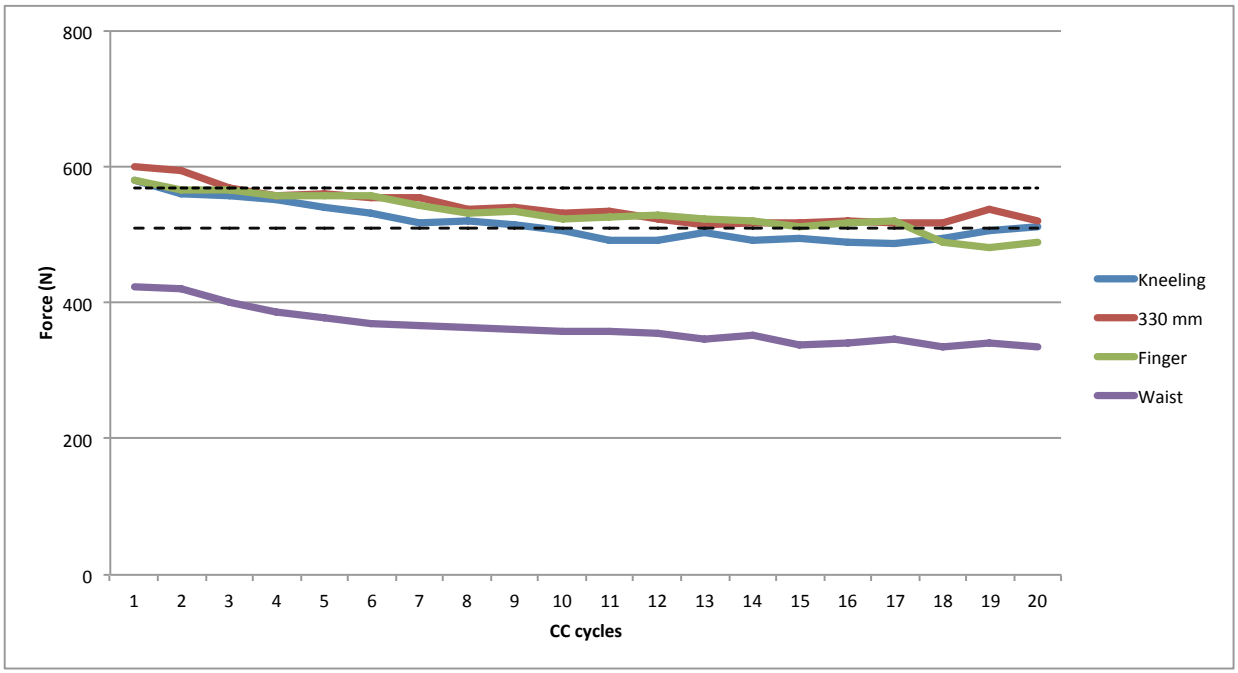

Figure 31: Average CC force across each CC cycle and CPR position. CC force was averaged across CC per CC cycle. The upper dashed horizontal line indicates a force of 568.09 N and the lower dashed horizontal line indicates a force of 510.06 N. These forces are representative of the minimum exerted force required to reach a depth of 50 mm and 60 mm, respectively, derived from the manikin in the current study.

There were no significant differences in the rate of change of CC force across all CPR positions. Extrapolated CC force did however significantly decrease throughout all CPR positions. Force decreased by 110.8 N, 98.05 N, 80.58 N, and 91.73 N during KH (p<0.001), LH (p=0.001), FH (p=0.001), and WH (p=0.001), respectively (fig 32). Furthermore, extrapolated CC force significantly decreased throughout CPR positions

when the data was pooled by sex. Male participants decreased by 119.9 N and 95.6 N during KH (p=0.008) and WH (p=0.027), respectively. Female participants decreased by 90.4 N, 88.9 N, 62.1 N, and 66.1 N during KH (p=0.002), LH(p<0.001), FH(p=0.01), and WH(p=0.004), respectively.

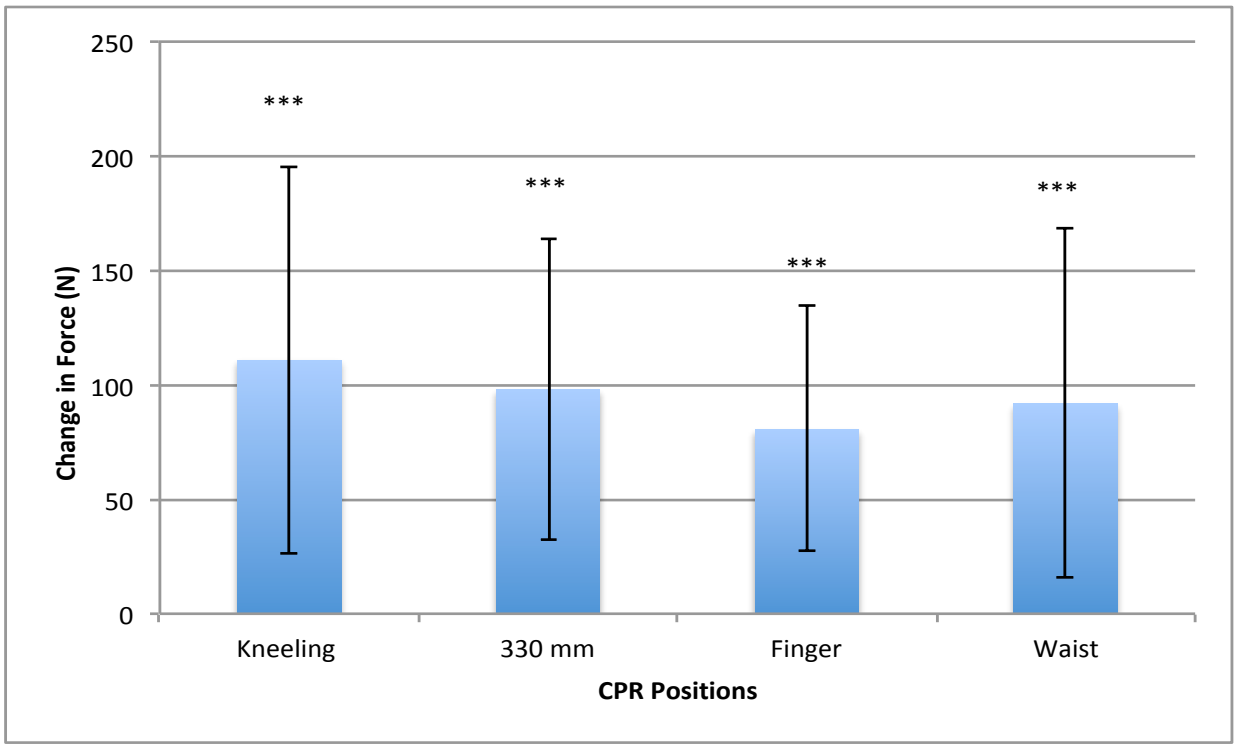

Figure 32: Magnitude and direction of the difference between cycle one and cycle twenty of the extrapolated CC force values per CPR position. Positive values indicate a drop in CC force from cycle one to cycle twenty. Error bars indicate ±1 standard deviation. *** indicates a significance at p<0.001.

3.3.2 chest compression depth.

Averaged across twenty CC cycles, CC depth during KH, LH, FH, and WH were 43.49 mm±7.83, 45.36 mm±9.44, 43.57 mm±10.28, and 33.96 mm±6.59, respectively. WH had a significantly shallower depth compared to KH (p<0.001), LH (p<0.001), and FH (p<0.001) (fig. 33).

In examining each CC cycle across all positions the standardized minimum depth (50 mm) was not attained, furthermore all positions displayed a linear decrease in depth. The slopes of KH, LH, FH, and WH were -0.329 mm/cycle, -0.229 mm/cycle, -0.195 mm/cycle, and -0.304 mm/cycle, respectively.

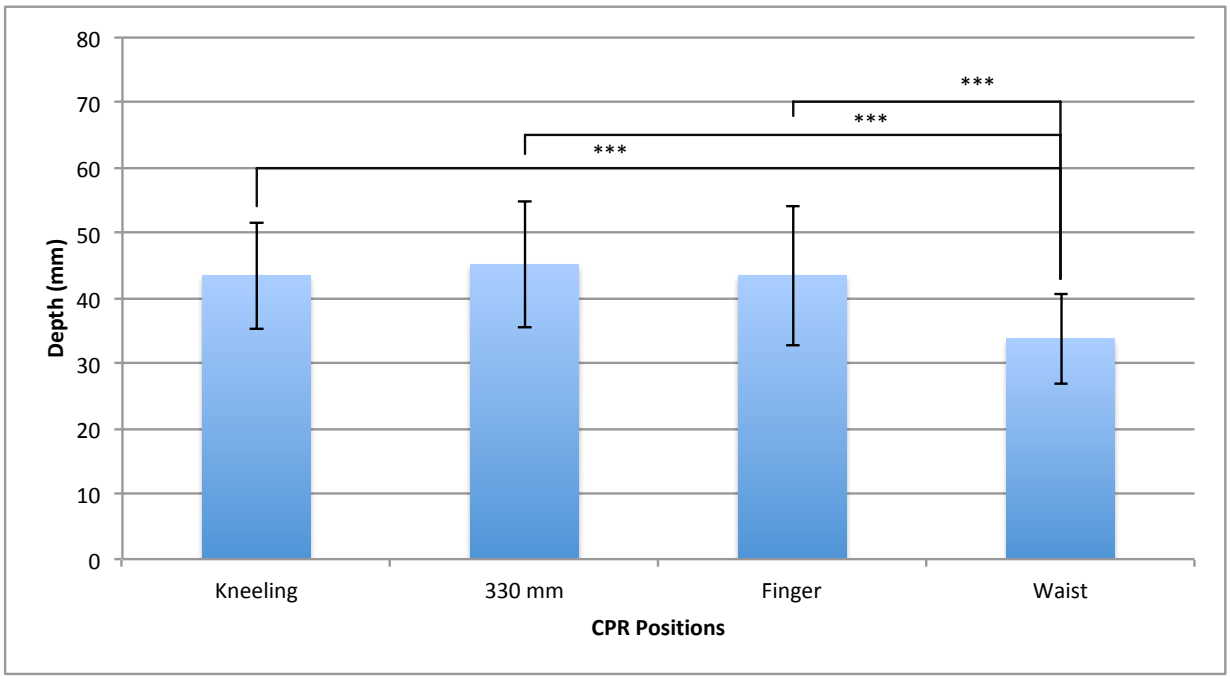

Figure 33: Average CC depth across each CPR position. CC depth was averaged across all CC and CC cycles per CPR position. Error bars indicate ±1 standard deviation. *** indicates a significance at $p<0.001$.

During KH cycles ten ($p=0.009$), eleven ($p<0.001$), twelve ($p<0.001$), thirteen ($p=0.001$), fourteen ($p=0.002$), fifteen ($p=0.001$), sixteen ($p=0.001$), seventeen ($p<0.001$), and eighteen ($p=0.003$) were found to be significantly different from cycle one (47.23 mm). Displaying a significantly decrease in CC depth at approximately 2 minutes and 9.34 seconds. During WH cycles six ($p=0.004$), eight ($p=0.029$), nine ($p<0.012$), eleven ($p=0.013$), twelve ($p=0.013$), thirteen ($p=0.002$), fourteen ($p=0.001$), fifteen ($p=0.001$), and six ($p=0.029$) were found to be significantly different from cycle two (37.93 mm).

Displaying a significantly decrease in CC depth at approximately 1 minutes and 14.5 seconds. While, during LH and FH there were no significant differences in depth when compared between CC cycles (fig. 34).

In controlling for participants' BMI the estimated marginal means of the overall CC depth during KH, LH, FH, and WH were 42.08 mm, 39.14 mm, 40.82 mm, and 33.6 3mm. KH displayed a significant increase in depth compared to WH ($p<0.001$). Furthermore, in examining the interaction effect of sex and position, male participants displayed a significant decrease in depth during WH compared to KH ($p<0.001$), LH ($p<0.001$), and FH ($p=0.001$) positions. However, there was no significant interaction between sex and position for female participants.

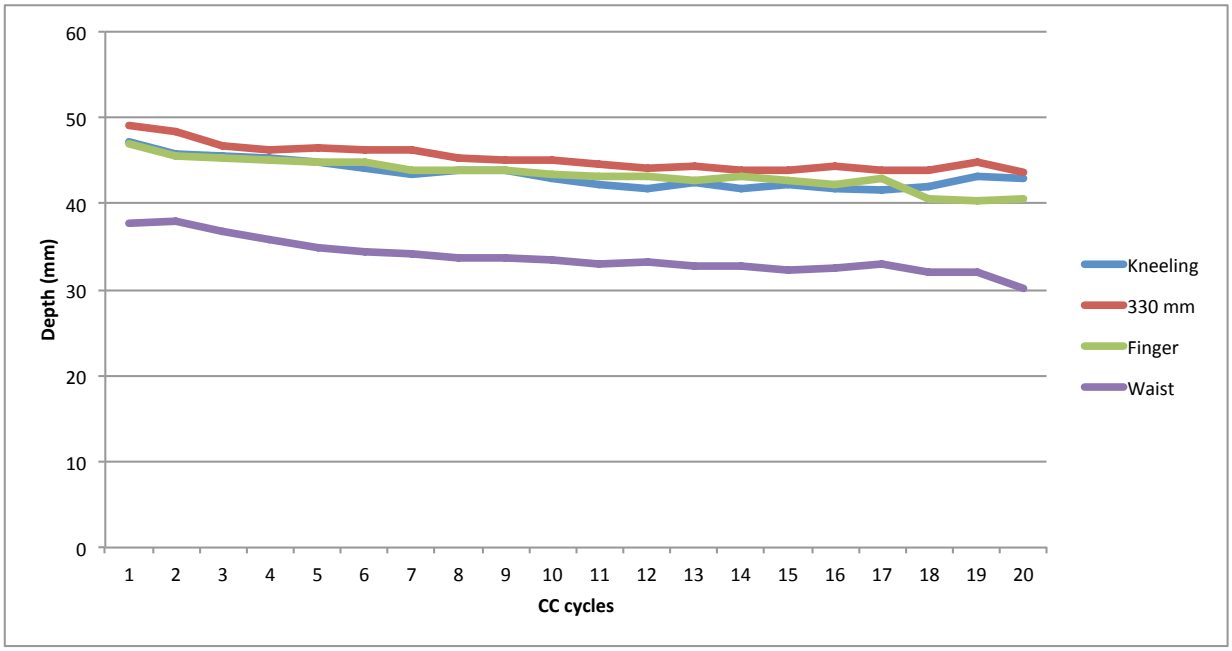

Figure 34: Average CC depth across each CC cycle and CPR position. CC depth was averaged across CC per CC cycle.

There were no significant differences in the rate of change of CC depth across all CPR positions. Extrapolated CC depth did however significantly decrease throughout all

CPR positions. Depth decreased by 6.26 mm, 4.35 mm, 3.71 mm, and 5.78 mm during KH ($p<0.001$), LH ($p=0.003$), FH ($p=0.008$), and WH ($p<0.001$), respectively (fig. 35). Furthermore, extrapolated CC depth significantly decreased throughout CPR positions when the data was pooled by sex. Male participants decreased by 6.12 mm and 5.75 mm during KH ($p=0.021$) and WH ($p=0.022$), respectively. Female participants decreased by 6.37 mm, 6.44 mm, 4.03 mm, and 5.81 mm during KH ($p=0.003$), LH ($p<0.001$), FH ($p=0.036$), and WH ($p=0.005$), respectively.

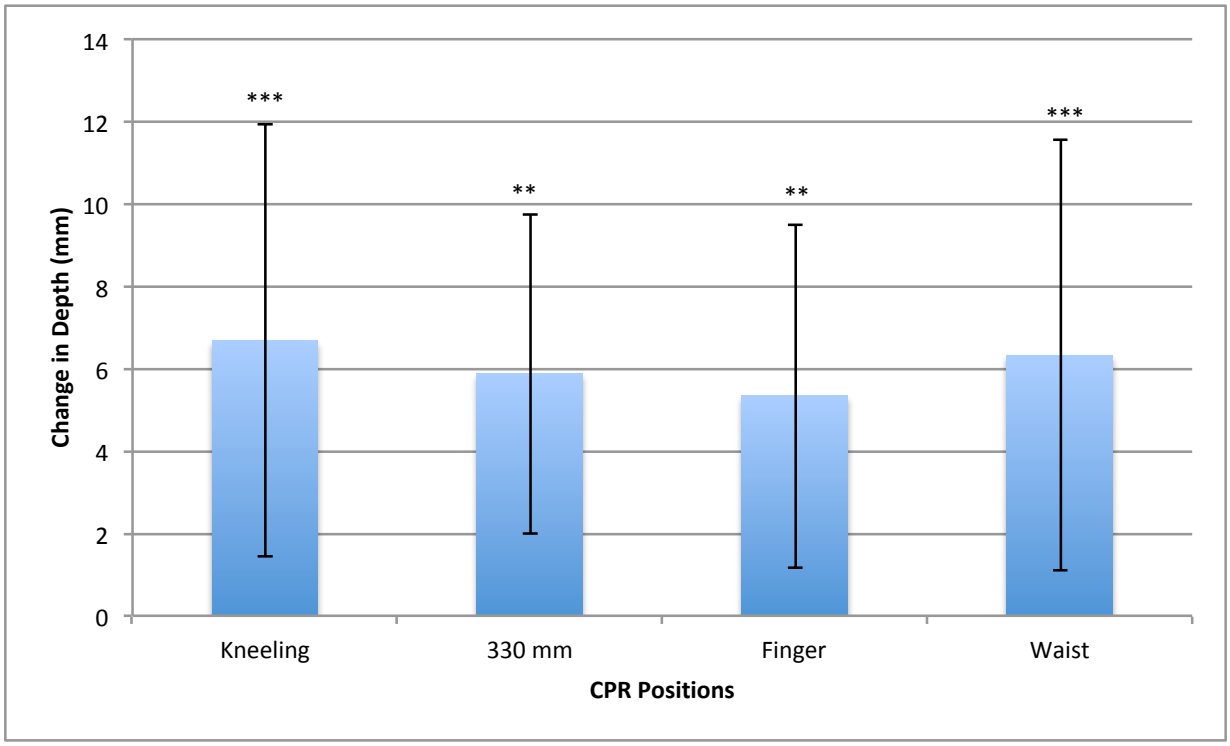

Figure 35: Magnitude and direction of the difference between cycle one and cycle twenty of the extrapolated CC depth values per CPR position. Positive values indicate a drop in CC depth from cycle one to cycle twenty. Error bars indicate ±1 standard deviation. ** indicate a significance at $p<0.01$, *** indicates a significance at $p<0.001$.

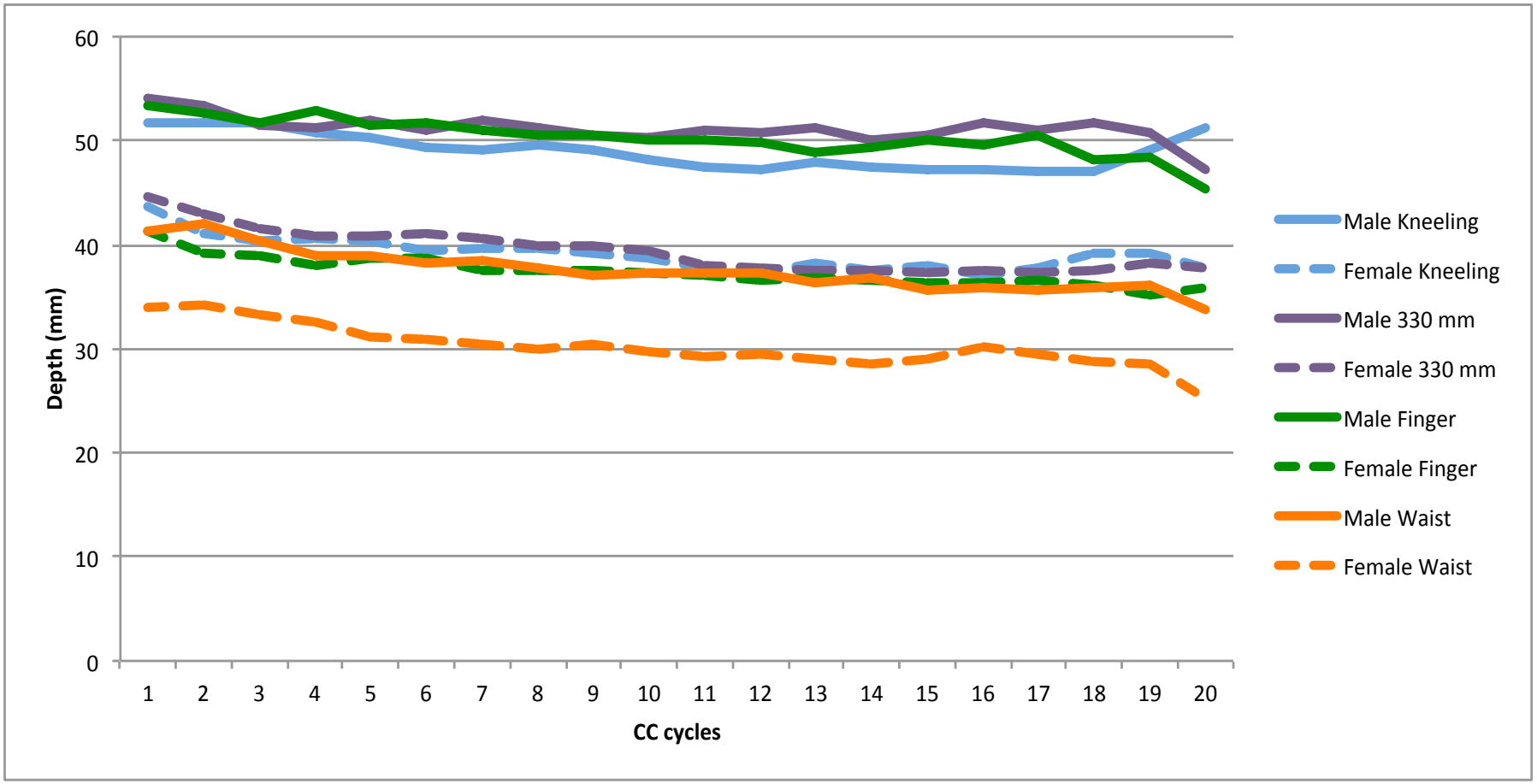

Figure 36: Average CC depth of females and males across each CC cycle and CPR position. CC depth was averaged across CC per CC cycle.

3.3.3 chest compression rate.

When averaged across twenty CC cycles, the rate of CC during KH, LH, FH, and WH were 126.15 bpm±14.7, 130.66 bpm±16.02, 130.05 bpm±18.55, and 123.81 bpm±19.19 respectively.

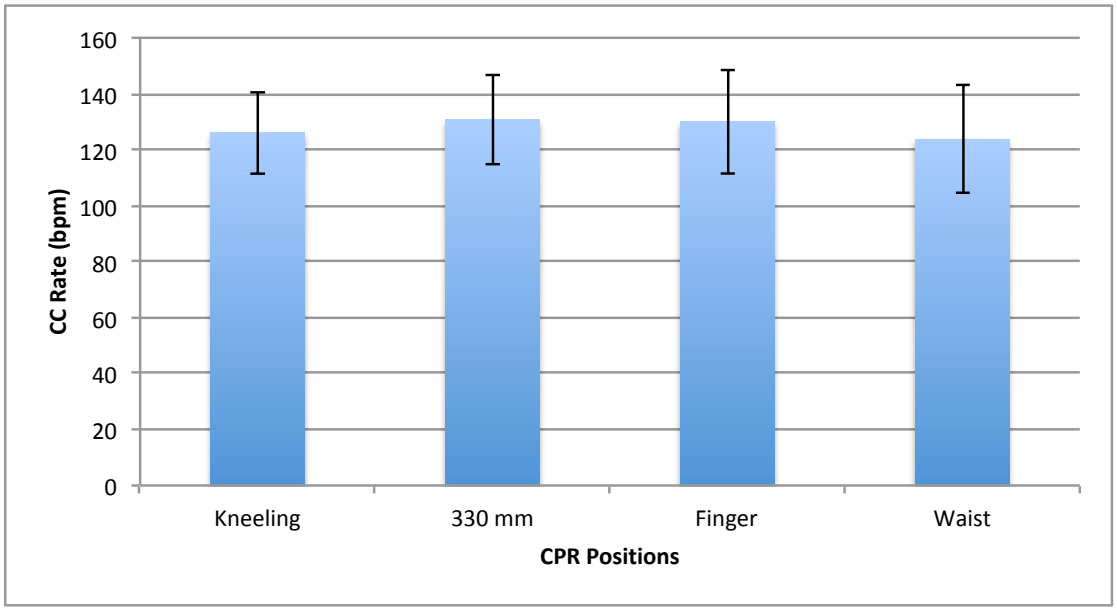

Figure 37: Average CC rate across each CPR position. CC rate was averaged across all CC and CC cycles per CPR position.

In examining each CC cycle, all cycles other than WH cycle one and two were completed at a faster rate than the guideline (100-120 bpm). In further evaluation of the data there were no significant differences in CC rates between positions. The slopes were 0.259 bpm/cycle, -0.006 bpm/cycle, 0.123 bpm/cycle, and 0.235 bpm/cycle during KH, LH, FH, and WH, respectively.

During WH, cycles fifteen ($p=0.025$), seventeen ($p=0.009$), eighteen ($p=0.01$), nineteen ($p=0.003$), and twenty ($p=0.006$) were significantly different from cycle one (118.22 bpm). While KH, LH, and FH displayed no significant differences between cycles.

In controlling for participants' BMI the estimated marginal means of the overall CC rate during KH, LH, FH, and WH were 117.53 bpm, 110.66 bpm, 106.52 bpm, and 112.55 bpm. KH displayed significantly faster CC rate compared to FH ($p<0.001$). Furthermore, in examining the interaction effect of sex and position, male participants had significantly faster CC rate during KH (130.24 bpm) compared to LH ($p=0.017$) and FH ($p=0.022$). However, there were no significant interactions between sex and position for female participants.

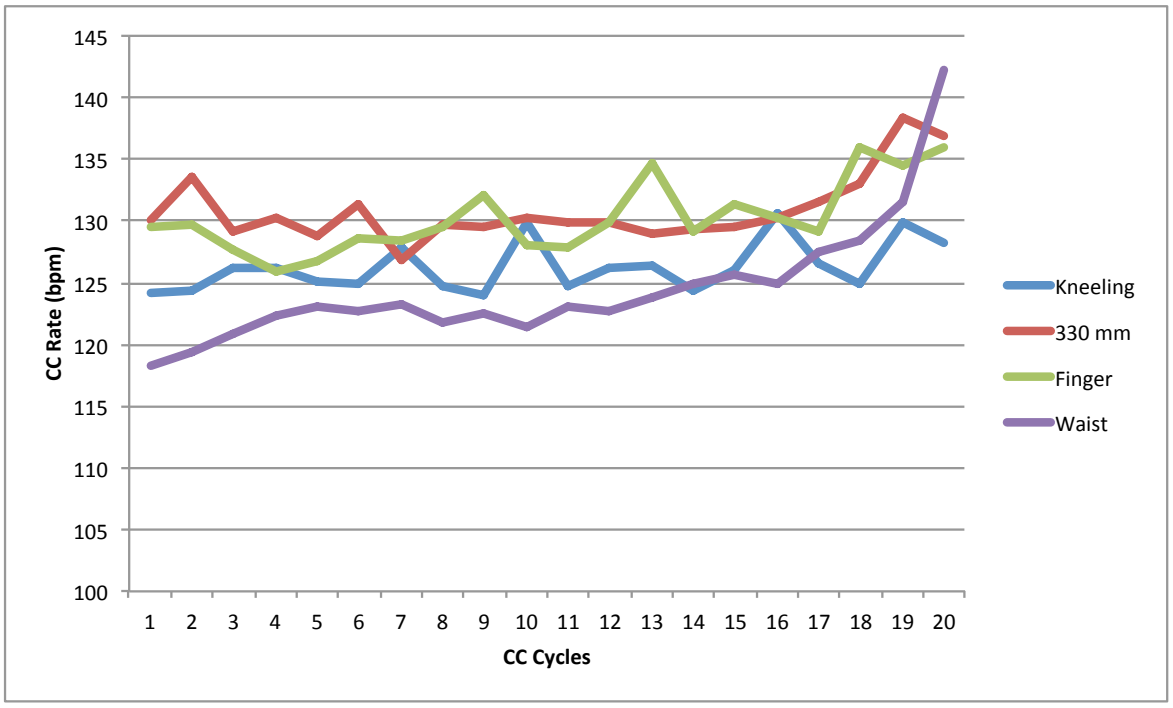

Figure 38: Average CC rate across each CC cycle and CPR position. CC rate was averaged across CC per CC cycle.

There were no significant differences in the rate of change of CC rate across all CPR positions. There were also no significant changes to extrapolated CC rate throughout all CPR positions. However, when the data was pooled by sex, male participants increased extrapolated CC rate by 9.31 bpm from cycle one to twenty during the WH ($p=0.006$).

3.3.4 chest recoil of the manikin.

When averaged across twenty CC cycles, chest recoil during KH, LH, FH, and WH were 3.61 mm±2.6, 3.41 mm±2.42, 3.91 mm±2.52, and 2.39 mm±1.62, respectively. Furthermore, it was identified that WH displayed significantly lower chest recoil compared to KH ($p=0.002$), LH ($p<0.001$), and FH ($p<0.001$) (fig. 39).

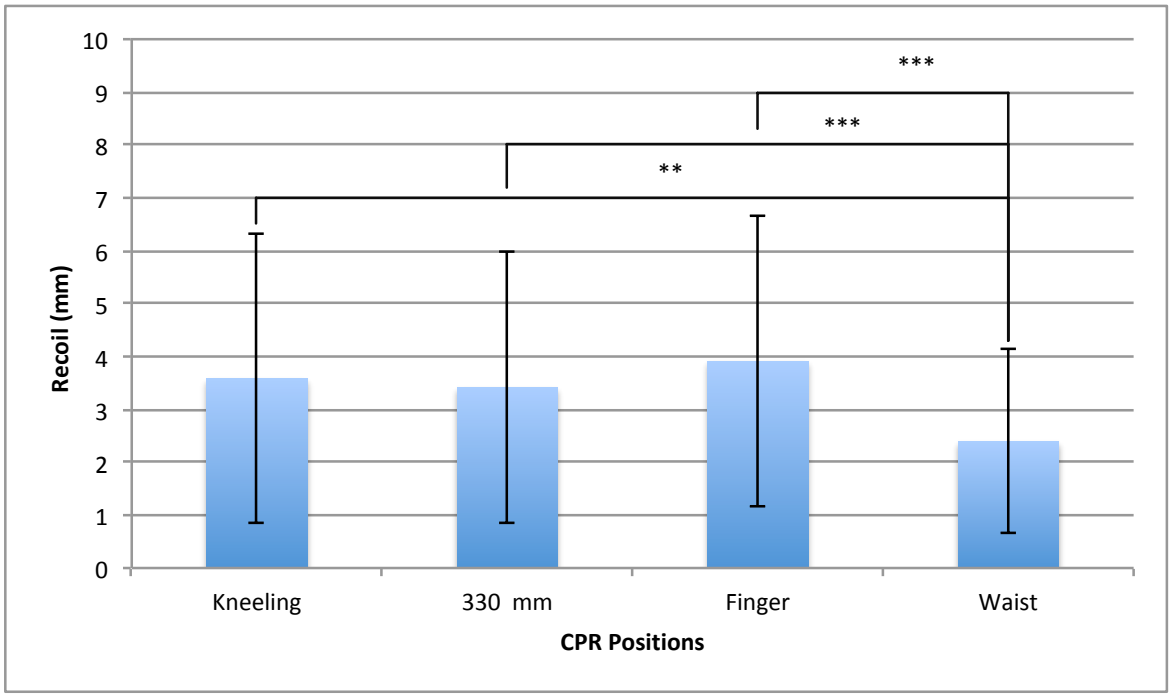

Figure 39: Average chest recoil across each CPR position. Chest recoil was averaged across all CC and CC cycles per CPR position. A positive value indicates full chest recoil was not attained. Error bars indicate ±1 standard deviation. ** indicates a significance at $p<0.01$, *** indicates a significance at $p<0.001$.

In examining each CC cycle, all positions displayed chest recoils of greater than 2 mm. In further evaluations of the cycles, there were no significant differences in the rate of change of chest recoil between positions (fig. 40). The slopes were 0.039 mm/cycle, -0.006 mm/cycle, 0.05 mm/cycle, and -0.01 mm/cycle during KH, LH, FH, and WH, respectively.

In controlling for participants' BMI the estimated marginal means of the overall chest recoil during KH, LH, FH, and WH were 3.5 mm, 3.00 mm, 2.08 mm, and 1.86 mm, respectively. LH was found to have significantly larger recoil compared to WH (p=0.023). Furthermore, in examining the interaction effect of sex and position there were no significant interactions.

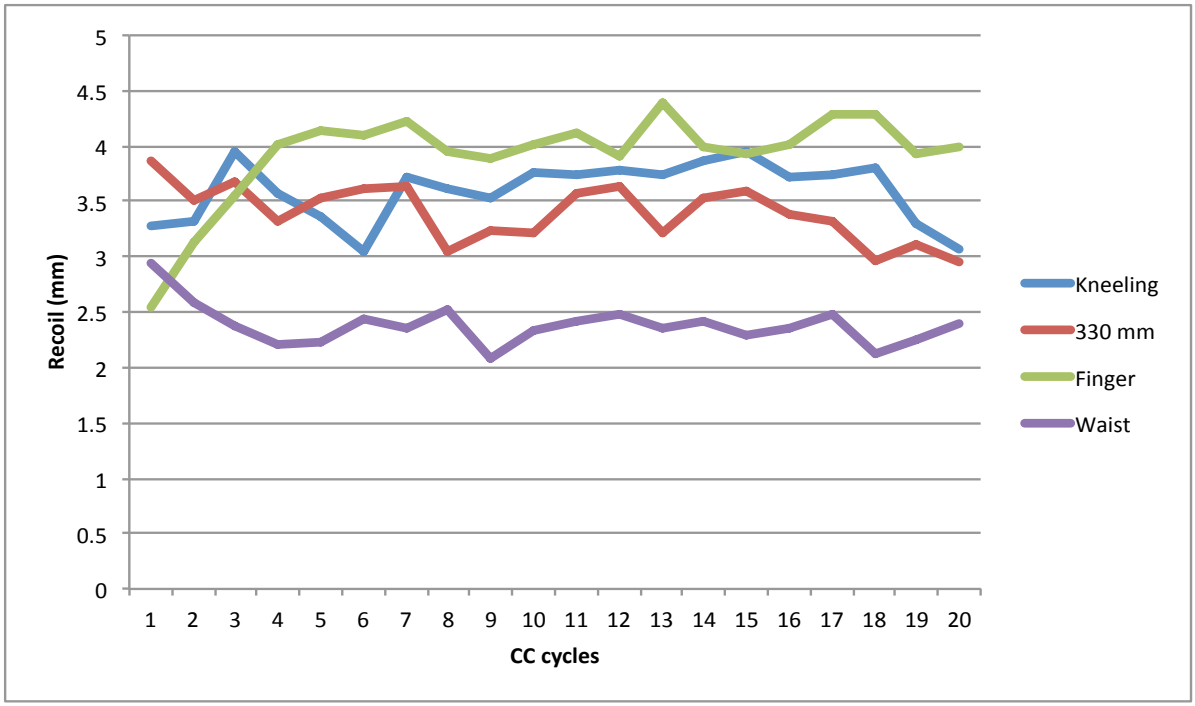

Figure 40: Average chest recoil across each CC cycle and CPR position. Chest recoil was averaged across CC per CC cycle. A positive value indicates the distance away from complete chest recoil.

There were no significant differences in the rate of change of chest recoil across all CPR positions. There were also no significant changes to extrapolated chest recoil throughout all CPR positions. However, when the data was pooled by sex, female participants increased in extrapolated chest recoil by 1.09 mm from cycle one to twenty during the FH (p=0.042).

3.4 Manikin Characteristics

3.4.1 chest angle.

When averaged across twenty CC cycles, chest angle during KH, LH, FH and WH were 11.48°±1.94, 10.85°±1.89, 10.77°±2.15, and 8.81°±1.63, respectively (fig. 41). It was identified that WH displayed significantly lower changes in angle compared to KH ($p<0.001$), LH ($p<0.001$), and FH ($p<0.001$).

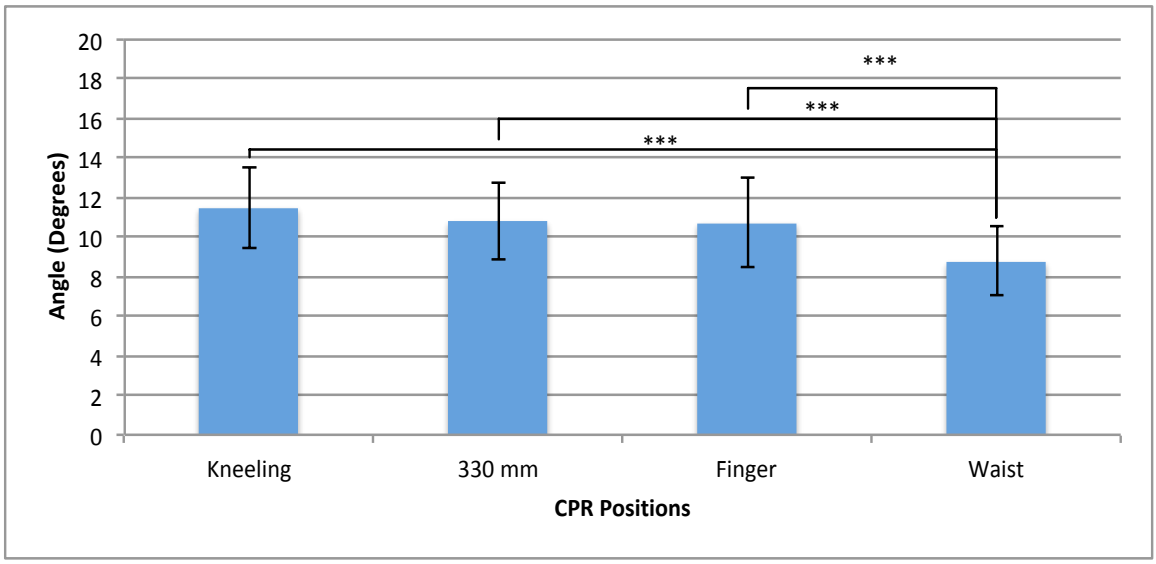

Figure 41: Average chest angle across each CPR position. Chest angle was averaged across all CC and CC cycles per CPR position. Error bars indicate ±1 standard deviation. *** indicates a significance at $p<0.001$.

Overall there were no significant differences in the rate of change of the change in chest angle between positions. The slopes were -0.092°/cycle, -0.047°/cycle, -0.051°/cycle, and -0.081°/cycle during KH, LH, FH, and WH, respectively. Furthermore, cycle eight ($p=0.03$), ten ($p=0.024$), eleven ($p=0.001$), twelve ($p=0.001$), thirteen ($p=0.002$), fourteen ($p=0.008$), fifteen ($p=0.017$), sixteen ($p=0.002$), seventeen ($p<0.000$), and eighteen ($p=0.001$) were significantly lower than cycle one (12.51°) during KH. Displaying a significant decrease in chest angle at approximately 1 minute and 40.2

seconds. During LH cycles seventeen (p=0.034) and eighteen (p=0.026) were significantly lower compared to cycle one (11.64°). While, during WH cycle five (p=0.046), six (p=0.002), seven (p=0.026), eight (p=0.007), nine (p=0.002), eleven (p=0.004), twelve (p=0.005), thirteen (p=0.001), fourteen (p<0.000), fifteen (p<0.000), and sixteen (p=0.009) were significantly lower compared to cycle two (9.87°). Displaying a significant decrease in chest angle after approximately 59.92 seconds (fig. 42).

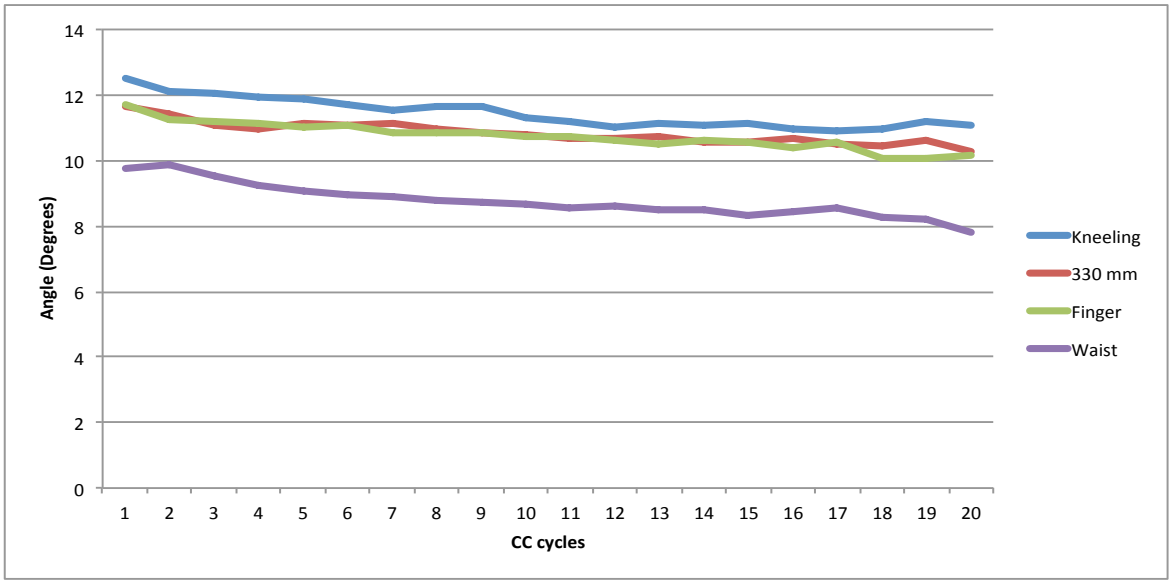

Figure 42: Average chest angle across each CC cycle and CPR position. Chest angle was averaged across CC per CC cycle.

There were no significant differences in the rate of change of chest angle across all CPR positions. Extrapolated chest angle did however significantly decrease throughout all CPR positions. Extrapolated chest angle decreased by 1.76°, 0.89°, 0.97°, and 1.54° during KH (p<0.001), LH (p=0.006), FH (p=0.008), and WH (p<0.001), respectively (fig. 43). Furthermore, extrapolated chest angle significantly decreased throughout CPR positions when the data was pooled by sex. Male participants decreased

by 1.68° and 1.5° during KH (p=0.031) and WH (p=0.013), respectively. Female participants decreased by 1.82°, 1.44°, 1°, and 1.57° during KH (p=0.002), LH (p<0.001), FH (p=0.039), and WH (p=0.005), respectively.

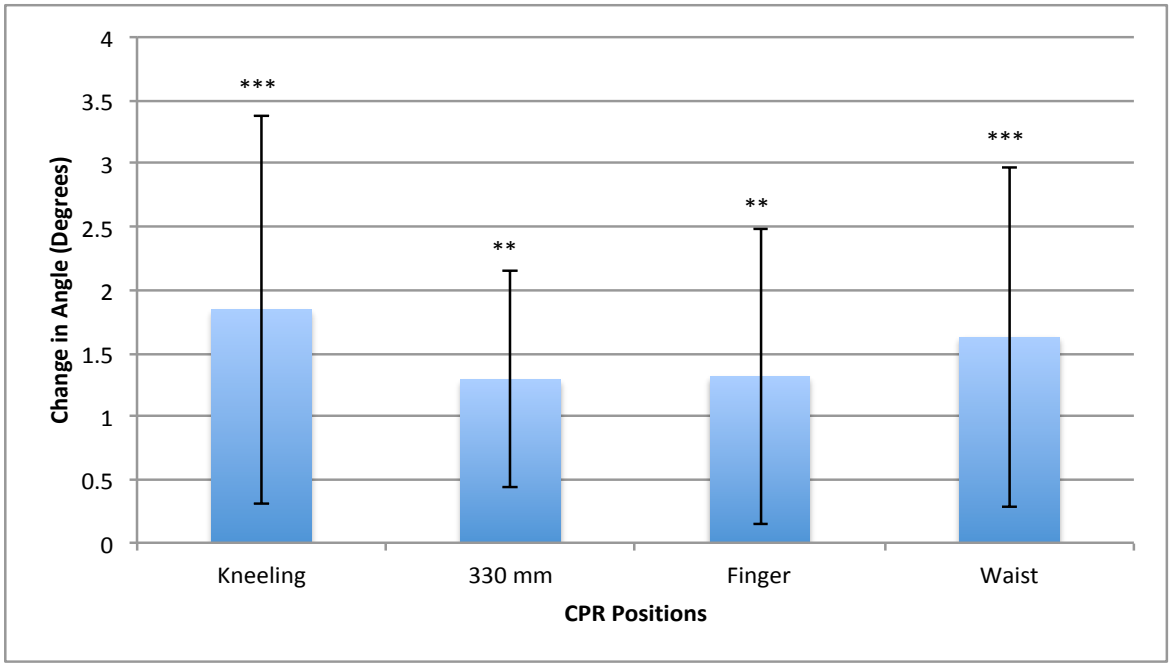

Figure 43: Magnitude and direction of the difference between cycle one and cycle twenty of the extrapolated chest angle values per CPR position. Positive values indicate a drop in chest angle from cycle one to cycle twenty. Error bars indicate ±1 standard deviation. ** indicate a significance at p<0.01, *** indicates a significance at p<0.001.

3.4.2 prediction of CC force and depth.

A linear regression was calculated during all CPR positions to predict CC force and CC depth based on the change in angle of the chest wall of the manikin. The results were significant across all CPR positions; the results were also significant when the positions were pooled together. When positions were pooled together, 91.9% of the variability in CC depth can be accounted for in changes in sternal angle ($F(1,1549) = 17475, p<0.001$), while 70.9% of the variability in CC force can be accounted for in changes in sternal angle ($F(1,1549) = 3768, p<0.001$). During KH, 96.3% of the

variability in CC depth can be accounted for in changes in sternal angle ($F(1,368) = 9446, p<0.001$), while 60.4% of the variability in CC force can be accounted for in changes in sternal angle ($F(1,368) = 561, p<0.001$). During LH, 91.4% of the variability in CC depth can be accounted for in changes in sternal angle ($F(1,383) = 4059, p<0.001$), while 73.4% of the variability in CC force can be accounted for in changes in sternal angle ($F(1,383) = 1057, p<0.001$). During FH, 93.5% of the variability in CC depth can be accounted for in changes in sternal angle ($F(1,400) = 5779, p<0.001$), while 74.1% of the variability in CC force can be accounted for in changes in sternal angle ($F(1,400) = 1144, p<0.001$). During WH, 97.7% of the variability in CC depth can be accounted for in changes in sternal angle ($F(1,392) = 16458, p<0.001$), while 70.1% of the variability in CC force can be accounted for in changes in sternal angle ($F(1,392) = 919, p<0.001$).

A line of best fit based on a logarithmic polynomial was fit to the data in figure 45 as it was speculated that a logarithmic polynomial might better represent the data.

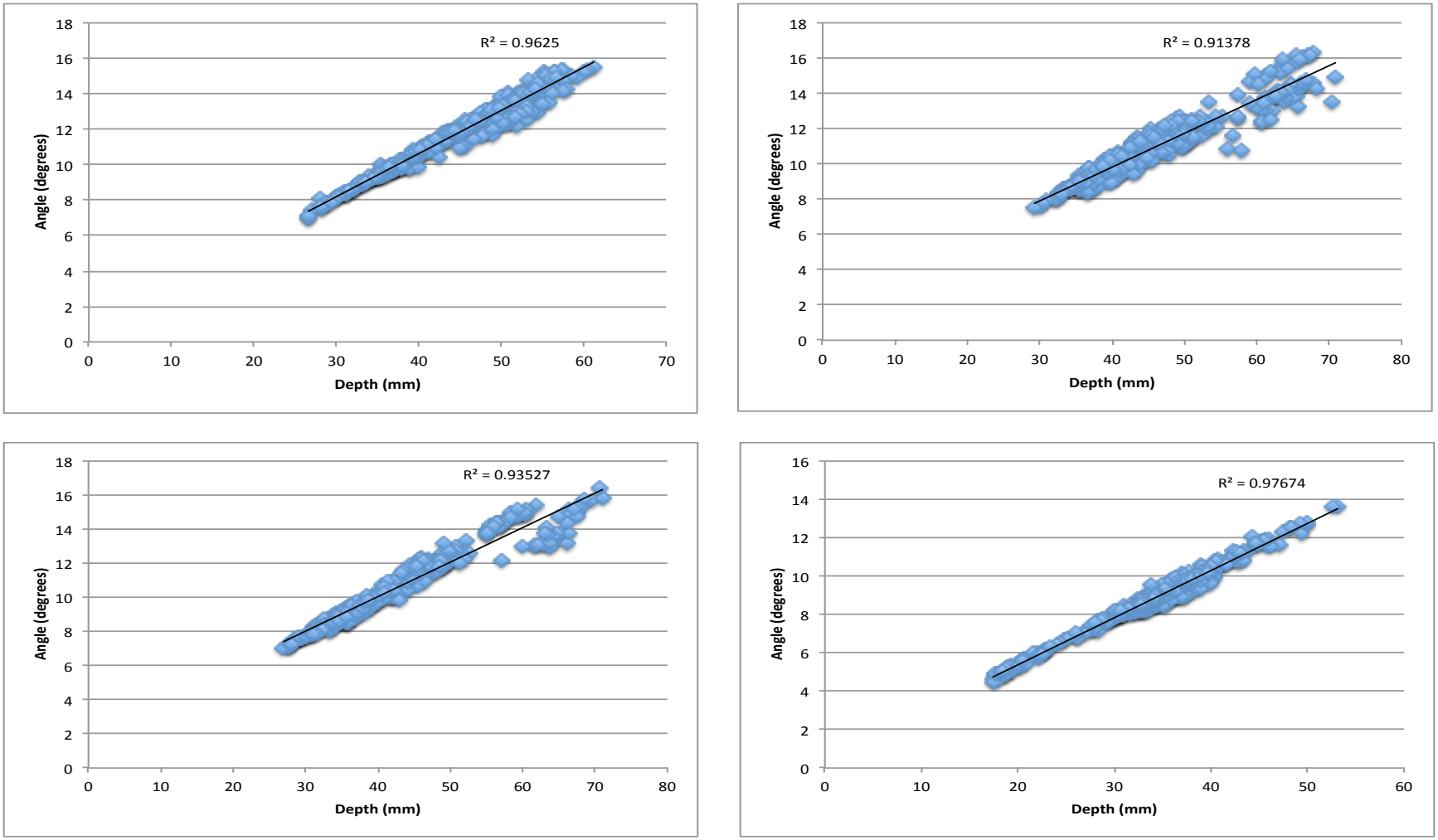

Figure 44: Average change in angle of the chest wall of a manikin during CPR and average depth of CC during CPR. Each data point represents the average CC depth and chest angle of a single CC cycle. The lines of best fit, calculated from the linear polynomial have been drawn. Top left = KH, top right = LH, bottom left = FH, bottom right = WH.

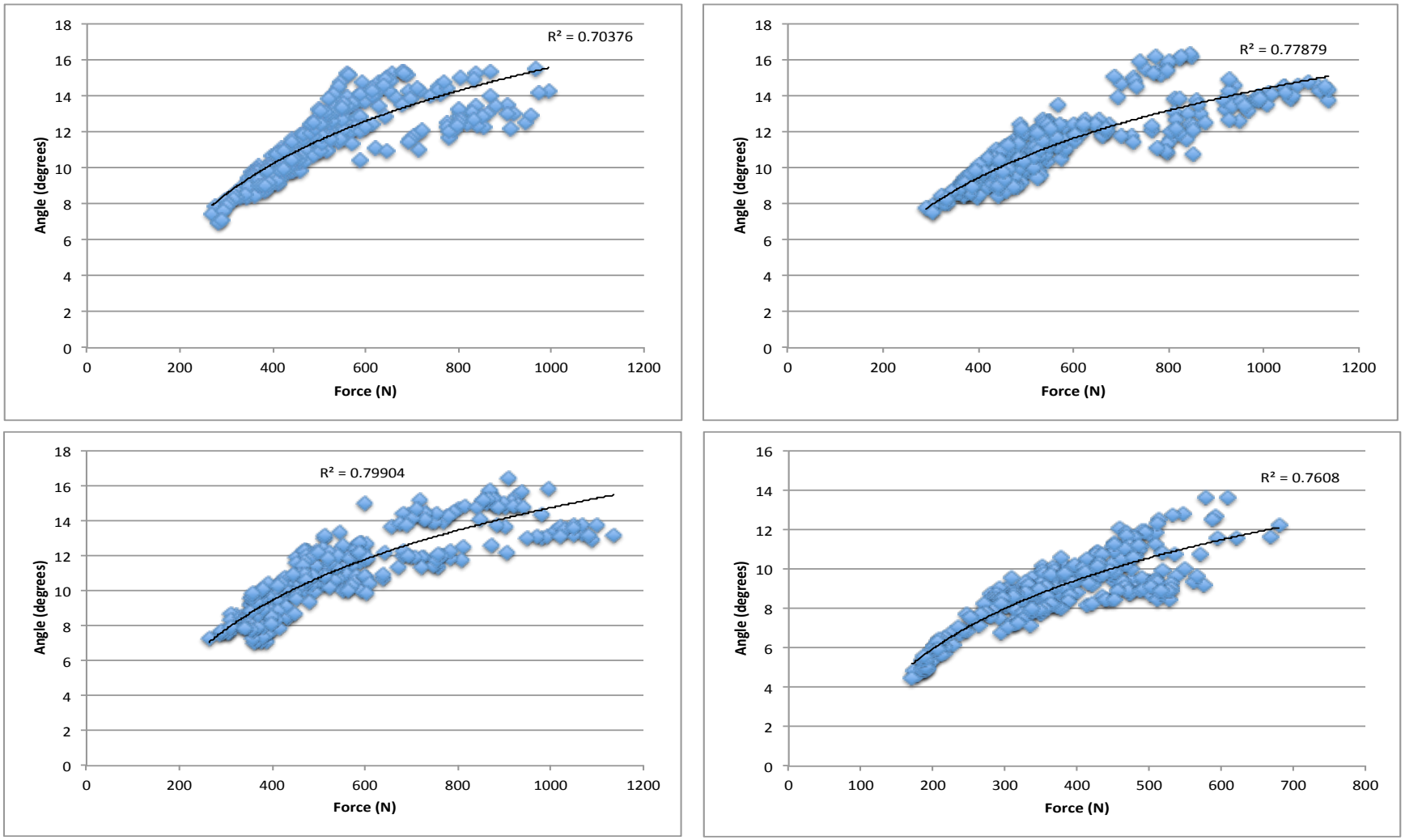

Figure 45: Average change in angle of the chest wall of a manikin during CPR and average force of CC during CPR. Each data point represents the average CC force and chest angle of a single CC cycle. The lines of best fit, calculated from the logarithmic polynomial have been drawn. Top left = KH, top right = LH, bottom left = FH, bottom right = WH.

3.4.3 spring dynamics.

The spring dynamics of the manikin were evaluated prior to commencement of the study. It was identified that maximum spring compression was 63.24 mm with an exerted force of 597.51 N. Furthermore, to reach a depth of the 50 mm an applied external force must be greater than or equal to 510.06 N and to reach a depth of 60 mm an applied external force must be greater than or equal to 568.09 N. When graphed the spring displayed a linear increase in force and depth during the compression phase and displayed evidence of hysteresis during the releases phase (fig. 46).

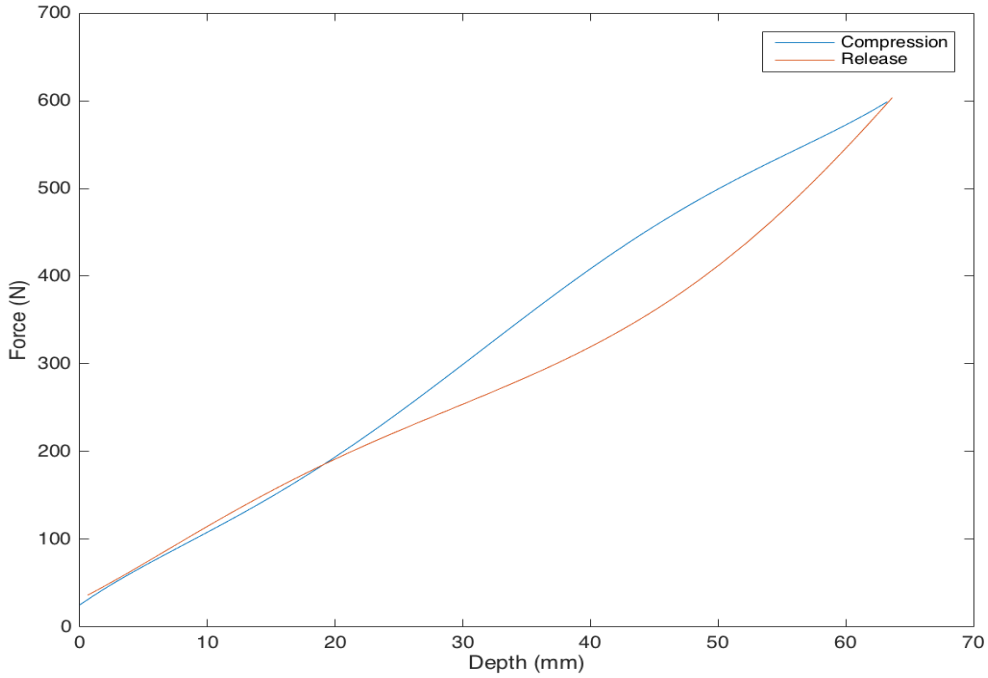

Figure 46: Spring dynamics of the Little Anne Manikin used in the current study. Results are averaged over four compression/release phases.

Chapter 4, Discussion

4.1 Revisiting the Hypotheses

The current study was driven by six hypotheses (section 1.3), which will now be revisited. Hypothesis one, which stated limiting muscles, indicated by a significant drop in MPF, would differ based on CPR position, was partially accepted. Of the sixteen muscles evaluated, eight displayed evidence of fatigue during CPR positions (section 3.1.1). The right and left TB were the only muscles to fatigue during each CPR position. During KH, EO and left GM fatigued, while during LH, left GM, LD, and TES fatigued. Lastly, during FH, LES and TES fatigued, whereas during WH, EO, LES, TES, RA, and LD fatigued. Hypothesis two, which stated muscles fatigued at different rates, based on a significant change in EMG over time compared between CPR positions, was partially accepted. Of the muscles that fatigued (hypothesis 1), three were found to have significant differences in the rate of change in peak (force development) or static (rest utilization) EMG between positions. EO displayed a significantly different peak EMG rate of change between WH and KH. Right TB and LD displayed significantly different static EMG rates of change between positions. EO displayed a steeper peak EMG rate of change during KH compared to WH, whereas the right TB displayed a steeper static EMG rate of change during LH compared to WH and LD displayed the steepest static EMG rate of change during LH. Hypothesis three, which stated muscles would fatigue at different rates during CPR positions, producing compensation methods, indicated by a muscle with a significant increase in activity compared to a muscle with a significant decrease in activity during the same position, was rejected. This hypothesis is rejected at this time as no significant increases in activity were observed. Hypothesis four, which

stated CC force, CC depth, and chest angle would decrease within each CPR position, was accepted. There was a significant decrease in CC force, CC depth, and chest angle within each position; additionally the rate of change of each measure was not significantly different between CPR positions. It should be noted that while the above measures decreased at the same rate between CPR positions, the initial values during WH were significantly lower. Hypothesis five, which stated chest recoil and CC rate would increase during CPR positions, was rejected. There was no difference in the rate of change of chest recoil and CC rate during CPR positions, or between positions. Hypothesis six, which stated perceived fatigue time would not differ from actual fatigue time, was rejected. As actual fatigue was defined as the cycle that was significantly lower in CC force compared to the higher of cycle one or two, all CPR positions except FH displayed evidence of fatigue. The difference between actual fatigue time and later occurring perceived fatigue time were as follows: 143.7 seconds, 176.6 seconds, and 101.49 seconds, during KH, LH, and WH, respectively. Furthermore, participants on average perceived fatigue 64.8 seconds before the end of the trial during FH.

4.2 Muscular Fatigue

4.2.1 Triceps Brachii.

It is evident that of all the muscles evaluated TB played one of the most significant roles, contributing to the transfer of force from the torso of the rescuer to the chest wall of the manikin. The TB consist of three heads, the long head, which was evaluated during the study, lateral head, and medial head. As all three heads act as a single unit it is a fair assumption that the observed sEMG activity of a single head may be representative of the general activity of the entire TB, however the fatigue rates, defined

as a decrease in RMS over time during sustain submaximal voluntary contractions, are different amongst the heads (Ali et al., 2015; Hussain et al., 2018). In referencing the anatomical architecture and functions of the long head of the TB, the muscle originates on the infraglenoid tubercle of the scapula and inserts on the olecranon process of the ulna. As such, it serves three main functions: extension of the elbow and shoulder, in addition to adduction of the shoulder. As the foremost upper limb posture adopted by participants across CPR positions was adduction and flexion of the shoulder in addition to extension of the elbow, the TB played an agonist role stabilizing the shoulder and elbow. As participants remained in this posture during each cycle of thirty CC the TB were required to repetitively activate and produce an extension moment at the elbow, allowing for the transfer of force distally from the trunk of the participant to the manikin. Furthermore, the TB activated approximately 10 – 25 msec prior to peak force, displayed the largest peak EMG activation, and displayed constant peak EMG activation during all positions, except LH. The aforementioned results suggest that the main responsibility of the TB is to stabilize the elbow prior to peak force, allowing for the transfer of force to the chest wall of the manikin.

Physiologically, the fibre type percentage within muscles influences the rate at which muscles fatigue. The TB are mainly composed of type II (fast-twitch) fibres, with studies identifying up to 78% of the TB fibre type to be composed of type II fibres (Jennekens et al., 1971; Mittendorfer et al., 2005). Furthermore, studies have shown that physiologically, muscles with a greater percentage of type II fibres are highly susceptible to fatigue (Deluca, 1997; Fuchs et al., 1970; Hamada et al., 2003; Komi and Tesch, 1979; Lin et al., 2002; Nakamaru and Schwartz, 1972). Nilsson and colleagues, identified a

positive correlation between the percentage of type II fibres and the time lag between EMG activity and force output (Nilsson et al., 1977). It was suggested that the drop in force and constant EMG activity is most likely attributed to the drop out of type II fibres and increase in Type I fibre recruitment (Nilsson et al., 1977). Nilsson and colleagues further suggest that this result may be influenced by SEC exhaustion, lack of substrates, and/or accumulation of lactic acid (Nilsson et al., 1977). These findings are similar to the current study, as both the right and left TB displayed an increase in time lag in almost all CPR positions (exception of the right TB during WH and left TB during LH).

To the author's knowledge there are two studies that evaluated EMG activity of the TB during CPR. Both studies evaluated participants performing CPR while at KH, where the study by Trowbridge and colleagues found that the IEMG of the TB did not change from start to end of the trial, whereas the study by Dainty and Gregory found that the left TB decreased in average EMG over the course of the trial (Dainty and Gregory, 2017; Trowbridge et al., 2009). As Trowbridge and colleagues found no difference in IEMG from start to the end of the CPR trial, the current study is in agreement with these results for all positions except for LH, which decreased similar to the results of Dainty and Gregory. The current study identified a change in peak EMG over time of the left TB, specifically a decrease in EMG over time during LH. Various explanations have been suggested for differences in EMG results of the TB, such as: migration of electrical activity to another muscle, and underling tissue geometry / electrode location during an almost fully extended elbow posture (Doheny et al., 2008; Komi and Tesch, 1979). This is evident when the relative angle of the elbow changes during CC, which could also lead

to a decrease in the amount of force, transferred from the trunk. This however will be further investigated when the participants' kinematic results are analyzed.

To the author's knowledge, an APDF has not before been applied to EMG data during CPR. Evaluating static EMG activity of the TB, the left TB displayed significantly lower static activity during WH compared to all other CPR positions. Static activity ranged from 0.42 - 1.54%MVC, suggesting that the TB had the potential to rest during ventilations. Studies have shown that in the workplace, static muscle activation above 1%MVC increases risk of muscle injuries (Aarås and Westgaard, 1987), however as CPR relies on peak activation of the TB, it is suggested that the muscle's static activation attempted to compensate for fatigue produced during peak activation. As ventilations make up approximately 21% of a CC cycle, activity of the TB is most likely lowest during ventilations, as it is speculated the TB are not highly recruited when participants performed ventilations. Furthermore, as previously mentioned static EMG over time decreased during all positions, implying that as the TB fatigued, the muscle had the potential to rest at lower activations during ventilations. These results suggest that although the right and left TB fatigued during each position, peak EMG remained constant, ensuring stability of the elbow allowing for the transfer of force, the TB also attempted to compensate for fatigue during ventilations.

4.2.2 Positional Limiting Muscles.

The current study evaluated shifts in the PSDF of sixteen muscles following CPR performed in four positions. Three previous studies set out to evaluate muscle activation while performing CPR, at KH (Dainty and Gregory, 2017; Trowbridge et al., 2009; Tsou et al., 2014). Of these studies, two evaluated shifts in the PSDF (MdPF) (Dainty and

Gregory, 2017; Tsou et al., 2014). In evaluating shifts in the PSDF Dainty and Gregory found no significant differences in LES between pre and post isometric back extension tests (Dainty and Gregory, 2017), which was in agreement with results of this study, suggesting the LES did not fatigue during KH. Tsou and colleagues evaluated shifts in the PSDF of PM, LD, RA, LES, and GM using a Hanning window of at least twelve CC in the first, third, and fifth minute of the CPR trial (Tsou et al., 2014). The results were similar to this study, except Tsou and colleagues found no evidence of fatigue in the left GM during KH (Tsou et al., 2014). A possible reason for the differences in findings may have resulted from not measuring EMG activity at the onset of the CPR trial, as participants may have fatigued (decreased MdPF) during the first minute of CC. The difference in MdPF in the third and fifth minute compared to the first would have been minimized. Furthermore, there was no control of hand force level during CC, which may have furthermore influenced the PSDF. Another possibility may be that participants adopted a slightly different posture while performing CPR. All of the participants in the study by Tsou and colleagues were healthcare professionals or first responders, whereas in this study 81% of participants were classified as either standard first aiders or first responders (first aid). As experience influences how a worker completes their job duties (Salas et al., 2016), it is speculated that experienced rescuers may adopt slightly different postures compared to non-experienced rescuers. A fourth possibility may have to do with sex, 19% of the participants were female in the study by Tsou and colleagues and 52% of participants were female in this study. Furthermore, in this study, when MPF was evaluated based on sex, females displayed a significant decrease in MPF of the left GM, whereas males did not.

Overall four muscles fatigued during KH, which included: the left and right TB, EO, and left GM. Major functions of the EO are rotation and lateral bending of the trunk, however as CPR is mainly performed in the sagittal plane, it is suggested that the main function of the EO is stabilization of the spine. This speculation is supported by the findings of Gardner-Morse and colleagues who identified that the EO offers the greatest gains in stability for the spine, however there is a trade off, as there is a greater percentage increase in fatigue (Gardner-Morse and Stokes, 1998). The GM functions as a major hip extensor, however as the GM is tightly interwoven with the lumbar paraspinal muscles it also acts as a trunk extensor, assuming the lower limbs are kept in equilibrium (Clark et al., 2003, 2002; Vleeming et al., 1995). A study by Clark and colleagues found that as the lumbar paraspinals fatigue GM increases in activity in an attempt to continue the motion (Clark et al., 2003). The findings by Clark and colleagues suggest that the GM not only extends the trunk during the release phase of CC, but may also increase in activity to compensate for fatiguing paraspinal muscles.

Overall five muscles fatigued during LH, which included: the left and right TB, left GM, LD, and TES. It is evident that LH is indicative of a stooped posture, such that the participants' trunk is flexed, as they remained standing. As the LES did not fatigue it is suggested that participants relied on the passive structures surrounding the spine (ligaments) to provide support, which required less extensor muscle activation (Salas et al., 2016). However, increased risk of ligament creep, increased intervertebral laxity, decreased muscle strength up to 1 hour and sensitivity up to 30 minutes after stretch, may result from loading passive structures (Avela et al., 1999; Fowles et al., 2000; Rose et al., 2001; Salas et al., 2016), these effects on passive structures can put the spine at risk as

much as muscle fatigue could. As the LD plays a minor role in horizontal abduction of the shoulder it is speculated that fatigue of the LD may have been exacerbated from producing an abduction moment. Assuming the elbows remained fully extended during CC, horizontal adduction moments about the shoulders are created by force at the hands. Furthermore, previous studies have shown that the LD plays a role in stabilizing the spine during trunk flexion (Cholewicki and VanVliet Iv, 2002), providing further evidence for fatigue of the LD during LH.

In evaluating FH and WH an important similarity between the two positions emerged. The TES and LES fatigued during both positions. This finding suggested that geometrical changes between positions may have caused the muscles stabilizing and extending the spine to fatigue, possibly due to a change in the direction of force. Further, neuromuscular stabilization of the spine becomes compromised due to fatigue of the trunk extensor musculature (Granata and Gottipati, 2008). Other than the TB, similarities between the two positions end there, as the EO, RA, and LD fatigued during WH. Fatigue of the RA and EO is most likely attributed to the decreased moment arm of the weight of the upper body with respect to L4/L5 (fig. 47). With the chest wall of the manikin positioned at the height of the participants' iliac crest, there was less flexion of the participants' trunk during CC. Therefore, even though the moment arm of the force at the hands with respect to L4/L5 may have also been reduced, the moment arm of the weight of the upper body would have contributed less to force production during WH compared to other CPR positions. As such, to produce a flexion moment participants relied heavily on the trunk flexors. Fatigue of the LD is most likely attributed to the increased moment arm of the force at the hands with respect to the shoulder (fig. 47). Due to the height of

the manikin during WH, the moment arm of the force at the hands with respect to the shoulder, increased, as there was decreased flexion of the participants' trunk, which resulted in the participants inability to align the shoulders, vertically, over the manikins' sternum. To compensate, participants recruited the LD to produce a shoulder extension moment.

When fatigue data was compared between sexes one of the main differences identified was that females fatigued the TB in each CPR position, while males fatigued the TB during FH and WH. This suggests that females actively recruit the TB to a level of fatigue regardless of CPR position, whereas fatigue may be position dependent for males. Curiously both sexes fatigued the TES during KH, however males fatigued during the pull isometric exercise and females fatigued during the push isometric exercises. This result suggests that fatigue of the TES during KH may be attributed to anthropometric differences between sexes, specifically trunk height. As the position participants adopted during the push/pull isometric exercises were standardized in an absolute sense, anthropometric differences between sexes could have changed the relative moment arms. This would suggest that slightly different postures might have been adopted between sexes. Lastly males fatigued the right ECRB during LH and left ECRB during WH. Furthermore, the left ECRB displayed a significant increase in amplitude (RMS) and in controlling for hand position displayed a significant drop in MPF with the left hand in contact with the manikin and during WH. These findings suggest that males actively extend their wrist during these positions to a point of fatigue. While wrist extension may be counter intuitive, ECRB is often an agonist muscle with force development in the hand, as it is required to counteract the wrist flexor moment created by the extrinsic

finger flexor muscles (flexor digitorum profundus (FDP) & FDS). In this case, active wrist extension would have the effect of moving the centre of pressure of force development on the hand closer to the wrist and more directly up the arm.

4.3 Roles of the Evaluated Muscles

As participants performed CC their muscles were repetitively activated at various time intervals and to various amplitudes, allowing for force transmission and/or force production. However, changes in electrical activity of the muscles cannot be seen as a direct causal effect for changes to CC force, as there are various physiological factors (section 1.5.1) that influence changes in EMG. As such, in evaluating EMG during CC, peak and static activity in conjunction with the time lag of the EMG signals can provide a clearer picture of the muscles roles during CPR.

Cross-correlations, which compared past, present, and future time points (Winter, 2009) of the EMG and hand force signals, were performed to determine the phase differences between the two signals, during each CPR position. Based on these analyses three distinct muscle groupings were identified. CC initiators (RA, EO, IO), displayed a time advance ranging approximately 32 to 67 msec. Upper limb stabilizers (LD, left and right FDS, PM, TB, ECRB), displayed a time advance or lag ranging approximately -15 to 30 msec. Lastly, CC terminators (LES, TES, left and right GM), displayed a time lag ranging approximately -111 to -38 msec. As the order of the three muscle groups remained constant during all CPR positions, it is suggested that order is not position dependent.

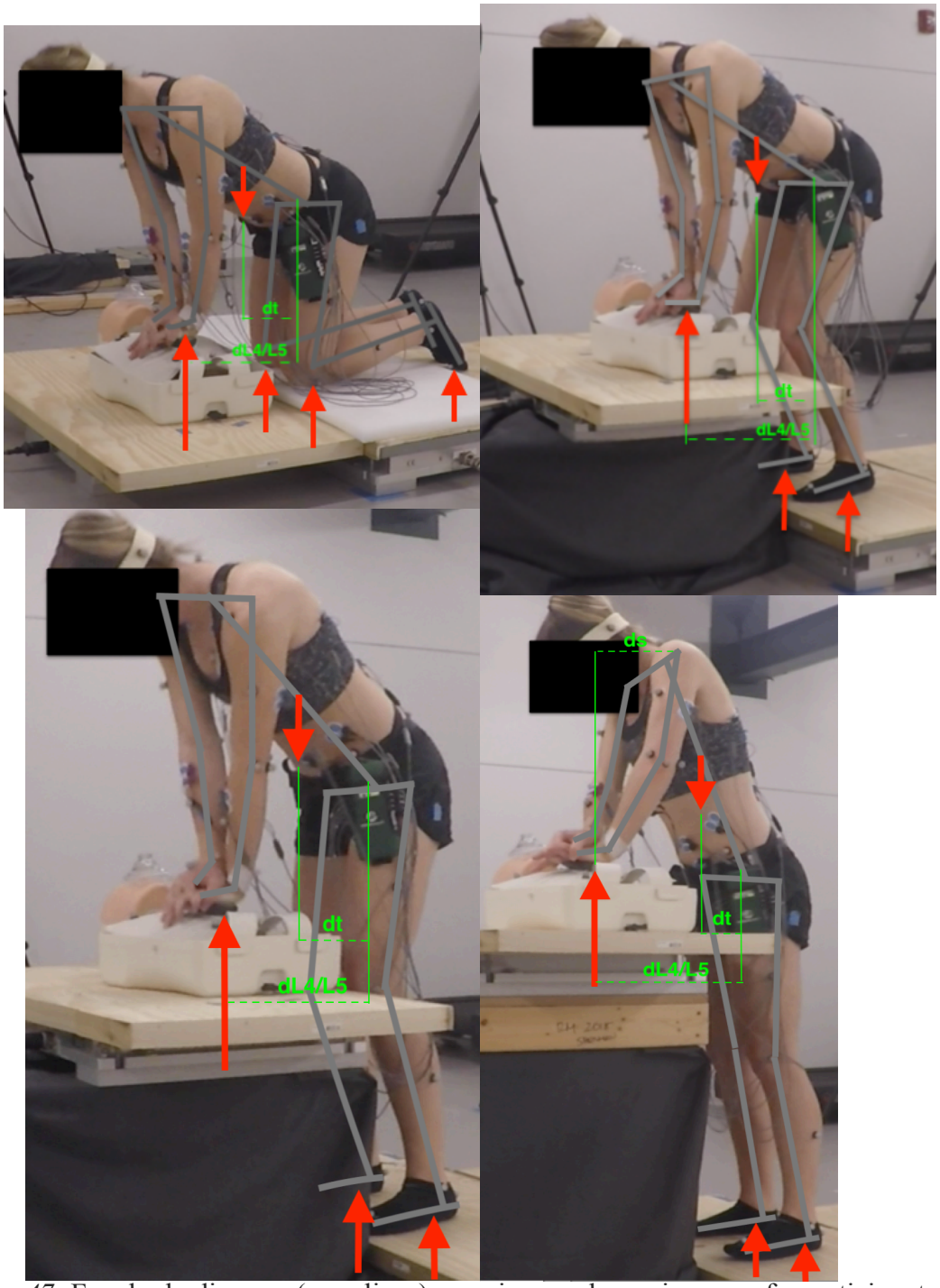

Figure 47: Free body diagram (grey lines) superimposed over images of a participant during the compression phase of CC. Red arrows pointing up represent the ground reaction forces at the hands, feet, and knees. Red arrows pointing down represent the centre of gravity of the torso. The variable dt represents the moment arm of the weight of the upper body with respect to L4/L5. The variable dL4/L5 represents the moment arm of the force at the hands with respect to L4/L5. The variable ds represents the moment arm of the force at the hands with respect to the shoulder. Top left denotes KH. Top right denotes LH. Bottom left denotes FH. Bottom right denotes WH

In evaluating peak EMG rate of change of the CC initiators, RA, EO, and IO decreased during KH, LH, and FH, while only RA decreased during WH. As peak EMG activity is closely related to force, conclusions may be drawn in regards to the CC initiators roles during the compression phase of each CC. A decreasing rate of change in peak EMG activity of RA during each CPR position suggests that RA played a role in force production, as the rate of change of CC force was also decreased during each position. The role of RA is most evident during WH, where the moment arm of the weight of the upper body with respect to L4/L5 was reduced compared to the other CPR positions. Subsequently a statistical increase in overall peak EMG activity of RA during WH, compared to the other CPR positions was observed. This result supports the findings of a study by Tsou and colleagues, who found that there was less flexion of the trunk at higher table heights and speculated that trunk flexor muscles would therefore need to compensate (Tsou et al., 2009). However, the tallest table height in the study by Tsou and colleagues was 63 cm, which is comparable to the average FH (67.4 cm) in this study. Additionally, as peak EMG over time of the EO and IO decreased during three of the four CPR positions and considering the major functions of the muscles, it is suggested that the major role of these muscles were to stabilize the spine during CC.

In evaluating the rate of change of peak EMG activity of the CC stabilizers the TB displayed constant activation during all CPR positions, except during LH. This result supports the previous conclusion that TB stabilizes the elbows prior to peak force. Furthermore, the PM displayed constant activation during all CPR positions, except KH. This finding suggests that PM stabilizes the shoulder through adduction and internal rotation. As peak EMG of the ECRB remained above 16%MVC it is evident that the

wrists were actively held in extension prior to peak force. As previously mentioned, active wrist extension may serve to move the centre of pressure of force development on the hand closer to the wrist and more directly up the arm. In addition ECRB displayed static EMG activity above 2.2%MVC during each CPR position. This may be attributed to participants delivering ventilations to the manikin using a mask. As the use of a mask requires participants to create a seal around the manikins' mouth and nose with both hands, the task requires activation of the wrist extensors. Therefore participants were unable to rest ECRB between cycles of CC.

In evaluating the rate of change of peak EMG activity of the CC terminators, TES, LES and GM displayed constant activation during all CPR positions. This result supports the previous conclusion that participants actively extended their trunk during the release-phase of CC. Furthermore the rate of change of static EMG activity of the LES displayed constant activation during all CPR positions, while the TES decreased in activity during LH. It is speculated that participants were unable to rest the LES and TES during ventilations at KH, FH, and WH, as performing ventilations required participants to actively extend the trunk. Whereas, during LH participants relied on passive structures surrounding the spine to support them during ventilations.

A study by Tsou and colleagues speculated that greater trunk extensor activity would be required to overcome the flexion moment of the trunk just after the compression-phase of CC, during KH and low table heights (Tsou et al., 2009). The results of this study do no support these speculations, as peak EMG activity of the trunk extensors were not significantly different during KH and LH compared to FH and WH, except for the left GM, which was significantly higher during LH compared to WH.

Overall, peak EMG activity was similar to a study by Tsou and colleagues, who suggested PM, RA, and LD displayed higher activity during the compression phase of CC, therefore generating the compression force, while LES and GM exhibited activity that produced trunk and hip extension (Tsou et al., 2014). This study is in agreement with the findings of Tsou and colleagues suggesting that PM, RA, and LD displayed higher activation during the compression phase of CC, while LES and GM displayed higher activation during the release phase of CC. However, results of this study suggest that the PM and LD do not produce the compression force but stabilize the upper limbs allowing for the transfer of force.

4.4 CPR Measured Outcomes

The current international CPR guidelines recommend rescuers reach a depth of 50 - 60 mm, complete CC at a rate of 100 - 120 bpm, and allow for full chest recoil (Hazinski et al., 2015). These guidelines do not vary based on the posture or height CPR is completed at, therefore it is important to evaluate CPR quality in varying positions to determine CPR quality based on the environment. In general, the results of the current study are in agreement with previous studies suggesting that over time CC depth and CC force decrease throughout the trial (Bjørshol et al., 2011, 2008b; Chi et al., 2010; Dainty and Gregory, 2017; McDonald et al., 2013; Russo et al., 2011; Sugerman et al., 2009; Trowbridge et al., 2009; Wang et al., 2015). In addition, overall CC depth and CC force were not significantly different between KH, LH, and FH, which is in agreement with the results of a previous study by Tsou and colleagues (Tsou et al., 2009). This study is also in agreement with findings of previous studies, suggesting that CC rate does not change over time (Hwang et al., 2016; Trowbridge et al., 2009). Additionally, there are a number

of studies that evaluated chest recoil as a percentage of incomplete recoils, which ranged from 2.2 – 47.2% (Aufderheide et al., 2006; Shin et al., 2014; Wang et al., 2015; Zhou et al., 2015). The results of the current study do not support these findings, as on average complete chest recoil was not attained during CPR positions.

Results of this study suggest that CC depth and CC force decrease over time regardless of CPR position, and the rate of decrease did not statistically differ between positions. Furthermore, overall CC depth and CC force were significantly lower during WH compared to all other positions. Lastly, chest recoil was found to be significantly lower during WH compared to all other positions, however chest recoil over time remained constant during each position.

4.4.1 Chest Compression Depth.

CC depth displayed one of the most unexpected results, as on average participants did not reach a minimum depth of 50 mm during any CPR position. This result is in contrast to a study by Wang and colleagues, who in following the 2010 AHA guidelines, found that 71.7% of the time participants reached the appropriate CC depth, while a total of 79.1% of participants displayed an average CC depth of greater than 50 mm (Wang et al., 2015). A possible explanation for the difference in results may have been attributed to differences in participants and training effects. Wang and colleagues recruited military medical school students six months after CPR training, whereas 81% of participants in this study were classified as either standard first aiders or first responders (first aid) and time from CPR training was not controlled for. However, results of this study were in agreement with a study by Tsou and colleagues who found that CC depth was not significantly different during KH, high table height (63 cm), and low table height (37 cm)

(Tsou et al., 2009). This suggests that rescuers were able to consistently perform CC to similar depths during KH, LH, and FH, however they were unable to reach the minimum CC depth.

As previously mentioned there was a decrease in CC depth over time during each position, with a decrease of 6.68 mm during KH, 5.88 mm during LH, 5.33 mm during FH, and 6.32 mm during WH. In pooling data across sex, dramatic differences emerge, most evident being that males were able to reach minimum depth during KH, LH, and FH. Females, however, were unable to reach the minimum depth. These results are in contrast to a study by Jaafar and colleagues who found there was no difference between sex and correct CC depth (Jaafar et al., 2015). A possible explanation for these findings may have resulted from statistically controlling for BMI in the current study, as increases in BMI have been positively correlated with CC quality (Russo et al., 2011; Sayee and McCluskey, 2012). It is speculated that the reason for the differences between sexe may not directly be attributed to BMI but anthropometric differences, specifically mass of the upper body. As previously shown, the moment arm of the weight of the upper body with respect to L4/L5 (fig. 47) contributed to generating force at the hands during the compression phase of CC. An upper body with a decreased mass would subsequently generate less force, assuming all else remains constant.

4.4.2 Chest Compression Force.

CC force is another important factor to consider in evaluating CC quality, as it is the direct cause of CC depth. The dynamics of the manikins' spring were evaluated prior to the study (section 3.4.3) and it was identified that a force of 510 – 568 N was required to depress the sternum 50 – 60 mm. Furthermore, in graphing the compression and

release phases of the spring there was evidence of hysteresis (figure 46). As the compression phase displayed a linear increase in force and depth it was suggested that damping in the release phase produced hysteresis. Previous studies identified that the human chest is best modeled using a non-linear spring and dashpot, suggesting that viscous and viscoelastic structures produced the damping effect, while an applied external force of approximately 556 N would produce a depth of 50 mm (Bankman et al., 1990; Geddes, A et al., 2007; Tsitlik et al., 1983). However, as previous studies have implemented linear springs in their methodologies (Stanley et al., 2012) it is suggested that the dynamics of the spring used in this study were consistent with the norms of simulation manikins.

As previously mentioned CC force decreased over time during all positions and was significantly lower during WH. In evaluating each position there was a decrease of 110.8 N during KH, 98.05 N during LH, 80.58 N during FH, and 91.73 N during WH. Furthermore, as no greater than 423 N was applied to the manikin during WH, participants should have fallen well below a depth of 50 mm, which was shown (fig. 31). However, CC force remained above 510 N during LH and did not drop below 510 N until the tenth cycle of KH and eighteenth cycle of FH. CC depth data did not support these findings, as a depth of 50 mm was never attained during these positions, yet a simple explanation exists, which may explain these contradicting results. The amount the manikins' sternum travels (CC depth) is dictated by the end range of the spring. At 63.24 mm the spring is fully compressed with an external force application of approximately 600 N, however participants can still exert force on the spring. This is most evident in examining the APDF of CC force at the 90^{th} percentile, where during KH, LH, FH, and

WH the respective values were 748.02 N, 849.77 N, 859.07 N, and 499.24 N. It is clear that while performing CPR during KH, LH, and FH participants may have overestimated the amount of force required to compress the spring or may have underestimated their ability to produce force. As such, when the data is pooled across CPR positions the mean values, influenced by large forces, were shifted such that it would seem as though all participants were able to achieve the minimum CC depth within three of the four positions.

When the data was pooled across sex, CC force data supports the CC depth results in that at no point during each CPR position did females apply a force greater than 504 N, therefore a depth of 50 mm was not attained. Similar CC force results were seen in studies by Dainty et al., 2015 and Trowbridge et al., 2009 who evaluated CPR during KH and found CC force dropped to 450 N by two minutes. Where, overall, females in this study began at approximately the same force level during KH, LH, and FH then dropped below 450 N by approximately 1 minute and 11.6 seconds, 1 minute and 10.7 seconds, and 1 minute and 10.3 seconds, respectively. In contrast to these results, males consistently applied a force greater than 510 N during KH, LH, and FH.

4.4.3 Chest Recoil of the Manikin.

Within the current literature there are a number of studies that evaluated chest recoil as a percentage of incomplete recoils, which ranged from 2.2 – 47.2% (Aufderheide et al., 2006; Shin et al., 2014; Wang et al., 2015; Zhou et al., 2015). All of the aforementioned studies implemented various devices specifically developed to provide results on the participants' CPR quality, whereas this study measured kinematic changes of the manikins' chest using a widely accepted motion capture system.

Furthermore, one study noted that the software defined a complete chest recoil as a return of at least 2 mm from baseline (Aufderheide et al., 2006), whereas in this study, full chest recoil was defined as a return to baseline.

This study found that chest recoil over time remained constant within CPR positions, whereas overall, participants were not able to achieve complete chest recoil, and WH displayed significantly lower chest recoil compared to all other CPR positions. As a quantitative value, which defined full chest recoil did not exists within the guidelines at the time of the study, the author assumed this value to be 0 mm or return to baseline. This value was chosen as previous studies identified that on average rescuers exerted approximately 1.7 kg of residual force, equating to approximately 3 mm of incomplete chest recoil (Tomlinson et al., 2007), where similar residual force levels, using a swine model, identified a significant decrease in cardiac index and left ventricular myocardial blood flow (Zuercher et al., 2010). However, if the value was assumed to be 2 mm, as outlined by a previous study, participants of this study were still unable to reach full chest recoil. These results suggest that participants leant on the chest wall of the manikin during each position, which did not allow for full chest recoil. The effects of leaning on the chest wall and not allowing complete chest recoil, have shown to increase diastolic intrathoracic pressure and right atrial pressure, using adult and paediatric swine models (Yannopoulos et al., 2005; Zuercher et al., 2010). Furthermore, incomplete chest recoil resulted in decreases to systolic, diastolic, mean arterial pressures, and coronary perfusion pressure (Yannopoulos et al., 2005).

4.4.4 Rate of Chest Compressions.

CC rate governs the minimum velocity CC are completed at, it does not provide a count of the actual number of CC completed per minute (Berg et al., 2010). Multiple studies have evaluated CC rate and on average it ranged from 100 – 121 bpm between studies (Betz et al., 2008; Bjørshol et al., 2008b; Jaafar et al., 2015; Pavo et al., 2016; Tsou et al., 2014; Wik et al., 2005). This study identified that on average the compression rates during KH, LH, FH, and WH were 126.1 bpm, 130.7 bpm, 130.1 bpm, and 123.1 bpm. Furthermore, CC rates over time remained constant during all CPR positions. As the current AHA guidelines recommend a rate of 100 – 120bpm, results suggest that participants completed CC too rapidly during all CPR positions. The upper limit of 120 bpm, introduced by the AHA in 2015, was in response to a large registry study that identified a dose-dependent response between CC rate and CC depth (Hazinski et al., 2015). The findings of the study suggested that CC depth became inadequate 50% of the time at CC rates between 120 - 139 bpm, while CC depth became inadequate 70% of the time at CC rates over 140 bpm (Hazinski et al., 2015). Furthermore, a single study has shown that the likelihood of return to spontaneous circulation peaks at a CC rate of 125 bpm during the first five minutes of CPR (Idris et al., 2012). As on average participants completed CC at a rate above 120 bpm during all CPR positions, results suggest that the rapid CC rate may have influenced the participants ability to reach minimum CC depth. Therefore, it is recommended that rescuers attempt to decrease CC rate during all CPR positions in an attempt to attain minimum CC depth.

When the data was pooled across sex, the results displayed that there were no significant differences in CC rate between sexes. However, male participants

significantly increased the rate of change of CC during WH. These results were in contrast to studies by Jaafar et al., 2015 and Russo et al., 2011, who identified that females performed CC more rapidly than males. Russo and colleagues suggested that BMI influences CC rate, proposing that females with a lower BMI may perform faster CC (Russo et al., 2011). Therefore, similar CC rates, in the current study, may have been caused by statistically controlling for BMI when pooling the data by sex.

4.4.5 Change in Chest Wall Angle.

As participants compress the manikins' chest wall the sternum acts as a hinge, which is fixed at the sterno-clavicular joint (Pickard et al., 2006; Shin et al., 2007). The most superior portion of the sternum cannot be compressed due to support from the clavicles and the costal cartilage connecting the manubrium of the sternum to the first and second rib, which are wide and short providing additional support for the superior portion of the sternum (Shin et al., 2007). As a result of this anatomical architecture, the sternum undergoes angular changes during CC. As the actual depth of compression cannot be measured directly with motion capture, the sternum provided a vector to estimate the compression depth directly below the hands. Similar to in-vivo, simulation manikins are a combination of sternal angle changes and linear chest wall movement. To calculate the changes in angle the superior and inferior ends of the sternum were used as landmarks in order to create a vector. To the authors knowledge there is only one study that attempted to extrapolate compression depth from angular measurements (Roskos et al., 2011). Roskos and colleagues undertook similar methodologies to this study, however they used the most distal portion of the sternum and a point on the body that did not move during CC (clavicle) to create a vector. This study identified minimal movement of the superior

portion of the manikins' sternum, however this issue was easily resolved by calculating the angle between the push and release phase vectors using the dot product and vector magnitudes. Therefore, this method allowed the author to utilize the landmarks of the sternum instead of attempting to find a point on the chest wall that does not move. Furthermore, in this study, sternal angles were calculated using two-dimensional measurements, z-axis (anterior-posterior) and x-axis (superior-inferior) in reference to the manikin.

When results were pooled across CPR positions a high correlation coefficient (R=0.958) between sternal angle and CC depth was identified, where 91.9% of the variability in CC depth can be accounted for in changes in the sternal angle. Similarly, high correlation coefficients were seen when the data was evaluated based on the CPR position, suggesting changes in sternal angle are a good predictor of CC depth during all CPR positions and the majority of depth is achieved through angular changes. These findings are supported by Roskos and colleagues, as they identified a mean absolute error of 18 mm between changes in CC depth and measured inclination using an accelerometer in two-dimensions (Roskos et al., 2011).

Changes in sternal angles were further evaluated to identify if changes in angles were a good predictor of CC force. When results were pooled across CPR positions a high correlation coefficient (R=0.842) between sternal angle and CC force was identified, where 70.9% of the variability in CC force can be accounted for in changes to the sternal angle. These results are similar to those of CC depth and change in angle, however a possible explanation for the lower correlation coefficient may be due to the participants' ability to exert force after the spring is fully compressed. Figure 45 displays graphs

comparing sternal angle and CC force; it is clear that variability within the data increases once the spring begins to reach full compression. This suggests that changes in sternal angle are a good predictor of CC force prior to full spring compression.

4.5 Perceived Fatigue and Rating of Perceived Exertion

Two measures were used in an attempt to quantify the participants' perceived level of fatigue and exertion during and between CPR positions. The Borg 15-grade scale, a validated scale that has been highly correlated to heart rates (Borg, 1982), was filled out by participants at the end of each CPR position. Participants were also asked to let the researcher know when they felt fatigued during each CPR position. Perceived fatigue time during KH, LH, FH, and WH were 4 minutes 33 seconds, 4 minutes 33.6 seconds, 4 minutes 55.2 seconds, and 2 minutes 41.4 seconds, respectively. These results were then compared to the identified actual fatigue times, defined as the CC cycle that was significantly lower in CC force compared to the higher of cycle one or two. Actual fatigue occurred at 2 minutes and 9.34 seconds during KH, 1 minute and 37 seconds during LH, and 59.91 seconds during WH. These results suggest that participants perceived fatigue time did not represent the point where CC force significantly decreased, as perceived fatigue was overestimated during KH, LH, and WH, while underestimated during FH. These results are in agreement with a study by Hightower and colleagues who found that participants perceived CC efficacy, defined as correct CC depth and hand placement, was at least 90% into 5-minutes of CPR, while CC efficacy truly fell below 90% after 1-minute of CPR (Hightower et al., 1995). As the most current advanced care life support guidelines suggests rescuers change compressors every two-minutes or sooner if fatigue (Duff et al., 2018), the results of this study find that the point at which a

rescuer perceives fatigue is past the point of actual fatigue. Therefore, based on the lowest actual fatigue time of KH and LH it is recommended that rescuers change compressors every 1 minute and 30 seconds and/or prior to the point at which the rescuer perceives fatigue.

There are a number of studies that used the 15-grade Borg or the modified Borg scale in an attempt to evaluate rescuer fatigue during CPR (Bridgewater et al., 2000; Cason et al., 2011; Chi et al., 2008; Hasegawa et al., 2014; Kwak et al., 2016; Trowbridge et al., 2009; Vaillancourt et al., 2011). Three of these studies identified a significant increase in RPE from pre to post CPR (Bridgewater et al., 2000; Hasegawa et al., 2014; Trowbridge et al., 2009), suggesting participants fatigued during CPR. This study, however, implement the RPE to determine if participants perceived exertion varied between CPR positions. The findings suggested that overall, RPE was highest during WH and there were no significant differences between KH, LH, and FH. These results are in agreement with a study by Chi and colleagues, who found no difference in RPE between CPR positions (Chi et al., 2008). The study by Chi and colleagues evaluated CPR positions of similar heights to KH, LH, and FH, however CC and ventilations were completed at a ratio of 15:2. The results suggest that perceived exertion during KH, LH, and FH were similar, which is supported by CC force and CC depth findings. Furthermore, in this study as overall CC force was significantly lower and perceived exertion was significantly higher during WH, it is suggested that rescuers perceived they worked harder, however they exerted the lowest amount of force in this position. As WH is more shoulder dominant than the other CPR positions, from an ergonomic perspective RPE is more sensitive to the use of the smaller muscles of the upper limb.

Chapter 5, Limitations

This study is not without its limitations. First, the study was conducted using a manikin in a controlled laboratory environment. Although the manikin was previously shown to be consistent with the norms of simulation manikins (section 3.4.3), the laboratory environment did not replicate the environment during actual cardiac arrest situations. Second, no data was collected using the CPRmeter 2. At the start of the study it was the authors' intention to collect data using the CPRmeter 2 and compare it to the kinetic and kinematic data. However, at the time of the study, a software package had not been released and therefore data could not be downloaded from the CPRmeter 2. As such, conclusions could not be drawn as to the validity of the CPR measures provided to the participants during CPR positions. Third, only surface upper limb and trunk muscle activity was evaluated during the study. Due to the scope of the study and number of EMG amplifiers, sixteen muscles were evaluated. The muscles were chosen for two reasons: first, they were based on a previous pilot study, completed by the author, which identified upper limb muscles with the highest activation during CPR, second, based on the literature, the evaluated muscles were expected to significantly contribute to the compression or release phases of CC. Lastly, 81% of the participant population were lay rescuers and there were minimal ranges in age between participants. At the start of the study it was the authors' intent to create three classifications, lay rescuers, first responders, and healthcare providers, in an effort to determine if there were any differences between the classifications. Lay rescuers would have been defined as participants who do not regularly treat or have the opportunity to treat patient's in-hospital and/or out-of-hospital, however are trained to a minimum of CPR-C. First

responders would have been defined as participants who regularly treat patient's out-of-hospital and healthcare providers would have been defined as participants who regularly treat patient's in-hospital. However, due to the length of the study and participant recruitment protocol it may be difficult to generalize the results of this study to the entire working population.

Chapter 6, Future Direction

First and foremost the remaining kinetic and kinematic data must be analyzed. Due to the scope and length of the study a portion of the kinetic and kinematic data remained unanalyzed. This includes kinetic data at the feet and knees, along with kinematics of the participants. This data would allow for further conclusions to be drawn in regards to the roles of the evaluated muscles during CPR positions. Results of these findings would not only provide critical ergonomic details in regards to strain placed on rescuers, it would also be clinically relevant, in identifying the appropriate posture to adopt based on the environment.

One large assumption made during the study was that the change in rate of EMG and CPR measures were linear. Albeit, previous studies have stated linear decrease in CPR measures (Bigland-Ritchie et al., 1983; Bjørshol et al., 2008a; McDonald et al., 2013; Sugerman et al., 2009), the assumption of linearity may not hold true across CPR positions or time. Therefore, future direction would be to evaluate the rate of change in EMG and CPR measures across and within participants using the spline fill methodology.

Due to the inherent variability of environments in which lay rescuers perform CPR, it is important for future studies of lay rescuer populations to focus on common CPR positions lay rescuers would adopt, such as kneeling next to a patient. However, as many first responders and healthcare providers have the means of manipulating the height of the patient, such as changing stretcher or bed height, it is imperative to place the rescuer in an optimal posture to not only minimize strain on the rescuer but optimize CPR quality. Therefore, future research should focus on identifying a position below WH that

is optimal for the rescuer and focus on a means of safely placing the rescuer in that position.

Chapter 7, Recommendations

Studies have found that during both out-of-hospital and in-hospital cardiac arrests, rescuers most often do not reach minimum guideline recommendations, defined by CC rate, CC depth ventilation rate, and no-flow fraction (Abella et al., 2005a; Wik et al., 2005). As fatigue of the rescuer plays a critical role in CPR quality, implementation of an exercise program is recommended. The exercises should focus on strengthening the muscles that fatigued during this study in conjunction to improving cardiovascular endurance. These exercises should be prescribed to rescuers whom find themselves predisposed to increased bouts of CPR such as, paramedics and members of in-hospital code teams.

CC force, CC depth, and change in angle of the chest wall were all found to be significantly lower during WH, in addition, the largest amount of muscles fatigued during WH. Furthermore, participants perceived exertion was significantly higher during WH and perceived fatigue time occurred significantly earlier during WH compared to all other CPR positions. For these reasons it is recommended that rescuers perform CPR when the patients' sternum is below the level of the rescuers' iliac crest. From the onset of CPR, CC were ineffective and declined in quality at a similar rate to KH, LH, and FH, indicating that CPR became less effective throughout the trial. Therefore, it is recommended that rescuers take time prior to CPR onset, such as when checking for signs of life, to adjust the height of the stretcher or bed to an appropriate height, for example FH. If adjusting the height of the stretcher or bed is not possible or due to variability in rescuers heights, rescuers who find themselves in a position where they may

perform CPR at or above WH, may want to consider the use of a platform that would safely elevate them off the ground.

CC rate did not change during CPR positions, however, overall CC rate was approximately 6 – 10 bpm faster, depending on the CPR position, than the upper limit of the current AHA guidelines. As a CC rate above the recommended guideline has been previously shown to be detrimental to CC depth, it is recommended that rescuers reduce their rate of CC. This is particularly important for female rescuers as decreasing CC rates may influence their ability to attain minimum CC depth. Another CPR measure, CC force was over exerted during CC. It was identified that approximately 600 N was required to fully compress the spring of the manikin, however in examining the APDF of peak CC force, force exceeded 700 N during KH, LH, and FH, suggesting that participants exert more force than required to compress the spring. In exerting more force than required rescuers may fatigue sooner, therefore it is recommended that feedback devices be improved to detect full chest compression or measure force, informing the rescuer when they exert too much force. To the authors knowledge there is currently no feedback device on the market that provides information on force exerted by the rescuer. As CC force is an important variable to consider in rescuer fatigue a feedback device that displays CC force and CC depth comparisons would be useful for the rescuer to either decrease or increase force in order to attain the minimum depth.

Lastly, the author recommends that rescuers attempt to rest the TB during ventilations. As it has been shown that the TB play a critical role in the transfer of force through the upper limbs and receive minimal rest during CC, it is recommended that the rescuer rest the TB during ventilations if CPR is being performed by two or more

rescuers. The rest the TB receives during ventilations may play an important role in attempting to decrease the rate at which the TB fatigues during CPR. Furthermore, as rescuers overestimated their perceived fatigue in three of the four positions, it is important for rescuers to implement a change in compressors early into CPR to ensure CPR quality remains high. Therefore, it is recommended a change in rescuer performing CC occur at one minute and thirty seconds and/or prior to the point of perceived fatigue. This recommendation should be implemented across all recommended positions in an attempt to reduce the rate of rescuer fatigue during CPR.

Chapter 8, Conclusion

Of the sixteen muscles analyzed during this study, eight fatigued. The right and left TB, EO, and left GM fatigued during KH. The right and left TB, LD, TES, and left GM fatigued during the LH. The right and left TB, TES, and LES fatigued during FH. Lastly, the right and left TB, RA, EO, LES, TES, and LD fatigued during WH. During KH it was suggested that the major function of the EO was stabilization of the spine, while the left GM extended the trunk during the release phase of CC. During LH participants relied on the passive structures surrounding the spine, which required less extensor muscle activity. During FH and WH changes in the direction of the force may have caused the TES and LES to fatigue. Lastly fatigue of RA and EO during WH is most likely attributed decreased moment arm of the weight of the upper body with respect to L4/L5.

It is evident that the TB plays a critical role during CC, by stabilizing the elbowing allowing for the transfer of force. The TB fatigued during each CPR position, displayed the highest peak EMG activation, and the peak EMG activity over time remained constant during all positions, except during LH, implying that the highly repetitive actions of CC leads to fatigue of the muscle. However, it is suggested that participants attempted to compensate for fatigue of the TB by decreasing static activation during ventilations.

Three distinct muscle groupings were identified within the four CPR positions, CC initiators (RA, EO, IO), upper limb stabilizers (LD, left and right FDS, PM, TB, ECRB), and CC terminators (LES, TES, left and right GM). It was identified that the CC

initiators played a role in force production and spine stabilization at the onset of CC. The upper limb stabilizers were found to stabilize the upper limbs during the compression phase of CC, allowing for force transmission, while the CC terminators were found to extend the trunk during the release phase of CC.

CC depth and CC force decreased over time during each CPR position, however the rate of decrease did not statistically differ between positions. Furthermore, overall CC depth and CC force were significantly lower during WH. On average participants were unable to reach minimum depth and decreased on average 6.68 mm, 5.88 mm, 5.33 mm, and 6.32 mm during KH, LH, FH, and WH, respectively. When CC depth was evaluated based on sex it was identified that males were able to achieve minimum depth during KH, LH, and FH, however females were unable to achieve minimum depth. Lastly, during KH, LH, and FH participants exerted more force than required to compress the spring.

CC rate and chest recoil remained constant over time during each CPR position. As chest recoil results found that participants did not attain full chest recoil during CPR positions, it is suggested that participants leant on the chest wall of the manikin during the release phase of CC. Further results suggest that participants completed CC at a rate above the recommended range during all CPR positions.

In conclusion CPR is a life saving technique performed by rescuers during out-of-hospital and in-hospital scenarios that place the rescuer in varying postures and expose the body to highly repetitive forces. As CPR will remain the standard of care for patients experiencing a cardiac arrest, until automated CC devices become more prevalent, it is essential to identify a rotational timeline and an optimal rescuer position based on the environment. As such, a rotational timeline of one minute and thirty seconds should be

implemented across recommended CPR positions and rescuers should perform CPR to a point in time prior to when they perceive fatigue. Furthermore, rescuers are advised to take advantage of breaks during CC, such as ventilations (if two or more rescuers are performing CPR) to rest. It is also advised that rescuers perform CPR below WH, by taking time to lower the patient or safely raising the rescuer prior to commencement of CPR.

.

References

Aarås, A., Westgaard, R.H., 1987. Further studies of postural load and musculo-skeletal injuries of workers at an electro-mechanical assembly plant. Appl. Ergon. 18, 211–219. doi:10.1016/0003-6870(87)90006-8

Abella, B., Alvarado, J., Myklebust, H., Barry, A., Hearn, N., Hoek, T.L. Vanden, Becker, L., Edelson, D., Barry, A., O'Hearn, N., Vanden Hoek, T., Becker, L., 2005a. Quality of cardiopulmonary resuscitation during in-hospital cardiac arrest. Jama 293, 305–10. doi:10.1001/jama.293.3.305

Abella, B., Sandbo, N., Vassilatos, P., Alvarado, J., O'Hearn, N., Wigder, H., Hoffman, P., Tynus, K., Vanden Hoek, T., Becker, L., 2005b. Chest compression rates during cardiopulmonary resuscitation are suboptimal: A prospective study during in-hospital cardiac arrest. Circulation 111, 428–434. doi:10.1161/01.CIR.0000153811.84257.59

Abella, B.S., Alvarado, J.P., Myklebust, H., Barry, A., Hearn, N.O., Hoek, T.L. Vanden, Becker, L.B., 2012. Quality of Cardiopulmonary Resuscitation During In-Hospital Cardiac Arrest 293, 305–310.

Ali, M.A., Sundaraj, K., Ahmad, R.B., Ahamed, N.U., Islam, M.A., Sundaraj, S., 2015. Muscle Fatigue in the Three Heads of the Triceps Brachii during a Controlled Forceful Hand Grip Task with Full Elbow Extension Using Surface Electromyography. J. Hum. Kinet. 46, 69–76. doi:10.1515/hukin-2015-0035

Allison, G.T., Fujiwara, T., 2002. The relationship between EMG median frequency and low frequency band amplitude changes at different levels of muscle capacity. Clin. Biomech. 17, 464–469.

Arendt-Nielsen, L., Mills, K.R., 1988. Muscle fibre conduction velocity, mean power frequency, mean EMG voltage and force during submaximal fatiguing contractions of human quadriceps. Eur. J. Appl. Physiol. Occup. Physiol. 58, 20–25. doi:10.1007/BF00636598

Aufderheide, T.P., Pirrallo, R.G., Yannopoulos, D., Klein, J.P., von Briesen, C., Sparks, C.W., Deja, K. a., Kitscha, D.J., Provo, T. a., Lurie, K.G., 2006. Incomplete chest wall decompression: A clinical evaluation of CPR performance by trained laypersons and an assessment of alternative manual chest compression-decompression techniques. Resuscitation 71, 341–351. doi:10.1016/j.resuscitation.2006.03.021

Avela, J., Kyröläinen, H., Komi, P. V, 1999. Altered reflex sensitivity after repeated and prolonged passive muscle stretching. J. Appl. Physiol. 86, 1283–91. doi:10.1007/bf00436748

Babbs, C.F., 1980. New versus old theories of blood flow during CPR. Crit Care Med 8, 191–195. doi:10.1097/00003246-198003000-00026

Babbs, C.F., Voorhees, W.D., Fitzgerald, K.R., Holmes, H.R., Geddes, L.A., 1983.

Relationship of blood pressure and flow during CPR to chest compression amplitude: Evidence for an effective compression threshold. Ann. Emerg. Med. 12, 527–532. doi:10.1016/S0196-0644(83)80290-X

Bankman, I.N., Gruben, K.G., Halperin, H.R., Popel, A.S., Guerci, A.D., Tsitlik, J.E., 1990. Identification of dynamic mechanical parameters of the human chest during manual cardiopulmonary resuscitation. IEEE Trans. Biomed. Eng. 37, 211–217. doi:10.1109/10.46262

Berg, R.A., Hemphill, R., Abella, B.S., Aufderheide, T.P., Cave, D.M., Hazinski, M.F., Lerner, E.B., Rea, T.D., Sayre, M.R., Swor, R.A., 2010. Part 5: Adult Basic Life Support: 2010 American Heart Association Guidelines for Cardiopulmonary Resuscitation and Emergency Cardiovascular Care. Circulation 122, S685–S705. doi:10.1161/CIRCULATIONAHA.110.970939

Betz, A.E., Callaway, C.W., Hostler, D., Rittenberger, J.C., 2008. Work of CPR During Two Different Compression to Ventilation Ratios With Real-time Feedback. Resuscitation 76, 278–282. doi:10.1007/s11103-011-9767-z.Plastid

Bigland-Ritchie, B., 1981. EMG/force relations and fatigue of human voluntray contractions. Exerc. Sport Sci. Rev. 9, 75–118.

Bigland-Ritchie, B., Donovan, E.F., Roussos, C.S., 1981. Conduction velocity and EMG power spectrum changes in fatigue of sustained maximal efforts. J. Appl. Physiol. 51, 1300–1305.

Bigland-Ritchie, B., Johansson, R., Lippold, O.C., Woods, J.J., 1983. Contractile speed and EMG changes during fatigue of sustained maximal voluntary contractions. J. Neurophysiol. 50, 313–324.

Bjørshol, C.A., Søreide, E., Torsteinbø, T.H., Lexow, K., Nilsen, O.B., Sunde, K., 2008a. Quality of chest compressions during 10 min of single-rescuer basic life support with different compression: ventilation ratios in a manikin model. Resuscitation 77, 95–100. doi:10.1016/j.resuscitation.2007.11.009

Bjørshol, C.A., Søreide, E., Torsteinbø, T.H., Lexow, K., Nilsen, O.B., Sunde, K., 2008b. Quality of chest compressions during 10min of single-rescuer basic life support with different compression: ventilation ratios in a manikin model. Resuscitation 77, 95–100. doi:10.1016/j.resuscitation.2007.11.009

Bjørshol, C.A., Sunde, K., Myklebust, H., Assmus, J., Søreide, E., 2011. Decay in chest compression quality due to fatigue is rare during prolonged advanced life support in a manikin model. Scand. J. Trauma. Resusc. Emerg. Med. 19, 46. doi:10.1186/1757-7241-19-46

Blackwell, J.R., Kornatz, K.W., Heath, E.M., 1999. Effect of grip span on maximal grip force and fatigue of flexor digitorum superficialis. Appl. Ergon. 30, 401–405. doi:10.1016/S0003-6870(98)00055-6

Borg, G.A.V., 1982. Psychophysical Bases of Perceived Exertion. Med. Sci. Sports Exerc. 14, 377–381. doi:10.1249/00005768-198205000-00012

Bridgewater, F.H.G., Bridgewater, K.J., Zeitz, C.J., 2000. Using the ability to perform CPR as a standard of fitness: A consideration of the influence of aging on the physiological responses of a select group of first aiders performing cardiopulmonary resuscitation. Resuscitation 45, 97–103. doi:10.1016/S0300-9572(00)00172-6

Bryan, M., Robb, R., Mehta, M., Vellano, K., Valderrama, A.L., Yoon, P.W., Sasson, C., Crouch, A., Perez, A.B., Merritt, R., Kellermann, A., 2011. Out-of-hospital cardiac arrest surveillance. Cardiac Arrest Registry to Enhance Survival (CARES), United States, October 1, 2005 - December 31, 2010. Morb. Mortal. Wkly. Rep. 60, 1–19. doi:ss6008a1 [pii]

Cason, C.L., Trowbridge, C., Baxley, S.M., Ricard, M.D., 2011. A counterbalanced cross-over study of the effects of visual, auditory and no feedback on performance measures in a simulated cardiopulmonary resuscitation. BMC Nurs. 10, 15. doi:10.1186/1472-6955-10-15

Cavanagh, P.R., Komi, P. V., 1979. Electromechanical delay in human skeletal muscle under concentric and eccentric contractions. Eur. J. Appl. Physiol. Occup. Physiol. 42, 159–163. doi:10.1007/BF00431022

Chi, C.-H., Tsou, J.-Y., Su, F.-C., 2008. Effects of rescuer position on the kinematics of cardiopulmonary resuscitation (CPR) and the force of delivered compressions. Resuscitation 76, 69–75. doi:10.1016/j.resuscitation.2007.06.007

Chi, C.H., Tsou, J.Y., Su, F.C., 2010. Effects of compression-to-ventilation ratio on compression force and rescuer fatigue during cardiopulmonary resuscitation. Am. J. Emerg. Med. 28, 1016–1023. doi:10.1016/j.ajem.2009.06.022

Cholewicki, J., VanVliet Iv, J.J., 2002. Relative contribution of trunk muscles to the stability of the lumbar spine during isometric exertions. Clin. Biomech. 17, 99–105. doi:10.1016/S0268-0033(01)00118-8

Chung, T.N., Kim, S.W., You, J.S., Cho, Y.S., Chung, S.P., Park, I., Kim, S.H., 2012. The specific effect of metronome guidance on the quality of one-person cardiopulmonary resuscitation and rescuer fatigue. J. Emerg. Med. 43, 1049–1054. doi:10.1016/j.jemermed.2012.01.021

Clark, B.C., Manini, T.M., Mayer, J.M., Ploutz-Snyder, L.L., Graves, J.E., 2002. Electromyographic activity of the lumbar and hip extensors during dynamic trunk extension exercise. Arch. Phys. Med. Rehabil. 83, 1547–1552. doi:10.1053/apmr.2002.34828

Clark, B.C., Manini, T.M., Ploutz-Snyder, L.L., 2003. Derecruitment of the lumbar musculature with fatiguing trunk extension exercise. Spine (Phila. Pa. 1976). 28, 282–287. doi:10.1097/00007632-200302010-00015

Crenshaw, A.G., Karlsson, S., Gerdle, B., Friden, J., 1997. Differential responses in intramuscular pressure and EMG fatigue indicators during low- vs. high-level isometric contractions to fatigue. Acta Physiol Scand. 160, 353–361. doi:10.1046/j.1365-201X.1997.00168.x

Dainty, R.S., Gregory, D.E., 2017. Investigation of low back and shoulder demand during cardiopulmonary resuscitation. Appl. Ergon. 58, 535–542. doi:10.1016/j.apergo.2016.04.013

Deluca, C.J., 1997. The use of Surface Electromyography in Biomechanics. Journale Appl. Biomech. 13, 135–163. doi:citeulike-article-id:2515246

Dine, C.J., Gersh, R.E., Leary, M., Riegel, B.J., Bellini, L.M., Abella, B.S., 2008. Improving cardiopulmonary resuscitation quality and resuscitation training by combining audiovisual feedback and debriefing. Crit. Care Med. 36, 2817–2822. doi:10.1097/CCM.0b013e318186fe37

Doheny, E.P., Lowery, M.M., FitzPatrick, D.P., O'Malley, M.J., 2008. Effect of elbow joint angle on force-EMG relationships in human elbow flexor and extensor muscles. J. Electromyogr. Kinesiol. 18, 760–770. doi:10.1016/j.jelekin.2007.03.006

Dolan, P., Mannion, A.F., Adams, M.A., 1995. Fatigue of the erector spinae muscles. Spine (Phila. Pa. 1976). 20, 149–159.

Drake, J.D.M., Callaghan, J.P., 2006. Elimination of electrocardiogram contamination from electromyogram signals: An evaluation of currently used removal techniques. J. Electromyogr. Kinesiol. 16, 175–187. doi:10.1016/j.jelekin.2005.07.003

Duff, J.P., Panchal, A.R., Hazinshi, M.F., 2018. Highlights of the 2018 Focused Upfates to the American Heart Association Guidelines for CPR and ECC: Advanced Cardiovascular Life Support and Pediatric Advanced Life Support.

Eberstein, A., Beattie, B., 1985. Simultaneous measurement of muscle conduction velocity and EMG power spectrum chaanges during fatigue. Muscle and Nerve 8, 768–773.

Foo, N.P., Chang, J.H., Lin, H.J., Guo, H.R., 2010. Rescuer fatigue and cardiopulmonary resuscitation positions: A randomized controlled crossover trial. Resuscitation 81, 579–584. doi:10.1016/j.resuscitation.2010.02.006

Fowles, J.R., Sale, D.G., MacDougall, J.D., 2000. Reduced strength after passive stretch of the human plantarflexors. J. Appl. Physiol. 89, 1179–1188. doi:10.1152/jappl.2000.89.3.1179

Fuchs, F., Reddy, Y., Norman Briggs, F., 1970. The interaction of cations with the calcium-binding site of troponin. BBA - Protein Struct. 221, 407–409. doi:10.1016/0005-2795(70)90290-4

Gardner-Morse, M.G., Stokes, I.A.F., 1998. The effects of abdominal muscle coactivation on lumbar spine stability. Spine (Phila. Pa. 1976). doi:10.1097/00007632-199801010-00019

Geddes, A, L.., Boland, K, M., Taleyarkhan, R, P., Vitter, J., 2007. Chest compression force of trained and untrained CPR rescuers. Cardiovasc. Eng. 7, 47–50. doi:10.1007/s10558-007-9029-5

Go, A.S., Mozaffarian, D., Roger, V.L., Benjamin, E.J., Berry, J.D., Borden, W.B.,

Bravata, D.M., Dai, S., Ford, E.S., Fox, C.S., Franco, S., Fullerton, H.J., Gillespie, C., Hailpern, S.M., Heit, J.A., Howard, V.J., Huffman, M.D., Kissela, B.M., Kittner, S.J., Lackland, D.T., Lichtman, J.H., Lisabeth, L.D., Magid, D., Marcus, G.M., Marelli, A., Matchar, D.B., McGuire, D.K., Mohler, E.R., Moy, C.S., Mussolino, M.E., Nichol, G., Paynter, N.P., Schreiner, P.J., Sorlie, P.D., Stein, J., Turan, T.N., Virani, S.S., Wong, N.D., Woo, D., Turner, M.B., 2013. Heart disease and stroke statistics-2013 update: A Report from the American Heart Association. Circulation 127. doi:10.1161/CIR.0b013e31828124ad

Granata, K.P., Gottipati, P., 2008. Fatigue influences the dynamic stability of the torso. Ergonomics 51, 1258–1271. doi:10.1080/00140130802030722

Hamada, T., Sale, D.G., MacDougall, J.D., Tarnopolsky, M.A., 2003. Interaction of fibre type, potentiation and fatigue in human knee extensor muscles. Acta Physiol. Scand. 178, 165–173. doi:10.1046/j.1365-201X.2003.01121.x

Hasegawa, T., Daikoku, R., Saito, S., Saito, Y., 2014. Relationship between weight of rescuer and quality of chest compression during cardiopulmonary resuscitation. J. Physiol. Anthropol. 33, 16. doi:10.1186/1880-6805-33-16

Hazinski, M., Shuster, M., Donnino, M., Travers, A., Samson, R., Schexnayder, S., Sinz, E., Woodin, J., Atkins, D., 2015. Highlights of the 2015 American Heart Association - Guidelines Update for CPR and ECG 1–36.

Hermens, H.J., Freriks, B., Disselhorst-Klug, C., Rau, G., 2000. Development of recommendations for SEMG sensors and sensor placement procedures. J. Electromyogr. Kinesiol. 10, 361–374. doi:10.1016/S1050-6411(00)00027-4

Hightower, D., Thomas, S.H., Stone, C.K., Dunn, K., March, J.A., 1995. Decay in Quality of Closed-Chest Compressions Over Time. Ann. Emerg. Med. 26, 300–303. doi:10.1016/S0196-0644(95)70076-5

Hof, A.L., 1984. EMG and Muscle Force: An Introduction. Hum. Mov. Sci. 3, 119–153.

Hof, A.L., Van den Berg, J., 1981. EMG to force processing I: An electrical analogue of the hill muscle model. J. Biomech. 14. doi:10.1016/0021-9290(81)90031-2

Hong, C.K., Park, S.O., Jeong, H.H., Kim, J.H., Lee, N.K., Lee, K.Y., Lee, Y., Lee, J.H., Hwang, S.Y., 2014. The most effective rescuer's position for cardiopulmonary resuscitation provided to patients on beds: A randomized, controlled, crossover mannequin study. J. Emerg. Med. 46, 643–649. doi:10.1016/j.jemermed.2013.08.085

Hussain, J., Sundaraj, K., Low, Y.F., Lam, C.K., Sundaraj, S., Ali, M.A., 2018. A systematic review on fatigue analysis in triceps brachii using surface electromyography. Biomed. Signal Process. Control 40, 396–414. doi:10.1016/j.bspc.2017.10.008

Hwang, S.-O., Cha, K.C., Kim, K., Cho, Y.H., Shin, J., Lee, H., Chung, S.P., You, J.S., Park, Y.S., Kim, S., Choi, S.-C., Kim, W.Y., Seo, D.W., Moon, S., Han, G., Choi, H.S., Kang, H.G., Park, S.M., Kwon, W.Y., Park, E.J., 2016. A randomized

controlled trial of compression rates (COMPRATE trial) during cardiopulmonary resuscitation. J. Korean Med. Sci. 1491–1498. doi:10.3346/jkms.2016.31.9.1491

Idris, A.H., Guffey, D., Aufderheide, T.P., Brown, S., Morrison, L.J., Nichols, P., Powell, J., Bigham, B.L., Atkins, D.L., Berg, R., Davis, D., Stiell, I.G., Sopko, G., Nichol, G., 2012. The Relationship Between Chest Compression Rates and Outcomes from Cardiac Arrest Ahamed. Circulation 125, 3004–3012. doi:10.1161/CIRCULATIONAHA.111.059535.The

Jaafar, A., Abdulwahab, M., Al-Hashemi, E., 2015. Influence of Rescuers' Gender and Body Mass Index on Cardiopulmonary Resuscitation according to the American Heart Association 2010 Resuscitation Guidelines. Int. Sch. Res. Not. 2015. doi:10.1155/2015/246398

Jennekens, F.G., Tomlinson, B.E., Walton, J.N., 1971. Data on the distribution of fibre types in five human limb muscles. An autopsy study. J. Neurol. Sci. 14, 245–257.

Komi, P. V, Tesch, P., 1979. EMG Frequency Spectrum, Muscle Structure, and Fatigue During Dynamic Contractions in Man. Appl. Physiol. 50, 41–50. doi:10.1007/BF00421103

Körber, M.I., Köhler, T., Weiss, V., Pfister, R., Michels, G., 2016. Quality of basic life support - A comparison between medical students and paramedics. J. Clin. Diagnostic Res. 10, OC33-OC37. doi:10.7860/JCDR/2016/19221.8197

Krogh-Lund, C., Jorgensen, K., 1991. Changes in conduction velocity, median frequency, and root mean square-amplitue of the electromyogram during 25% maximal voluntray contractions of the triceps brachii muscle, to limit of endurance. Eur. J. Appl. Physiol. Occup. Physiol. 63, 60–69.

Kudenchuk, P.J., Sandroni, C., Drinhaus, H.R., Böttiger, B.W., Cariou, A., Sunde, K., Dworschak, M., Taccone, F.S., Deye, N., Friberg, H., Laureys, S., Ledoux, D., Oddo, M., Legriel, S., Hantson, P., Diehl, J.-L., Laterre, P.-F., 2015. Breakthrough in cardiac arrest: reports from the 4th Paris International Conference. Ann. Intensive Care 5, 22. doi:10.1186/s13613-015-0064-x

Kwak, S.-J., Kim, Y.-M., Baek, H.J., Kim, S.H., Yim, H.W., Sj, K., Ym, K., Hj, B., Sh, K., 2016. Chest compression quality, exercise intensity, and energy expenditure during cardiopulmonary resuscitation using compression-to-ventilation ratios of 15:1 or 30:2 or chest compression only: a randomized, crossover manikin study. Clin Exp Emerg Med 3, 148–157. doi:10.15441/ceem.15.105

Lang, A.H., Nurkkanen, P., Vaahtoranta, K.M., 1971. Automatic sampling and averaging of electromyographic unit potentials. Electroenecephalography Clin. Neurophysiol. 31, 404–406.

Leedham, J.S., Dowling, J.J., 1995. Force-length, torque-angle and EMG-joint angle relationships of the human in vivo biceps brachii. Eur. J. Appl. Physiol. 246–249.

Lin, J., Wu, H., Tarr, P.T., Zhang, C.-Y., Wu, Z., 2002. Transcriptional co-activator PGC-1a drives the formation of slow-twitch muscle fibre. Nature 418, 797–801.

doi:10.1038/nature00936.1.

Lurie, K.G., 1994. Active compression-decompression CPR : a progress report. Resuscitation 28, 115–122.

McDonald, C.H., Heggie, J., Jones, C.M., Thorne, C.J., Hulme, J., 2013. Rescuer fatigue under the 2010 ERC guidelines, and its effect on cardiopulmonary resuscitation (CPR) performance. Emerg. Med. J. 30, 623–627. doi:10.1136/emermed-2012-201610

McGill, S.M., Norman, R.W., Cholewicki, J., 1996. A simple polynomial that predicts low-back compression during complex 3-D tasks. Ergonomics 39, 1107–1118. doi:10.1080/00140139608964532

Meaney, P.A., Bobrow, B.J., Mancini, M.E., Christenson, J., De Caen, A.R., Bhanji, F., Abella, B.S., Kleinman, M.E., Edelson, D.P., Berg, R.A., Aufderheide, T.P., Menon, V., Leary, M., 2013. Cardiopulmonary resuscitation quality: Improving cardiac resuscitation outcomes both inside and outside the hospital: A consensus statement from the American heart association. Circulation 128, 417–435. doi:10.1161/CIR.0b013e31829d8654

Merchant, R.M., Yang, L., Becker, L.B., Berg, R.A., Nadkarni, V., Nichol, G., Carr, B.G., Mitra, N., Bradley, S.M., Abella, B.S., Peter, W., 2012. Incidence of treated cardiac arrest in hospitalized patients in the United States. Crit Care Med 39, 2401–2406. doi:10.1097/CCM.0b013e3182257459.Incidence

Mills, K.R., 1982. Power spectral analysis of electromyogram and compound muscle action potential during muscle fatigue and recovery. j. Physiol. 326, 401–409.

Mittendorfer, B., Andersen, J.L., Plomgaard, P., Saltin, B., Babraj, J.A., Smith, K., Rennie, M.J., 2005. Protein synthesis rates in human muscles: Neither anatomical location nor fibre-type composition are major determinants. J. Physiol. 563, 203–211. doi:10.1113/jphysiol.2004.077180

Nakamaru, Y., Schwartz, A., 1972. The influence of hydrogen ion concentration on calcium binding and release by skeletal muscle sarcoplasmic reticulum. J. Gen. Physiol. 59, pp.22-32.

Nichol, G., Thomas, E., Callaway, C.W., Hedges, J., Powell, J.L., Aufderheide, T.P., Rea, T., Lowe, R., Brown, T., Dreyer, J., Davis, D., Idris, A., Stiell, I., Resuscitation Outcomes Consortium Investigators, 2008. Regional variation in out-of-hospital cardiac arrest incidence and outcome. Jama 300, 1423–31. doi:10.1001/jama.300.12.1423

Niemann, J.T., Rosborough, J., Hausknecht, M., Brown, D., Criley, M., 1980. Cough-CPR, Documentation of systemic perfusion in man and in an experimental model: a "window" to the mechanism of blood flow in external CPR. Crit. Care Med. 8, 141–146.

Nieminen, H., Takala, E.-P., Viikari-Juntura, E., 1993. Normalization of electromyogram in the neck-shoulder region. Eur. J. Appl. Physiol. 199–207.

Nilsson, J., Tesch, P., Thorstensson, A., 1977. Fatigue and EMG of Repeated Fast Voluntary Contractions in Man. Acta Physiol. Scand. 101, 194–198. doi:10.1111/j.1748-1716.1977.tb05998.x

Olasveengen, T.M., Wik, L., Steen, P.A., 2008. Quality of cardiopulmonary resuscitation before and during transport in out-of-hospital cardiac arrest. Resuscitation 76, 185–190. doi:10.1016/j.resuscitation.2007.07.001

Pavo, N., Goliasch, G., Nierscher, F.J., Stumpf, D., Haugk, M., Breckwoldt, J., Ruetzler, K., Greif, R., Fischer, H., 2016. Short structured feedback training is equivalent to a mechanical feedback device in two-rescuer BLS: a randomised simulation study. Scand. J. Trauma. Resusc. Emerg. Med. 24, 70. doi:10.1186/s13049-016-0265-9

Phinyomark, A., Thongpanja, S., Hu, H., Phukpattaranont, P., Limsakul, C., 2012. The Usefulness of Mean and Median Frequencies in Electromyography Analysis, Computational Intelligence in Electromyography Analysis - A Perspective on Current Applications and Future Challenges. doi:10.5772/50639

Pickard, A., Darby, M., Soar, J., 2006. Radiological assessment of the adult chest: Implications for chest compressions. Resuscitation 71, 387–390. doi:10.1016/j.resuscitation.2006.04.012

Pozner, C.N., Almozlino, A., Elmer, J., Poole, S., McNamara, D., Barash, D., 2011. Cardiopulmonary resuscitation feedback improves the quality of chest compression provided by hospital health care professionals. Am. J. Emerg. Med. 29, 618–625. doi:10.1016/j.ajem.2010.01.008

Robertson, D.G.E., Caldwell, G.E., Hamill, J., 2004. Research Methods in Biomechanics, Second Edition.

Roger, V.L., Go, A.S., Lloyd-Jones, D.M., Benjamin, E.J., Berry, J.D., Borden, W.B., Bravata, D.M., Dai, S., Ford, E.S., Fox, C.S., Fullerton, H.J., Gillespie, C., Hailpern, S.M., Heit, J.A., Howard, V.J., Kissela, B.M., Kittner, S.J., Lackland, D.T., Lichtman, J.H., Lisabeth, L.D., Makuc, D.M., Marcus, G.M., Marelli, A., Matchar, D.B., Moy, C.S., Mozaffarian, D., Mussolino, M.E., Nichol, G., Paynter, N.P., Soliman, E.Z., Sorlie, P.D., Sotoodehnia, N., Turan, T.N., Virani, S.S., Wong, N.D., Woo, D., Turner, M.B., 2012. Heart disease and stroke statistics-2012 update: A report from the American heart association. Circulation 125. doi:10.1161/CIR.0b013e31823ac046

Rose, L., Örtengren, R., Ericson, M., 2001. Endurance, pain and resumption in fully flexed postures. Appl. Ergon. 32, 501–508. doi:10.1016/S0003-6870(01)00016-3

Roskos, D., Lentz, N., Grimmel, K., Bolz, A., 2011. Determination of compression depth during resuscitation using angular measurement. IFMBE Proc. 37, 434–437. doi:10.1007/978-3-642-23508-5_113

Rudikoff, M.T., Maughan, W.L., Effron, M., Freund, P., Weisfeldt, M.L., 1980. Mechanisms of blood flow during cardiopulmonary resuscitation. Circulation 61, 345–352. doi:10.1161/01.CIR.61.2.345

Russi, C.S., Myers, L.A., Kolb, L.J., Lohse, C.M., Hess, E.P., White, R.D., 2016. A Comparison of Chest Compression Quality Delivered During On-Scene and Ground Transport Cardiopulmonary Resuscitation. West. J. Emerg. Med. 17, 634–639. doi:10.5811/westjem.2016.6.29949

Russo, S.G., Neumann, P., Reinhardt, S., Timmermann, A., Niklas, A., Quintel, M., Eich, C.B., 2011. Impact of physical fitness and biometric data on the quality of external chest compression: a randomised, crossover trial. BMC Emerg. Med. 11, 20. doi:10.1186/1471-227X-11-20

Salas, E.A., Vi, P., Reider, V.L., Moore, A.E., 2016. Factors affecting the risk of developing lower back musculoskeletal disorders (MSDs) in experienced and inexperienced rodworkers. Appl. Ergon. 52, 62–68. doi:10.1016/j.apergo.2015.06.016

Sayee, N., McCluskey, D., 2012. Factors influencing performance of cardiopulmonary resuscitation (CPR) by foundation Year 1 Hospital Doctors. Ulster Med. J. 81, 14–18.

Sayre, M.R., Berg, R.A., Cave, D.M., Page, R.L., Potts, J., White, R.D., 2008. Hands-only (compression-only) cardiopulmonary resuscitation: A call to action for bystander response to adults who experience out-of-hospital sudden cardiac arrest - A science advisory for the public from the American heart association emergency cardiovas. Circulation 117, 2162–2167. doi:10.1161/CIRCULATIONAHA.107.189380

Shin, J., Hwang, S.Y., Lee, H.J., Park, C.J., Kim, Y.J., Son, Y.J., Seo, J.S., Kim, J.J., Lee, J.E., Lee, I.M., Koh, B.Y., Hong, S.G., 2014. Comparison of CPR quality and rescuer fatigue between standard 30:2 CPR and chest compression-only CPR: a randomized crossover manikin trial. Scand. J. Trauma. Resusc. Emerg. Med. 22, 59. doi:10.1186/s13049-014-0059-x

Shin, J., Rhee, J.E., Kim, K., 2007. Is the inter-nipple line the correct hand position for effective chest compression in adult cardiopulmonary resuscitation? Resuscitation 75, 305–310. doi:10.1016/j.resuscitation.2007.05.003

Smart, J.R., Kranz, K., Carmona, F., Lindner, T.W., Newton, A., 2015. Does real-time objective feedback and competition improve performance and quality in manikin CPR training--a prospective observational study from several European EMS. Scand J Trauma Resusc Emerg Med 23, 79. doi:10.1186/s13049-015-0160-9

Stanley, A.A., Healey, S.K., Maltese, M.R., Kuchenbecker, K.J., 2012. Recreating the feel of the human chest in a CPR manikin via programmable pneumatic damping. Haptics Symp. 2012, HAPTICS 2012 - Proc. 37–44. doi:10.1109/HAPTIC.2012.6183767

Stephan Riek, Richard G. Carson, Anthony Wright b, 2000. A new technique for the selective recording of extensor carpi radialis longus and brevis EMG. J. Electromyogr. Kinesiol. 10, 249–253. doi:10.1016/j.clinbiomech.2003.11.012

Stephens, J.A., Taylor, A., 1972. Fatigue of maintain voluntary muscle contraction in

man. j. Physiol. 220, 1–18.

Sugerman, N.T., Herzberga, D., Learya, M., Weidmanb, E.K., Edelsonb, D.P., Hoekc, T.L. Vanden, Beckera, L.B., Benjamin S. Abella, 2009. Rescuer fatigue during actual in-hospital cardiopulmonary resuscitation with audiovisual feedback: a prospective multicenter study. Resuscitation 80, 981–984. doi:10.1016/j.resuscitation.2009.06.002.Rescuer

Tomlinson, A.E., Nysaether, J., Kramer-Johansen, J., Steen, P.A., Dorph, E., 2007. Compression force-depth relationship during out-of-hospital cardiopulmonary resuscitation. Resuscitation 72, 364–370. doi:10.1016/j.resuscitation.2006.07.017

Trowbridge, C., Parekh, J.N., Ricard, M.D., Potts, J., Patrickson, W.C., Cason, C.L., 2009. A randomized cross-over study of the quality of cardiopulmonary resuscitation among females performing 30:2 and hands-only cardiopulmonary resuscitation. BMC Nurs. 8, 6. doi:10.1186/1472-6955-8-6

Tsitlik, J.E., Weisfeldt, M.L., Chandra, N., Effron, M.B., Halperin, H.R., Levin, H.R., 1983. Elastic properties of the human chest during cardiopulmonary resuscitation. Crit. Care Med.

Tsou, J.Y., Chi, C.H., Hsu, R.M.F., Wu, H.F., Su, F.C., 2009. Mechanical loading of the low back during cardiopulmonary resuscitation. Resuscitation 80, 1181–1186. doi:10.1016/j.resuscitation.2009.06.025

Tsou, J.Y., Su, F.C., Tsao, P.C., Hong, M.Y., Cheng, S.C., Chang, H.W., Yang, J.S., Chi, C.H., 2014. Electromyography activity of selected trunk muscles during cardiopulmonary resuscitation. Am. J. Emerg. Med. 32, 216–220. doi:10.1016/j.ajem.2013.10.044

Vaillancourt, C., Midzic, I., Taljaard, M., Chisamore, B., 2011. Performer fatigue and CPR quality comparing 30:2 to 15:2 compression to ventilation ratios in older bystanders: A randomized crossover trial. Resuscitation 82, 51–56. doi:10.1016/j.resuscitation.2010.09.003

Vaillancourt, C., Stiell, I., 2004. Chapter 24 : Cardiac arrest care and emergency medical services in Canada. Can. J. Cardiol. 20, 1081–1090.

Viitasalo, J.H.T., Komi, P. V., 1977. Signal characteristics of EMG during fatigue. Eur. J. Appl. Physiol. Occup. Physiol. 37, 111–121. doi:10.1007/BF00421697

Vleeming, A., Pool-Goudzwaard, A.L., Stoeckart, R., Wingerden, J.-P. van, Snijders, C.J., 1995. The Posterior Layer of the Thoracolumbar Fascia. Spine (Phila. Pa. 1976). 7, 753–758.

Wang, J., Zhou, C., Zhang, L., Gong, Y., Yin, C., Li, Y., 2015. Performance of cardiopulmonary resuscitation during prolonged basic life support in military medical university students: A manikin study. World J. Emerg. Med. 6, 179–185. doi:10.5847/wjem.j.1920

Wik, L., Kramer-Johansen, J., Myklebust, H., Sorebo, H., Svensson, L., Fellows, B., Steen, A, P., 2005. Quality of cardiopulmonary resuscitation. JAMA 293, 299–304.

doi:10.1016/0140-6736(92)91309-V

Winter, D., 2009. BIOMECHANICS AND MOTOR CONTROL OF HUMAN MOVEMENT, John Wiley & Sons, Inc. doi:10.1002/9780470549148

Winter, D.A., 1980. Units, Terms and Standards in the reporting of EMG Research. ISEK.

Yannopoulos, D., Mcknite, S., Aufderheide, T.P., Sigurdsson, G., Pirrallo, R.G., Benditt, D., Lurie, K.G., 2005. Effects of incomplete chest wall decompression during cardiopulmonary resuscitation on coronary and cerebral perfusion pressures in a porcine model of cardiac arrest. Resuscitation 64, 363–372. doi:10.1016/j.resuscitation.2004.10.009

Yao, W., Fuglevand, R.J., Enoka, R.M., 2000. Motor-unit synchronization increases EMG amplitude and decreases force steadiness of simulated contractions. J. Neurophysiol. 83, 441–452. doi:10.1007/BF00863403

Zhang, F.-L., Yan, L., Huang, S.-F., Bai, X.-J., 2013. Correlations between quality indexes of chest compression. World J. Emerg. Med. 4, 54–8. doi:10.5847/wjem.j.1920-8642.2013.01.010

Zhou, X.L., Li, L., Jiang, C., Xu, B., Wang, H.L., Xiong, D., Sheng, L.P., Yang, Q.S., Jiang, S., Xu, P., Chen, Z.Q., Zhao, Y., Lazzeri, C., 2015. Up-down hand position switch may delay the fatigue of non-dominant hand position rescuers and improve chest compression quality during cardiopulmonary resuscitation: A randomized crossover manikin study. PLoS One 10, 1–11. doi:10.1371/journal.pone.0133483

Zipp, P., 1982. Recommendations for the standardization of lead positions in surface electromyography. Eur. J. Appl. Physiol. Occup. Physiol. 50, 41–54. doi:10.1007/BF00952243

Zuercher, M., Hilwig, R.W., Ranger-Moore, J., Nysaether, J., Nadkarni, V.M., Berg, M.D., Kern, K.B., Sutton, R., Berg, R.A., 2010. Leaning during chest compressions impairs cardiac output and left ventricular myocardial blood flow in piglet cardiac arrest. Crit Care Med 38, 1141–1146. doi:10.1097/CCM.0b013e3181ce1fe2.Leaning

Appendix A

Table A1: Vicon marker names and placement locations on the human body.

Marker Label	Definition	Location
C7	7th cervical vertebra	On spinal process of 7th cervical vertebra
T10	10th Thoracic vertebra	On spinal process of 10th thoracic vertebra
CLAV	Clavicle	On the jugular notch
STRN	Sternum	On the xiphoid process
RBAK	Right Back	Anywhere on the right scapula
LSHO	Left Shoulder	On the acromio-clavicular joint
LUPA	Left upper arm	On the upper lateral 1/3 surface of the left arm
LELB	Left lateral elbow	On the lateral epicondyle
LEMB	Left medial elbow	On the medial epicondyle
LEOL	Left elbow	On the Olecranon process
LFRM	Left forearm	On the lower lateral 1/3 surface of the left forearm
LWRA	Left wrist marker A	On the lateral styloid process
LWRB	Left wrist marker B	On the medial styloid process
LFIN	Left finger	Just proximal to the middle knuckle on the left hand (*Dependent on whether or not the left hand was in contact with the manikin*)
RSHO	Right shoulder	On the acromio-clavicular joint
RUPA	Right upper arm	On the lower lateral 1/3 surface of the right arm
RELB	Right lateral elbow	On the lateral epicondyle

REMB	Right medial	On the medial epicondyle
REOL	Right elbow	On the Olecranon process
RFRM	Right forearm	On the lower lateral 1/3 surface of the right forearm
RWRA	Right wrist marker A	On the lateral styloid process
RWRB	Right wrist marker B	On the medial styloid process
RFIN	Right finger	Just below the middle knuckle on the right hand (Dependent on whether or not the left hand was in contact with the manikin)
SACR	Sacral	On the skin mid-way between the posterior superior iliac spines (PSIS) and positioned to lie in the plane formed by the ASIS and PSIS points.
LASI	Left ASIS	Left anterior superior iliac spine
RASI	Right ASIS	Right anterior superior iliac spine
LPSI	Left PSIS	Left posterior superior iliac spine (immediately below the sacro-iliac joints, at the point where the spine joins the pelvis)
RPSI	Right PSIS	Right posterior superior iliac spine (immediately below the sacro-iliac joints, at the point where the spine joins the pelvis)
LTHI	Left thigh	Over the lower lateral 1/3 surface of the left thigh
LKNE	Left knee	On the flexion-extension axis of the left knee
LTIB	Left tibia	Over the lower 1/3 surface of the left shank
LANK	Left ankle	On the lateral malleolus along an imaginary line that passes through the transmalleolar axis
LHEE	Left heel	On the calcaneous at the same height above the plantar surface of the foot as the toe marker
LTOE	Left toe	Over the second metatarsal head, on the mid-foot side of the equinus break between fore-foot and mid-foot
RTHI	Right thigh	Over the upper lateral 1/3 surface of the right thigh
RKNE	Right knee	On the flexion-extension axis of the right knee.

RANK	Right ankle	On the lateral malleolus along an imaginary line that passes through the transmalleolar axis
RHEE	Right heel	On the calcaneous at the same height above the plantar surface of the foot as the toe marker
RTOE	Right toe	Over the second metatarsal head, on the mid-foot side of the equinus break between fore-foot and mid-foot
LBHD	Head	Left back of head
RBHD	Head	Right back of head
LFHD	Head	Left front of head
RFHD	Head	Right front of head

Appendix B

Table B1: Vicon marker names and placement locations on the Little Anne manikin.

Marker Label	Definition	Location
STR	Sternal Notch	On the sternal notch
RCST	Right Clavical	On the sternal end of the clavical
LCST	Left Clavical	On the sternal end of the clavical
XYP	Xiphoid Process	On the xiphoid process
RRIB	Right Rib	On the costal cartilage of the 7th rib
LRIB	Left Rib	On the costal cartilage of the 7th rib

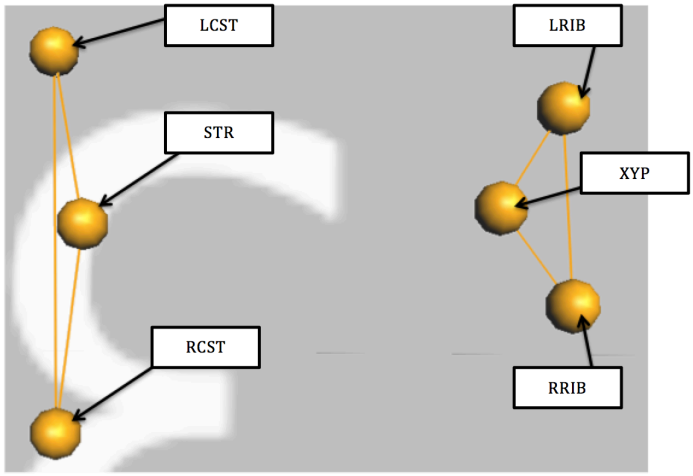

Figure B1: This figure depicts the coronal plane of the manikin, which has been labeled in Vicon Nexus.

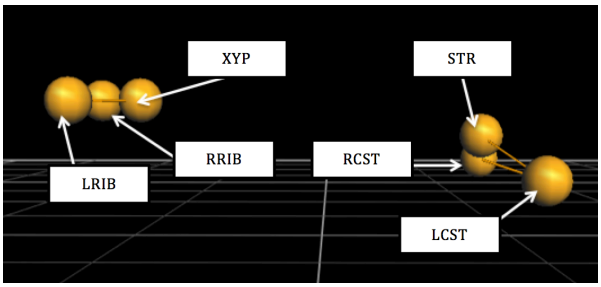

Figure B2: This figure depicts the sagittal plane of the manikin, which has been labeled in Vicon Nexus.

Appendix C.

_____ _____

Posture: _____

Fatigue Time:_____

Rating of Perceived Exertion

- Please circle the value that best describes how you currently perceive your exertion.

6	No exertion at all
7	Extremely light
8	
9	Very light
10	
11	Light
12	
13	Somewhat hard
14	
15	Hard (heavy)
16	
17	Very Hard
18	
19	
20	Maximal exertion

Figure C1: Rating of perceived exertion form completed by participants at the end of each six-minute trial.

Appendix D

Posture:_____ _____

Fatigue Questionnaire

Indicate which muscles feel fatigued or sore:

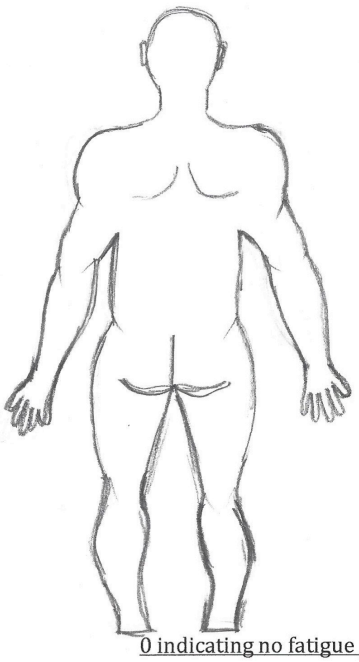

Mark location with:

0 indicating no fatigue / 10 indicating immense fatigue

Location 1:
1 2 3 4 5 6 7 8 9 10

Location 2:
1 2 3 4 5 6 7 8 9 10

Location 3:
1 2 3 4 5 6 7 8 9 10

Location 4:
1 2 3 4 5 6 7 8 9 10

Location 5:
1 2 3 4 5 6 7 8 9 10

Figure D1: Muscle fatigue location and classification form, filled out by participants at the end of each six-minute trial.

Appendix E

Sex: Female Male

1) Age: _____

2) Height (cm): _____

3) Weight (kg.): _____

4) Regular smoker? Yes No

5) Do you have any allergies to adhesives (ex: Band-Aid, double-sided tape)?

   Yes No

6) Has a physician and/or medical/exercise professional ever advised you against performing moderate-to-vigorous intensity physical activity?

   Yes No

7) Are you currently diagnosed with any musculoskeletal disorders? Yes No

   If you answered, "**Yes**" have you received treatment in the last six months?

   Yes No

8) Have you incurred any musculoskeletal injuries in the past year? Yes No

9) During/following the last time you completed CPR, either in training or on a human did you experience any musculoskeletal pain? Yes No

10) During/following the last time you completed CPR, either in training or on a human did you experience any muscular fatigue? Yes No

11)In general do you experience muscular fatigue in any of the following muscles during/following CPR?

a) Forearm(s): Yes No

b) Bicep(s): Yes No

c) Tricep(s): Yes No

d) Deltoid(s) (shoulders): Yes No

e) Latissimus Dorsi (back): Yes No

f) Abdominals: Yes No

g) Gluteus: Yes No

h) Hamstring(s): Yes No

i) Quadricep(s): Yes No

12) Do you have any history of lower back pain? Yes No

If you answered "**Yes**" please complete the following questions:

a) How long ago were you first diagnosed with LBP? _____

b) What motion(s) provoke your LBP?

_____

_____

c) Have you experienced LBP during activities directly related to your professional duties? Yes No

d) Have you experience LBP during or shortly after CPR? Yes No N/A

e) Using a scale of 0-10, (0 indicating no pain, and 10 being the worst pain you have ever felt) how would you rate your LBP on:

Average _____

During CPR _____ N/A

13) How many times have you completed cardiopulmonary resuscitation on a human? _____

14) On average, how many days per week do you perform moderate-to-vigorous physical activity, lasting 30 min or longer:

a) 0 days/week
b) 1-2 days/week
c) 3-4 days/week
d) 5+ days/week

15) What is your occupation?

_____

16) How many years have you worked/studied and/or been employed in your occupation? _____

17) What CPR certification level do you currently hold?

_____

18) What agency is/are your current CPR certification(s) under?

_____

19) When does your CPR certification(s) expire?

_____

20)In your opinion, how would you rate your current knowledge of CPR procedures?

a) No knowledge
b) Novice
c) Moderate
d) Expert

Figure E1: General questionnaire filled out by participants prior to the start of the study.

Appendix F

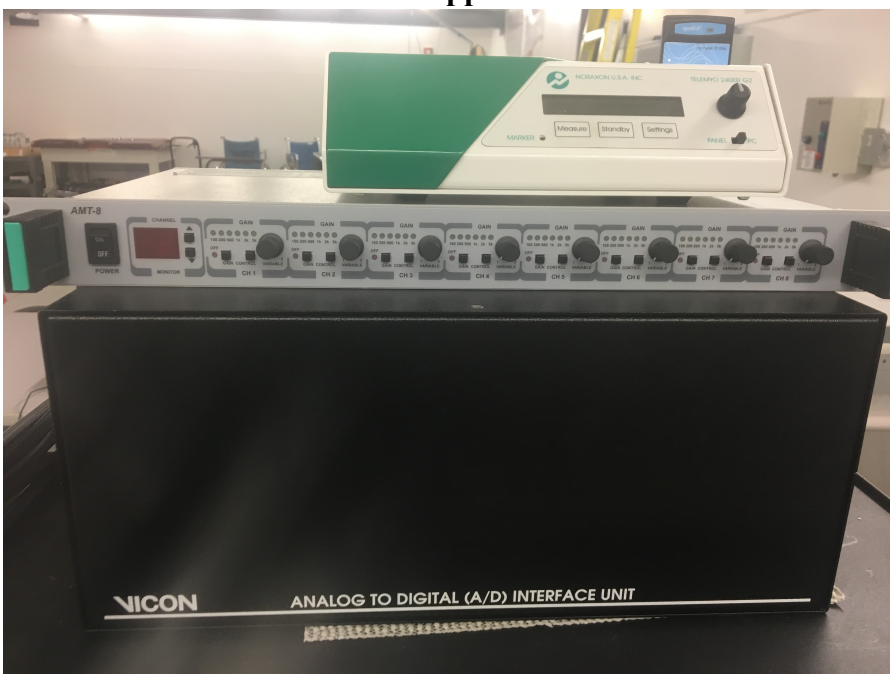

Figure F1: Vicon A/D board, AMT-8 EMG amplifier, TeleMyo 2400R G2; equipment used to collect EMG signals from participants.

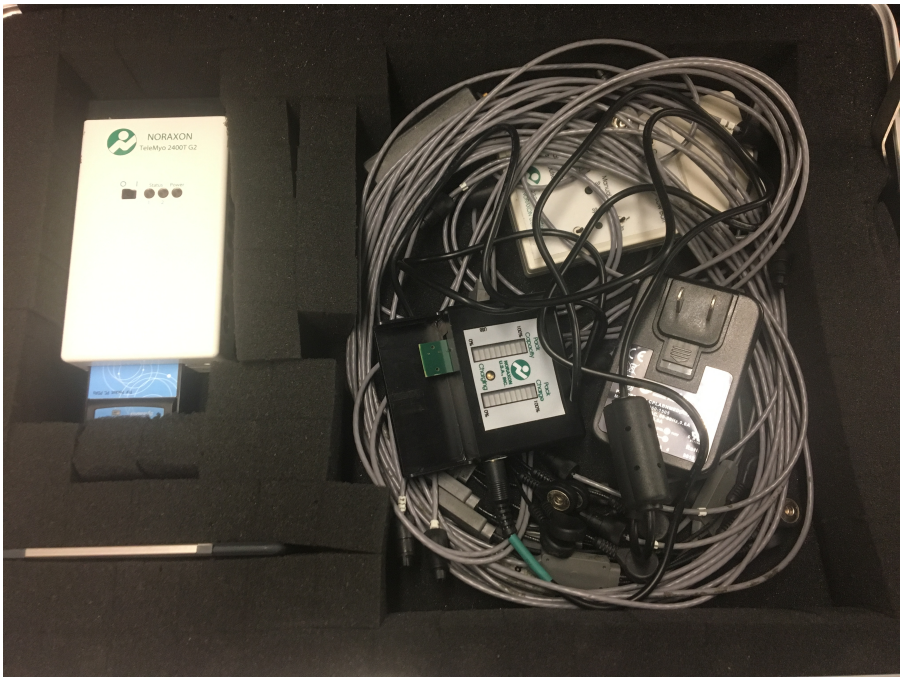

Figure F2: TeleMyo 2400T G2, battery, and leads used to collect EMG signals from participants.

Appendix G

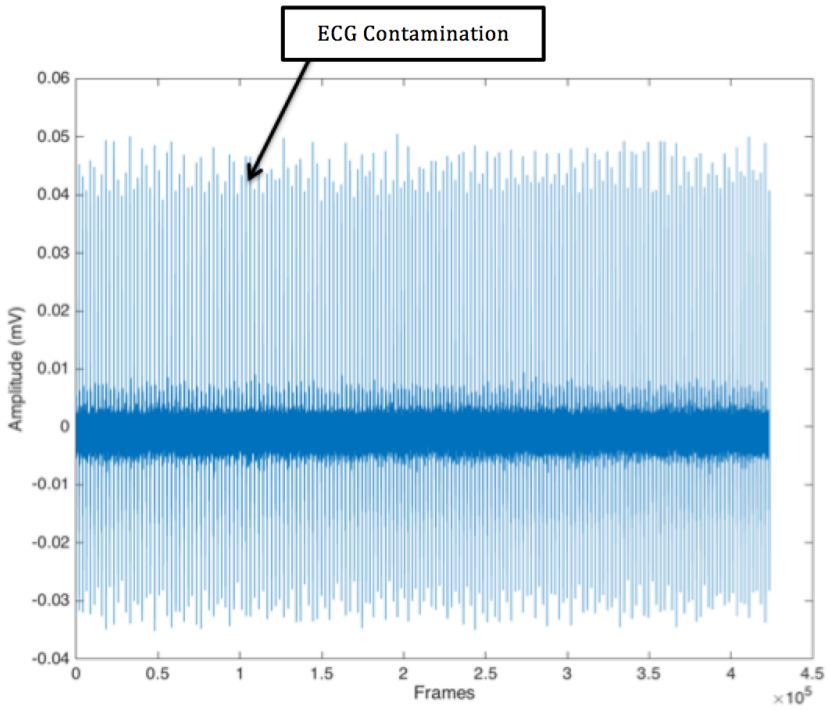

Figure G1: EMG signal of the left PM from a participant with ECG contamination.

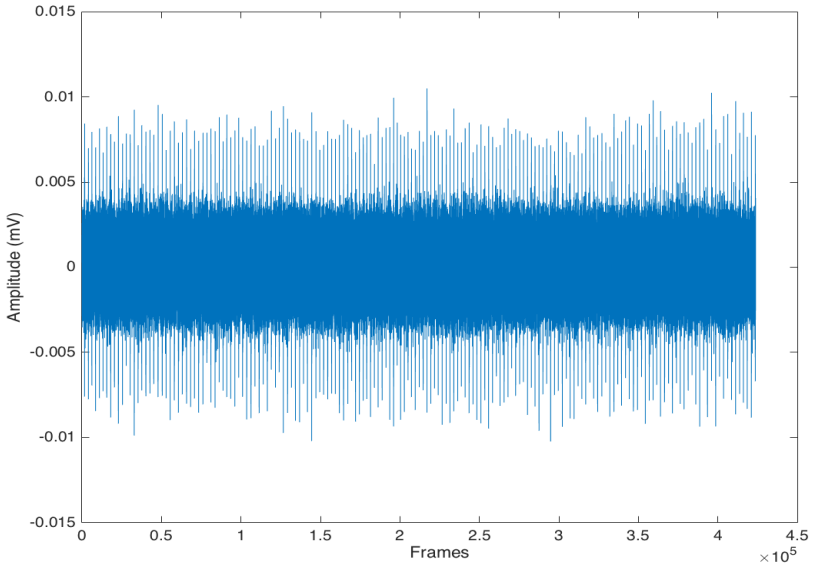

Figure G2: EMG signal of the left PM from the same participant in figure G1 with ECG contamination removed using the methodology from Drake and Callaghan, 2006.

Appendix H

H1.1 Resultant CC Force Vector

```
%% Force - Identifying the force vector
l(1,1:4) = NaN;
for i = 1:4;
    l(1,i) = length(force_xyz{1,i}(:,:));       %Identifying the
lengths of each posture
end
for i = 1:4;
    hand_force{1,i}(1:l(1,i),1) = NaN;          %Setting up a NaN
matrix for the force vector
end
for i = 1:l(1,1);       %Identifying the force vector of the kneeling
posture because there is an extra force plate
    hand_force{1,1}(i,1) = sqrt(force_xyz{1,1}(i,7)^2 +
force_xyz{1,1}(i,8)^2 + force_xyz{1,1}(i,9)^2);
end
for p = 2:4;
    for i = 1:l(1,p);   %Identifying the force vector of the table
postures
        hand_force{1,p}(i,1) = sqrt(force_xyz{1,p}(i,7)^2 +
force_xyz{1,p}(i,8)^2 + force_xyz{1,p}(i,9)^2);
    end
end

%% Force - Identifying the cutoff
for i = 1:4;
    plot(hand_force{1,i}(:,:))
    max_low_force(1,i) = input('Identify the highest force (N) that is
prior to a compression:');
end
```

H1.2 Start/End Times per CC

```
for i = 1:4;
    x_p{1,i}(1:40,1:120) = NaN;
end
%%
for i = 1:4;
    y_s{1,i}(1:40,1:120) = NaN;
end
%%
for a = 1:4;
    upflag=0;
    downflag=1;
    force = hand_force{1,a};
    F = max_low_force(1,a);       % Indication compression started and
ended
    timeflag = 0;               % flag used to indicate breathing space
    starttime = NaN(120,120);      % row 1 start times for compressions
in first series
```

```
    peaks = NaN(120,120);          % row 1 peak forces for compressions
in first series
    j=0;                        % counter for columns (compression)
approx max 28
    k=0;                        % counter for rows (series between
breaths) approx max 14  (22 sec /group in 300 sec)
    first=0;                    %flag for first compression in a series
    downcount = 0;
    l = length(force);
    firsttime = 1;
    for i=1:l;
        downcount=downcount+1;
        if force(i,1)> F && upflag==0
            upflag=1;
            downflag=0;
            if downcount > 3800 || firsttime==1; %**Change 3800 to
identify breaks between compression cycles (set to 1.32sec)**
                firsttime=0;
                k=k+1;
                downcount=0;
                first=1;
                j=0;
            else
                upsample=i;
                tempmin=F;
                j=j+1;
                for l=(i-downcount):i;
                    if force(l,1) <= tempmin
                        starttime(k,j)= l;   %ARRAY with sample times
for last minimum before the rise starts ie the start time of each
compression cycle
                                             %  for all but the first
                                             %  compression or end
times for
                                             %  all but last
compression
                        tempmin=force(l,1);
                    end
                end

            end
        end
        if force(i,1) < F && downflag==0
            downflag=1;
            upflag=0;
            downcount=0;
            if first==1
                first=0;
            else
                tempmax=F;
                for l=upsample:i;
                    if force(l,1) >= tempmax
                        peaks(k,j)= force(l,1);  %ARRAY with peak hand
force for
                                             %  for all but the first
```

```
compression
                        tempmax=force(l,1);
                    end
                end
            end
        end
    end
x_p{1,a}(1:length(peaks'),:) = peaks';
y_s{1,a}(1:length(starttime'),:) = starttime';
end

%% Identifying if there were more than 33 compression in the first
cycle
start(1,1:4) = NaN;
for i = 1:4;
    if sum(~isnan(y_s{1,i}(1:end,1))) > 29
       start(1,i) = y_s{1,i}(3,1);
    else
       start(1,i) = 2401;
    end
end

for i = 1:4;
    hand_force_1{1,i}(:,1) = hand_force{1,i}(start(1,i):end,1);
end

%% Find starttime and peaks after getting rid of first 3 compressions
for i = 1:4;
    x_p{1,i}(1:40,1:120) = NaN;
end
for i = 1:4;
    y_s{1,i}(1:40,1:120) = NaN;
end
%%
for a = 1:4;
    upflag=0;
    downflag=1;
    force = hand_force_1{1,a};
    F = max_low_force(1,a);       % Indication compression started and
ended
    timeflag = 0;               % flag used to indicate breathing space
    starttime = NaN(120,120);      % row 1 start times for compressions
in first series
    peaks = NaN(120,120);          % row 1 peak forces for compressions
in first series
    j=0;                        % counter for columns (compression)
approx max 28
    k=0;                        % counter for rows (series between
breaths) approx max 14  (22 sec /group in 300 sec)
    first=0;                   %flag for first compression in a series
    downcount = 0;
    l = length(force);
    firsttime = 1;
    for i=1:l;
```

```
        downcount=downcount+1;
        if force(i,1)> F && upflag==0
            upflag=1;
            downflag=0;
            if downcount > 3800 || firsttime==1; %**Change 3800 to
identify breaks between compression cycles (set to 1.32sec)**
                firsttime=0;
                k=k+1;
                downcount=0;
                first=1;
                j=0;
            else
                upsample=i;
                tempmin=F;
                j=j+1;
                for l=(i-downcount):i;
                    if force(l,1) <= tempmin
                        starttime(k,j)= l;   %ARRAY with sample times
for last minimum before the rise starts ie the start time of each
compression cycle
                                                %  for all but the first
                                                %  compression or end
times for
                                                %  all but last
compression
                        tempmin=force(l,1);
                    end
                end

            end
        end
        if force(i,1) < F && downflag==0
            downflag=1;
            upflag=0;
            downcount=0;
            if first==1
                first=0;
            else
                tempmax=F;
                for l=upsample:i;
                    if force(l,1) >= tempmax
                        peaks(k,j)= force(l,1);  %ARRAY with peak hand
force for
                                                %  for all but the first
compression
                        tempmax=force(l,1);
                    end
                end
            end
        end
    end
x_p{1,a}(1:length(peaks'),:) = peaks';
y_s{1,a}(1:length(starttime'),:) = starttime';
end
%     save('peaks_1.txt','peaks','-ascii','-tabs');
```

```
%     save('starttime_1.txt','starttime','-ascii','-tabs');
end
```

H1.3 CC Rate

```
for i = 1:4;
    temp = size(starttime{1,i});
    time_compression{1,i}(1:temp(1,1),1:temp(1,2)) = zeros;
    bpm_compression{1,i}(1:temp(1,1),1:temp(1,2)) = zeros;
    time_cyle{1,i}(1,1:temp(1,2)) = zeros;
    bpm_cyle{1,i}(1,1:temp(1,2)) = zeros;
end
%%
for a = 1:4;                            %Trial counter
    starttime_m = starttime{1,a};   %Using an individual array every
loop
    j = 0;                              %Row counter (compressions)
    k = 1;                              %Coloumn counter (cycles)
    for i = 1:numel(starttime_m)-(length(find(isnan(starttime_m))));
%Identifies how many NaN's are in the matrix and subtracts it from the
total number of elements.
        j = j + 1;
        if isnan(starttime_m(j+1,k));           %Identifies a NaN as
the next element, signalling the end of a compression cycle
            k = k + 1;  %Changing to the next compression cycle
            j = 0;      %Reverting to the first compression in that
cycle

        else
            time_compression{1,a}(j,k) = (starttime_m(j+1,k) -
starttime_m(j,k)) / 2400;    %Identifies the time per compressions
            bpm_compression{1,a}(j,k) = 60 /
(time_compression{1,a}(j,k));  %Identifies the rate of compressions
            time_cyle{1,a}(1,k) = (starttime_m(j,k) - starttime_m(1,k))
/ 2400; %Identifies the total time per compression cycle
            bpm_cyle{1,a}(1,k) = mean(bpm_compression{1,a}(1:j,k));
%Identifies the mean bpm per cycle
        end
    end
end

end
```

H1.4 Linear Envelope of the EMG

```
mc = 16;          %Input number of muscles collected

hfc= 30;        %High-Pass variables that can be changed.
hfs = 2400;
n = 2;
```

```
Wn = hfc/(hfs/2);
ftype = 'High';

lfc = 4;          %Low-Pass variables that can be changed.
lfs = 2400;
nl = 2;
Wnl = lfc/(lfs/2);
%% Time Shift (Noraxon)
for i = 1:4;                %Setting up a Zero matrix to align the
Noraxon EMG in time
    emg_ts{1,i}(1:length(emg{1,i}),1:mc) = zeros;
end

for i = 1:4;
    for p = 1:6;            %Places the AMT EMG into the blank matrix
        emg_ts{1,i}(:,p) = emg{1,i}(:,p);
    end
end

for i = 1:4;
    for p = 1:10;           %Gets rid of the first 240 data points to
align Noraxon with AMT, since it is delayed by 100msec
        emg_ts{1,i}(1:length(emg{1,i})-240,6+p) =
emg{1,i}(241:end,6+p);
    end
end

%% Removal of bias and High Pass filter
% for i = 1:mc;
%     quiet_noraxon(:,i) = quiet(1:175600,i); %Noraxon shut off half
way through the quiet trial.
% end
k = length(mvc);
bias(1,1:mc) = NaN;                 %Setting up empty NaN matrixs
for i = 1:4;
    l(1,i) = length(emg_ts{1,i});
    emg_bias{1,i}(1:l(1,i),1:mc) = NaN;
end
mvc_bias(1:k,1:mc) = NaN;                       %Sets up a NaN matrix
for mvc bias

[b,a] = butter(n,Wn,ftype);       %Set up transfer function for bias
ECG removal
ecg_quiet = filtfilt(b,a,quiet);  %dual pass Filter the quiet trial,
based on transfer function
bias = mean(ecg_quiet);                          %Identify mean voltage
during quiet trial.

for p = 1:4;
    ecg_emg{1,p} = filtfilt(b,a,emg_ts{1,p});    %dual pass Filter the
emg trial, based on transfer function
end

ecg_mvc = filtfilt(b,a,mvc);        %dual pass Filter the mvc trial,
```

```
based on transfer function

for p = 1:4;
    for i = 1:mc;
        emg_bias{1,p}(:,i) = ecg_emg{1,p}(:,i) - bias(1,i);   %Removing
bias from each EMG signal.
    end
end
for i = 1:mc;
    mvc_bias(:,i) = ecg_mvc(:,i) - bias(1,i);   %Removing bias from
each MVC signal.
end

%% Rectification
for i = 1:4;    %Taking the absolute value of the EMG after it has been
HP filtered.
    hp_emg_bias{1,i} = abs(emg_bias{1,i});
end
hp_mvc_bias = abs(mvc_bias);

%% Low-Pass Filter
[bl,al] = butter(nl,Wnl);

for i = 1:4;
    le_emg{1,i} = filter(bl,al,hp_emg_bias{1,i});
end

le_mvc = filter(bl,al,hp_mvc_bias);

%% Removing Padding Points
%Sampling Hz was 2400, therefore we take away 2400 data points off the
%start.
for i = 1:4;
    for p = 1:mc;
        x{1,i}(:,p) = le_emg{1,i}(start(1,i):end,p);
    end
end


for i = 1:mc;
    y(:,i) = le_mvc(2401:end,i);
end

%% Identifying Max MVC
mvc_max = max(y);
%% Identifying Max values for RMS normalizations
mvc_rms = max(mvc);
%% Normalization
for k = 1:4;
    for i = 1:mc;
        norm_emg{1,k}(:,i) = (x{1,k}(:,i) / mvc_max(1,i)) * 100;
    end
end
```

H1.5 Ensemble Averaged CC Force

```
%%
for i = 1:4;              %Set this to the number of postures that will
work.
    int_force_trial{1,i}(1,1) = NaN;
    int_force_cycle{1,i}(1,1) = NaN;
end
%%
for a = 1:4;          %Set this to the number of postures that will
work.
    force = hand_force_padd_removed{1,a};
    starttime_m = starttime{1,a};
    temp_force = NaN(900,101);
    inter_force = NaN(900,101);
    j = 0;
    k = 1;
    for i = 1:numel(starttime_m)-(length(find(isnan(starttime_m))));
%The if statement identifies a NaN as the end of the current
compression
        j = j + 1;
%cycle and start of the next one.
        if isnan(starttime_m(j+1,k));
            k = k + 1;
            j = 0;

        else
            v = force(starttime_m(j,k):starttime_m(j+1,k),1);   %The
Linear interpolation function is used here. Each individual compression
            c = numel(v);
%was completed with varying timing, thus absolute averaging would not
be
            xq = 1:c/101:c;
%appropriate in this situation. To remedy this the start of each
compression
            temp_force = interp1(v,xq);                              %is
defined as '1' and the end '101' to equal 100%. The number of samples
in

%each compression is counted and divided by 101, this equals the new
frequency
            inter_force(i,1:101) = temp_force(1,1:101);             %it
will be sampled at. Therefore this function begins at 1 increases at a
        end
%frequency of c/101 to c number of samples.
    end

    downcount = 1;      %Compression counter
    c = 1;              %Compression cycle counter
    for b = 1:length(inter_force);
    %while ~isnan(inter_force(downcount,1)) &&
~isnan(inter_force(downcount+1,1));
        downcount = downcount + 1;
```

```
        if isnan(inter_force(b,1)) && isnan(inter_force(b+1,1))
%Identifies the end of the trial with 2 NaN's back to back
            break
        elseif isnan(inter_force(downcount+1,1)) && c == 1;
%Identifies the first compression cycle
            int_force_cycle{c,a}(1:downcount,1:101) =
inter_force(1:downcount,1:101);
            c = c + 1;
            d = downcount;      %Holds the position of the last
compression in the cycle
        elseif isnan(inter_force(downcount+1,1));
%Identifies each compression cycle after the first
                last_comp = downcount - d;                  %Identifies
the position of the last compression in the cycle
                int_force_cycle{c,a}(1:last_comp - 1,1:101) =
inter_force(d+2:downcount,1:101);
                c = c + 1;
                d = downcount;
        end
    end

inter_force(any(isnan(inter_force),2),:)=[]; %Gets rid of the NaN rows
int_force_trial{1,a} = inter_force;          %Places each full posture
trial in its own array

temp_force = NaN(600,101);      %Re-sets the matrix to NaN's so there
is no overlap when evaluating the next posture
inter_force = NaN(600,101);


end
%%
end
```

H1.6 Ensemble Averaged EMG

```
%%
for i = 1:4;
    for a = 1:16;
       int_emg_trial{1,i} = NaN; %Added
%         int_emg_cycle{1,i}{1,a} = NaN; Original
        int_emg_cycle{1,i}{1,a} = NaN;
    end
end
%%
for a = 1:4;
    starttime_m = starttime{1,a};
    le_emg_m = le_emg{1,a};
    temp_emg = NaN(1,101);           %NaN Matrix for the rise and fall
of EMG per compression
    int_EMG = NaN(750,101);          %NaN Matrix for all EMG during the
trial
```

```
    n = 0;
    o = -100;
        %inter_EMG = NaN(3160,101);
        %mean_inter_EMG = NaN(101,8);          %NaN Matrix for final
interpolated data
        j = 0;                  %Counter for rows
        k = 1;                  %Counter for coloumns
        for f = 1:16;
            %le_emg_muscle = le_emg_m(1:end,f);
            k = 1;              %Re-set for the next muscle, since it
is in one data sheet
            for i = 1:numel(starttime_m)-
(length(find(isnan(starttime_m))));  %Identifies how many numbers
starttimes there are as a counter
                j = j + 1;

                if isnan(starttime_m(j+1,k));  %Identifies the end of
the current compression cycle
                    k = k + 1;
                    j = 0;                   %Re-sets row counter to 0.

                else
                    v =
le_emg_m(starttime_m(j,k):starttime_m(j+1,k),f);   %The Linear
interpolation function is used here.
                    c = numel(v);
                    xq = 1:c/101:c;
                    temp_emg = interp1(v,xq);
                    int_EMG(i,1:101) = temp_emg(1,1:101);
                end
            end

            downcount = 1;          %Compression counter
                c = 1;              %Compression cycle counter
                for z = 1:length(int_EMG);
                    downcount = downcount + 1;
                    if isnan(int_EMG(z,1)) && isnan(int_EMG(z+1,1))
%Identifies the end of the trial with 2 NaN's back to back
                        break
                    elseif isnan(int_EMG(downcount+1,1)) && c == 1;
%Identifies the first compression cycle
                        int_emg_cycle{1,a}{c,f}(1:downcount,1:101) =
int_EMG(1:downcount,1:101);
                        c = c + 1;
                        d = downcount;      %Holds the position of the
last compression in the cycle
                    elseif isnan(int_EMG(downcount+1,1));
%Identifies each compression cycle after the first
                            last_comp = downcount - d;
%Identifies the position of the last compression in the cycle
                            int_emg_cycle{1,a}{c,f}(1:last_comp -
1,1:101) = int_EMG(d+2:downcount,1:101);
                            c = c + 1;
                            d = downcount;
```

```
                    end
                end

            o = o+101; %Added
                n=n+101;   %Added
            int_EMG(any(isnan(int_EMG),2),:)=[];         %Clears all
the rows with NaN's in them
%             int_emg_trial{1,a}{1,n} = int_EMG; % origianal
            int_emg_trial{1,a}(1:length(int_EMG),o:n) = int_EMG;

        temp_emg = NaN(1,101);           %NaN Matrix for the rise and
fall of EMG per compression
        int_EMG = NaN(750,101);

%             d = length(int_EMG);                          %Identifies
how many compressions per trial
%             s = d * f;                                    %To place
the EMG of each muscle in a single file we need to keep adding the
%             a = ((d * f) + 1) - d;                        %total
amount of compressions per trial to it.
%             inter_EMG(a:s,1:101) = int_EMG;
%             mean_inter_EMG(1:end,f) = mean(int_EMG);
        end                                                  %Finds the
mean EMG per trial and copies it into the final matrix

end
```

H1.7 Mean Power Frequency and Root Mean Squared

```
mc = 16;                                                %muscles evaluated
fs = 2400;                                              %Sampling freq
l_trial = length(pre_post);                             %Number of trials

Starting point for the portion of the trial, numbers in excel document
l_s = length(s_points);

s_counter = 1;
for i = 1:l_s;  %taking 2048 sample points starting from the portion of
the trial
    pre_post_sp{1,i}(1:2048,1:16) =
pre_post{1,i}(s_points(1,s_counter):(s_points(1,s_counter) +
2047),1:mc);
    s_counter = s_counter + 1;
end

%% Mpf loop
mpf_1(l_trial,1:mc) = NaN;

for a = 1:l_trial
    mpf_1(a,1:mc) = meanfreq(pre_post_sp{1,a},fs,[10 250]);
end
```

```
%% RMS loop
rms_1(l_trial,1:mc) = NaN;

rms_emg_1 = pre_post_sp;
for a = 1:l_trial;
    for i = 1:mc
        rms_emg{1,a}(:,i) = (rms_emg_1{1,a}(:,i) / mvc_rms(1,i)) * 100;
    end
end
for a = 1:l_trial
    rms_1(a,1:mc) = rms(rms_emg{1,a});
end

%% Shifting into different matrix
for i = 1:4
    mpf{1,1}(i,1:mc) = mpf_1(i,1:mc);       %Kneeling
end
for i = 1:4
    mpf{1,2}(i,1:mc) = mpf_1(i+4,1:mc);     %330
end
for i = 1:4
    mpf{1,3}(i,1:mc) = mpf_1(i+8,1:mc);    %Finger
end
for i = 1:4
    mpf{1,4}(i,1:mc) = mpf_1(i+12,1:mc);    %Waist
end

%% Shifting RMS into different matrix
for i = 1:4
    rms_results{1,1}(i,1:mc) = rms_1(i,1:mc);       %Kneeling
end
for i = 1:4
    rms_results{1,2}(i,1:mc) = rms_1(i+4,1:mc);     %330
end
for i = 1:4
    rms_results{1,3}(i,1:mc) = rms_1(i+8,1:mc);    %Finger
end
for i = 1:4
    rms_results{1,4}(i,1:mc) = rms_1(i+12,1:mc);    %Waist
end

end
```

H1.8 CC Depth, Change in Chest Angle, and Chest Recoil

```
%% Identify the centroid of the triangle
for i = 1:4
    for a = 3:3:18
        z_axis{1,i}(:,a/3) = kine{1,i}(:,a);  %Placing the z-axis of
each marker in a seperate matrix
    end
end
```

```
b = 0;
for i = 1:4
    b = 0;
    for a = 2:3:17
        b = b + 1;
        y_axis{1,i}(:,b) = kine{1,i}(:,a);  %Placing the y-axis of each
marker in a seperate matrix
    end
end
b = 0;
for i = 1:4
    b = 0;
    for a = 1:3:16
        b = b + 1;
        x_axis{1,i}(:,b) = kine{1,i}(:,a);  %Placing the x-axis of each
marker in a seperate matrix
    end
end

for i = 1:4  %Identifying the middle of each triangle in regards to
each axis
    x{1,i}(:,1) = (x_axis{1,i}(:,1) +  x_axis{1,i}(:,2) +
x_axis{1,i}(:,3))/3;
    x{1,i}(:,2) = (x_axis{1,i}(:,4) +  x_axis{1,i}(:,5) +
x_axis{1,i}(:,6))/3;
end
for i = 1:4
    y{1,i}(:,1) = (y_axis{1,i}(:,1) +  y_axis{1,i}(:,2) +
y_axis{1,i}(:,3))/3;
    y{1,i}(:,2) = (y_axis{1,i}(:,4) +  y_axis{1,i}(:,5) +
y_axis{1,i}(:,6))/3;
end
for i = 1:4
    z{1,i}(:,1) = (z_axis{1,i}(:,1) +  z_axis{1,i}(:,2) +
z_axis{1,i}(:,3))/3;
    z{1,i}(:,2) = (z_axis{1,i}(:,4) +  z_axis{1,i}(:,5) +
z_axis{1,i}(:,6))/3;
end

%% Converting the padding points to a sampling rate of 100Hz
start_1(1,1:4) = NaN;
for i = 1:4;
    start_1(1,i) =  round(start(1,i) / 24); %Kinematics sampled at
100hz, therefore we need to downsample the starttimes that were sampled
at 2400hz.
end

%% Removing the padding points from the start of the trial
for i = 1:4
    for a = 1:2 %identifyies the correct starttime of each vector and
removes all data prior to it
        x_clip{1,i}(:,a) = x{1,i}(start_1(1,i):end,a);
        y_clip{1,i}(:,a) = y{1,i}(start_1(1,i):end,a);
        z_clip{1,i}(:,a) = z{1,i}(start_1(1,i):end,a);
```

```
    end
end


%% Downsampling the starttimes to line up with the 100Hz sampling rate
for i = 1:4
    starttime{1,i} = round(starttime{1,i} / 24); %Downsampling the
starttimes to match the 100Hz
end

for i = 1:4
    s1(1,i) = length(z_clip{1,i});
end
s2=size(starttime{1,1});

%% Identifying the 1/4 the distance away from the xiphoid centroid
for i = 1:4 %Participants were pushing 3/4 the distance away from the
sternal notch
    c_x{1,i} = ((1/4) * x_clip{1,i}(:,1)) + ((3/4) * x_clip{1,i}(:,2));
    c_y{1,i} = ((1/4) * y_clip{1,i}(:,1)) + ((3/4) * y_clip{1,i}(:,2));
    c_z{1,i} = ((1/4) * z_clip{1,i}(:,1)) + ((3/4) * z_clip{1,i}(:,2));
end

%% Identifying the resultant vector
for p = 1:4                    %Calculating the resultant distance
vectors
    xyz{1,p}(:,1) = sqrt((x_clip{1,p}(:,1).^2) + (y_clip{1,p}(:,1).^2)
+ (z_clip{1,p}(:,1).^2));
    xyz{1,p}(:,2) = sqrt((x_clip{1,p}(:,2).^2) + (y_clip{1,p}(:,2).^2)
+ (z_clip{1,p}(:,2).^2));
    c_xyz{1,p}(:,1) = sqrt((c_x{1,p}(:,1).^2) + (c_y{1,p}(:,1).^2) +
(c_z{1,p}(:,1).^2));
end


%% Creating empty matrix's for the variables
for i = 1:4;
    compdist_z{1,i} = NaN(s2(1,1),s2(1,2));
end
for i = 1:4;
    chest_recoil_z{1,i} = NaN(s2(1,1),s2(1,2));
end
for i = 1:4;
    min_depth_z{1,i} = NaN(s2(1,1),s2(1,2));
end
for i = 1:4;
    compdist_xyz{1,i} = NaN(s2(1,1),s2(1,2));
end
for i = 1:4;
    chest_recoil_xyz{1,i} = NaN(s2(1,1),s2(1,2));
end
for i = 1:4;
    min_depth_xyz{1,i} = NaN(s2(1,1),s2(1,2));
end
```

```
for i = 1:4;
    zero_pos_xyz{1,i} = NaN(1,s2(1,2));
end
for i = 1:4;
    zero_pos_mid_z{1,i} = NaN(1,s2(1,2));
end

%% Calculating all variables
for a = 1:4
    j = 0;      %Row counter
    k = 1;      %Coloumn counter
    for i = 1:sum(sum(~isnan(starttime{1,a}),1))-1; %Identifies the
exact number of starttimes (compressions) in each trial
        j = j + 1;
        if isnan(starttime{1,a}(j+1,k));
            %zero_pos{1,a}(1,k) =
prctile(z_clip{1,a}(starttime{1,a}(j,k):starttime{1,a}(1,k+1),2),50);
%Identiying the zero position using the 50th percentile.

            temp =
(c_z{1,a}(starttime{1,a}(j,k):starttime{1,a}(1,k+1),1)); %Calculating
the zero position using the mid point of the breath
            f = round((length(temp)) / 2);
%Identifying the mid point
            zero_pos_mid_z{1,a}(1,k) = mean(temp(f-50:f,1));
%Moving half a second (50frames) backward
            temp = 0;
            f=0;

            temp =
(c_xyz{1,a}(starttime{1,a}(j,k):starttime{1,a}(1,k+1),1)); %Calculating
the zero position using the mid point of the breath
            f = round((length(temp)) / 2);
%Identifying the mid point
            zero_pos_xyz{1,a}(1,k) = mean(temp(f-50:f,1));
%Moving half a second (50frames) backward
            temp = 0;
            f=0;

            k = k + 1;
            j = 0;

        else    %This will index the time to max compression depth and
calculate the minimum comp depth. It will also find the comp depth in
the z axis
            [~,index_min{1,a}(i,1)] =
min(z_clip{1,a}(starttime{1,a}(j,k):starttime{1,a}(j+1,k),2)); %Indexs
the maximum depth of a compression
            index_min{1,a}(i,1) = index_min{1,a}(i,1) +
(starttime{1,a}(j,k) - 1); %because the min code pulls the index out of
the range we specified starting at 1 we have to add it back to the
start time
            min_depth_z{1,a}(j,k) =
max(c_z{1,a}(starttime{1,a}(j,k):starttime{1,a}(j+1,k),1));
```

```
%Identifies the minimum depth of the compression
            compdist_z{1,a}(j,k) = min_depth_z{1,a}(j,k) -
min(c_z{1,a}(starttime{1,a}(j,k):starttime{1,a}(j+1,k),1));

            %Calculate the comp distance in the xyz axis
            min_depth_xyz{1,a}(j,k) =
max(c_xyz{1,a}(starttime{1,a}(j,k):starttime{1,a}(j+1,k),1));
%Identifies the minimum depth of the compression
            compdist_xyz{1,a}(j,k) = min_depth_xyz{1,a}(j,k) -
min(c_xyz{1,a}(starttime{1,a}(j,k):starttime{1,a}(j+1,k),1));

            %Calculates the component form of the vector using the
x,y,z axis in the start and end locations
            res_v_start{1,a}(i,1) =
(x_clip{1,a}(starttime{1,a}(j,k),2)) -
(x_clip{1,a}(starttime{1,a}(j,k),1));
            res_v_start{1,a}(i,2) =
(y_clip{1,a}(starttime{1,a}(j,k),2)) -
(y_clip{1,a}(starttime{1,a}(j,k),1));
            res_v_start{1,a}(i,3) =
(z_clip{1,a}(starttime{1,a}(j,k),2)) -
(z_clip{1,a}(starttime{1,a}(j,k),1));
            res_v_finish{1,a}(i,1) =
(x_clip{1,a}(index_min{1,a}(i,1),2)) -
(x_clip{1,a}(index_min{1,a}(i,1),1));
            res_v_finish{1,a}(i,2) =
(y_clip{1,a}(index_min{1,a}(i,1),2)) -
(y_clip{1,a}(index_min{1,a}(i,1),1));
            res_v_finish{1,a}(i,3) =
(z_clip{1,a}(index_min{1,a}(i,1),2)) -
(z_clip{1,a}(index_min{1,a}(i,1),1));

            %Calculating the dot product in 2D and 3D
            dot_x{1,a}(i,1) = res_v_start{1,a}(i,1) *
res_v_finish{1,a}(i,1);
            dot_y{1,a}(i,1) = res_v_start{1,a}(i,2) *
res_v_finish{1,a}(i,2);
            dot_z{1,a}(i,1) = res_v_start{1,a}(i,3) *
res_v_finish{1,a}(i,3);
            dot_product_2D{1,a}(i,1) = dot_x{1,a}(i,1) +
dot_z{1,a}(i,1);
            dot_product_3D{1,a}(i,1) = dot_x{1,a}(i,1) +
dot_y{1,a}(i,1) + dot_z{1,a}(i,1);

            %Calculates the magnitude of the two vectors in 2D and 3D
            mag_start_2D{1,a}(i,1) = sqrt((res_v_start{1,a}(i,1).^2) +
(res_v_start{1,a}(i,3).^2));
            mag_start_3D{1,a}(i,1) = sqrt((res_v_start{1,a}(i,1).^2) +
(res_v_start{1,a}(i,2).^2) + (res_v_start{1,a}(i,3).^2));
            mag_finish_2D{1,a}(i,1) = sqrt((res_v_finish{1,a}(i,1).^2)
+ (res_v_finish{1,a}(i,3).^2));
            mag_finish_3D{1,a}(i,1) = sqrt((res_v_finish{1,a}(i,1).^2)
+ (res_v_finish{1,a}(i,2).^2) + (res_v_finish{1,a}(i,3).^2));
            mag_2D{1,a}(i,1) = mag_start_2D{1,a}(i,1) *
```

```
mag_finish_2D{1,a}(i,1);
            mag_3D{1,a}(i,1) = mag_start_3D{1,a}(i,1) *
mag_finish_3D{1,a}(i,1);

            %Calculates the change in angle in degrees between the two
vectors
            delta_2D{1,a}(i,1) = acosd(dot_product_2D{1,a}(i,1) /
mag_2D{1,a}(i,1));
            delta_3D{1,a}(i,1) = acosd(dot_product_3D{1,a}(i,1) /
mag_3D{1,a}(i,1));
            %acos = a*b(dot product) / magnitude of a*b

end
    end
end

%%
for i = 1:4;
    zero_length(1,i) = sum(sum(~isnan(zero_pos_mid_z{1,i}),1));
end
for i = 1:4
    for a = 1:zero_length(1,i)
        if a == zero_length(1,i)
            %Calculating the chest recoil for the 1st and 2nd cycle
since we couldn't get a zero prior to the start of compressions
            chest_recoil_z{1,i}(:,a) = zero_pos_mid_z{1,i}(1,a) -
min_depth_z{1,i}(:,a);
            chest_recoil_z{1,i}(:,a+1) = zero_pos_mid_z{1,i}(1,a) -
min_depth_z{1,i}(:,a+1);
            chest_recoil_xyz{1,i}(:,a) = zero_pos_xyz{1,i}(1,a) -
min_depth_xyz{1,i}(:,a);
            chest_recoil_xyz{1,i}(:,a+1) = zero_pos_xyz{1,i}(1,a) -
min_depth_xyz{1,i}(:,a+1);
        else
            chest_recoil_z{1,i}(:,a) = zero_pos_mid_z{1,i}(1,a) -
min_depth_z{1,i}(:,a);
            chest_recoil_xyz{1,i}(:,a) = zero_pos_xyz{1,i}(1,a) -
min_depth_xyz{1,i}(:,a);
        end
    end
end
end
```

H1.9 Amplitude probability distribution function

```
mc = 16;
for i = 1:4          %Trial counter
    for k = 1:mc     %Muscle counter
        APDF_emg{1,i}(k,:) = prctile(le_emg{1,i}(:,k),[10 50 90]); %No
need to reshape data here because each muscle is already in a single
vector
    end
```

```
end
```

H1.10 Time Lag of EMG and CC Force

```
mc = 16; %Number of muscles per trial evaluated
fs = 2400;
for x = 1:4;
    lag_sample{1,x}(1,1:mc) = NaN;
end
for x = 1:4;
    lag_time{1,x}(1,1:mc) = NaN;
end
%%
for a = 1:4; %Trial counter
    for m = 1:mc; %Muscle counter
        for cycle = 1:sum(~isnan(starttime{1,a}(1,:))); %Calculates the
number of cycles per trial
            [r,lag_temp] = xcorr(hand_force_padd_removed{1,
a}(starttime{1,a}(1,cycle):starttime{1,a}(sum(~isnan(starttime{1,a}(:,c
ycle))),cycle),1),...
            le_emg{1,
a}(starttime{1,a}(1,cycle):starttime{1,a}(sum(~isnan(starttime{1,a}(:,c
ycle))),cycle),m));
            [~,I] = max(r);
            lag_sample{1,a}(cycle,m) = lag_temp(I);
            lag_time{1,a}(cycle,m) = lag_temp(I)/fs;
            lag_temp = NaN;
            r = NaN;
            I = NaN;
        end
    end
end
```